THESIS

HAZARD MAPPING WITH DIRECT READING INSTRUMENTS FROM FACILITIES WITH HIGH AND LOW TEMPORAL VARIABILITY

Submitted by

Kirk Allen Lake

Department of Environmental and Radiological Health Sciences

In partial fulfillment of the requirements

For the Degree of Master of Science

Colorado State University

Fort Collins, Colorado

Spring 2014

Master's Committee:

Advisor: Kirsten Koehler

William Brazile
Pinar Omur-Ozbek

ABSTRACT

HAZARD MAPPING WITH DIRECT READING INSTRUMENTS FROM FACILITIES WITH HIGH AND LOW TEMPORAL VARIABILITY

The purpose of this study was to develop novel sampling techniques employing relatively lower-cost direct-reading instruments (DRIs, instruments that report hazard intensity at near real-time resolution) for hazard mapping. Normally, personal sampling equipment worn by workers is used to determine personal exposure (time-weighted average) to a hazard for comparison with an occupational exposure limit (OEL). However, time-weighted average methods give the industrial hygienists (IH) no information on the spatial or temporal variability of the exposures. Hazard maps have been suggested as a way to represent spatial variability in hazard intensity displayed as contours of hazard intensity on the facility floor plan. Traditionally, expensive direct-reading instruments (e.g., sound level meters) are used to create these hazard maps by collecting numerous individual measurements over a single-traverse of a workspace. These instruments fail to determine the temporal variability in exposures through the workplace and as such, may miss important, but transient exposures. To overcome these limitations, we proposed that we could enhance both the spatial and temporal resolution, compared to single traverse sampling strategies, by deploying lower-cost static personal monitors that captured temporal variability distributed throughout the facility and roving personal monitors that capture spatial variability over multiple traverses throughout whole work shifts.

These novel sampling techniques were evaluated at two locations with different temporal variabilities: a Plastic Manufacturing Facility (PMF), having low temporal variability, and the Engines and Energy Conversion Laboratory (EECL) at Colorado State University,

having high temporal variability. The goals of the sampling at these locations were three-fold. First, we wished to determine if hazards maps generated with different sampling techniques were similar, depending on the temporal variability. Relative similarity was assessed by comparison of overall mean squared difference between maps and percent differences from location-specific interpolated values between hazard maps. Second, since the new sampling technique was not validated, we wanted to determine if measurements taken from personal noise dosimeters, operated as static or roving monitors, and a sound level meter (SLM) exceeded instrument accuracy, when collected at the same time and in close spatial proximity. Third, in the course of these studies, several occupational hazard assessments were also carried out at these locations. These assessments included determination of effective hearing protector usage, characterization of noise, vibration, and diesel exhaust hazards, and evaluation of noise and diesel exhaust engineering controls.

TABLE OF CONTENTS

LIST OF TABLES

LIST OF FIGURES

1 Introduction

Workers are exposed to a variety of physical, chemical, and biological hazards in the workplace. This study was designed to determine if occupational exposures from hazards could be accurately mapped, utilizing hazard mapping techniques by novel sampling techniques with direct reading instruments (DRI) such as personal noise dosimeters and aerosol monitors. In the course of this study, we investigated occupational exposures to workers from noise, vibration, and diesel engine exhaust hazards. In this section, hazards and occupational exposure limits (OELs) will be discussed for the incidence of adverse health effects from noise, whole body vibration (WBV), and diesel particulate matter (DPM) hazards. Current hazard mapping techniques and studies from environmental and occupational scenarios will be related, and the novel techniques for collecting measurements from direct reading instruments to create high quality hazard maps will be introduced.

1.1 Noise Induced Hearing Loss (NIHL)

NIHL is one of the most common forms of occupational disease despite the Occupational Safety and Health Administration's (OSHA) requirements on the use of Hearing Conservation Programs (HCP) to protect workers in industries with hazardous noise levels. It is currently estimated that 30 million workers are exposed to hazardous noise levels and that 9 million workers are at risk for hearing loss from co-exposures to metals and organic solvents. The National Institute of Occupational Safety and Health (NIOSH) lists hearing loss as one of its twenty-one priority research areas for the 21th century (NIOSH, 2001).

NIHL is completely preventable and permanent; this form of hearing loss cannot be treated with surgery or corrected with hearing aids. Short-term exposures to loud noise can lead to symptoms including changes in hearing and ringing. These effects are generally temporary and pass in a matter of minutes or hours. Repeated or long-term exposures to loud noise can lead to permanent hearing loss making workers especially vulnerable to NIHL (Hong *et al*, 2013). Susceptibility to NIHL varies by subject and may worsen with co-exposure to some pharmaceuticals and organic solvents (Campo *et al*., 2013; Metwally *et al.*, 2012). A number of non-auditory physiological effects have also been associated with loud noise such as affected blood pressure, affected heart rate, blood pressure variation, reduced rates of breathing, hormonal changes, and brief skeletal-muscle tension. Physiological effects may also be dependent on noise frequency (Prashanth and Venugopalachar, 2011). High frequency noise is more damaging to hearing than medium and low frequencies (Ward *et al*., 2003). In general audiologists define noise frequency in low (10-200 Hz), medium (200-2000Hz), and high (2000-20000 Hz) band ranges, which are useful for describing noise characteristics (Leventhall, 2004 and OSHA, 2013).

OSHA regulates noise exposure with a permissible exposure limit (PEL) of 90 dBA for time-weight averages over an10 8-hour work shift (TWA (8 hr)) with a 5 dB exchange rate (ER). An ER, or doubling rate, of 5 dB refers 10 above the PEL (i.e., 16 hr at 85 dBA, 8 hr at 90 dBA, 4 hr at 95 dBA, and 2 hr at 100 dBA). Impulsive or impact noise is limited to 140 dB. The maximum level of continuous noise (i.e., noise lasting longer than 1 s) that a worker may be exposed to for any amount of time is limited to 115 dBA. Time-weighted average (TWA) exposure is the average worker exposure generally normalized for an 8 hr work shift and is used by OSHA to determine if noise levels are hazardous to workers. OSHA has set a noise action level such that any applicable business or governmental agency, having an employee TWA (8 hr)

equal to or greater than 85 dBA or personal dose greater than 50%, is required to implement a Hearing Conservation Program (HCP) to protect workers from increased risk of NIHL. The OSHA PEL is the only exposure limit with the "rule of law" resulting in citable exposures by regulatory agencies (OSHA, 2002).

The American Conference of Governmental Industrial Hygienists (ACGIH) and NIOSH recommend more protective OELs (Threshold Limit Values [TLV] and Recommended Exposure Limits [REL], respectively) of TWA (8 hr) 85 dBA with a 3 dB ER. This lower criterion level and ER result in more protective permissible exposure durations (i.e., 16 hr at 82 dBA, 8 hr at 85 dBA, 4 hr at 88 dBA, and 2 hr at 91 dBA). The TLV and REL are based on the probable incidence of adverse human health effects over time (NIHL in this case) but are not enforceable by law (NIOSH, 1998; ACGIH, 2001a). Cross-sectional studies by Daniell *el al.* (2006) found that employers using 5 dB exchange rates to control noise exposures subjected their employees to 150 to 300 % greater excessive noise than those using 3 dB exchange rates.

Risk in the present study will be defined as high for worker TWA (8 hr) greater than or equal to 85 dBA based on a significant proportion of the population (>10 %) developing NIHL overtime. The percentage risk increases to 19 % for impairment at 85 dBA for work exposures greater than 30 years. TWA (8 hr) from 80-84 dBA will be defined as medium in risk based on a lesser proportion (<10 %) of the population and those with illnesses or co-exposures developing NIHL overtime, and TWA (8 hr) less than 80 dBA will be defined as low in risk (ACGIH, 2001a). With the NIOSH 1-2-3-kHz model for hearing impairment at age 40 after 40 years of work exposure at average noise intensity levels, excess risk was estimated at 32 % for 90 dBA, at 14 % for 85 dBA, and at 5 % for 80 dBA (NIOSH, 1998).

1.2 Whole Body Vibration (WBV)

In the United States nearly seven million workers are annually exposed to WBV. The primary route of vibration exposure is from the ground, transmitting to the feet while standing, the bottom while sitting, and the entire body while reclining. Acute exposure to WBV can cause fatigue, lower back pain, motion sickness, and psychological effects such as irritation and stress (ACGIH, 2001b). Vibration exposures can be viewed in terms of cumulative trauma with injuries resulting from repeated overuse or trauma to parts of the human body over time. Accumulation of trauma can result in joint disorders, leading to back pain and degenerative spinal disc diseases (Wikstrom, 1994).

No OELs have been promulgated by OSHA for WBV. The ACGIH has established TLV values. While the TLV was designed to address WBV for vehicle operators, it is used as a rough guide to evaluate worker health and safety for WBV in buildings (ACGIH, 2001b). The TLV for WBV is determined by sampling time, frequency, and longitudinal (Z-axis) or transverse (X or Y-axis) orientation. These TLV values, which are called Fatigue Decreased Proficiency (FDP) boundaries, represent the maximum WBV exposure at which most people could control a vehicle and are protective against the incidence of back disorders and pain over time. FDP boundaries will be used as OELs in this study for the incidence of adverse health effects associated with vibration exposure over time (ACGIH, 2001b).

1.3 Diesel Exhaust (DE)

DE is a mixture of gaseous species and particulate matter. Gaseous components include nitrogen, carbon dioxide, oxygen, water vapor, carbon monoxide, nitrogen compounds, sulfur compounds, and low molecular weight hydrocarbons from incomplete combustion of diesel fuel and oils. The exposure criteria for the gaseous components of DE can be determined for each

hazardous component individually by Environmental Protection Agency (EPA) Ambient Air Criteria or OSHA PEL. These gaseous components were not assessed during the present study. Diesel particulate matter (DPM), is composed of elemental carbon (EC) with small amounts of absorbed nitrate, sulfate, trace metals, and low molecular weight hydrocarbons (several of which have been identified as carcinogenic). DPM is directly released from engines or form from gases during secondary reactions in the atmosphere. Contaminates absorbed on EC particles of DPM are of primary concern for potential adverse health effects (Ris, 2007). Varying DPM particle size distributions have been reported in the literature. While a review of risk assessments by Ris (2007) reported 80-95 % of particle mass for DPM in the fine particle size range (particle diameter $\leq$ 2.5 μm or $PM_{2.5}$) and 1-20 % in the ultrafine particle size range (particle diameter < 0.1 μm), analysis of particle size distributions from a Pennsylvania turnpike study by Abu-Allaban *et al*. (2002) resulted in far smaller count median diameters (CMD) from 11 to 17 nm in the ultrafine range for exhaust particle production rates dominated by heavy-duty diesel vehicles. Fine and ultrafine particles pose an inhalation risk because these particles have a tendency to penetrate to the deep alveolar region of the respiratory tract, where hazardous organic and inorganic compounds from the surface of the particle are rapidly absorbed into systemic circulation (Ris, 2007). Ultrafine EC particles have also been demonstrated to translocate to the liver in short-term (< 24 hr) rat inhalation models with carbon-13 labeled EC particles. Inhalation and ingestion pathways are both likely operating based on isotopic carbon ratios detected in the liver (Oberdorster *et al.,* 2002).

Intense, acute exposure to DE may result in increased immunological responses and irritation of eyes, nose, throat, and the respiratory system. Symptoms of headache, lightheadedness, nausea, vomiting, and numbness of extremities have been reported (Ris, 2007).

An EPA health assessment from 2002 identified low concentration, long-term inhalation exposure to DE as a human health hazard for lung cancer. Non-cancerous effects from long-term inhalation exposure to DE include impairment of lung function and lung injury, leading to chronic inflammation and pathological change in the lung (Hesterberg *et al*., 2009). Based on these dose-dependent findings, a lifetime reference concentration (RFC) of 5 $\mu g/m^3$ was set for the incidence of non-cancer adverse human health effects from long-term chronic inhalation of DE. The RFC of a chemical or substance represents the daily (24 hr) inhalation concentration level of exposure below which adverse health effect are expected to not occur (Hesterberg *et al*., 2009). OELs have not been specifically promulgated by OSHA for DPM. For fine and ultrafine DPM exposures, the OHSA PEL for particulates not otherwise regulated (respirable fraction) is utilized with a TWA of 5 mg/m^3. While this PEL is expected to be protective against the incidence of lung disease for respirable particles, it is hundreds of times greater than the RFC value for DE inhalation after converting from daily (24 hr) to equivalent work-shift exposures (8 hr). The ACGIH proposed several draft TLVs (0.15 mg/m^3 and then 0.05 mg/m^3 as total particulates) for DPM, which were subsequently withdrawn, leaving it currently designated as a substance under study. The ACGIH TLV for respirable particles is instead utilized with a TWA of 3 mg/m^3. This TLV is expected to be protective against the incidence of lung disease with compromised airway clearance for respirable particles in general but is not low enough for exposure based on the RFC value (OSHA, 2012). The Mining Safety and Health Administration (MSHA) has set a more protective occupational DPM standard of 0.16 mg/m^3 TWA for sub-micrometer total carbon ($PM_{1.0}$) (Rogers and Davies, 2005).

1.4 Hazard Mapping

Koehler and Volckens (2011) loosely defined hazard mapping as "… the depiction of relative levels of a quantifiable hazard as it varies across a geographical space." In application, this equates to the projection of hazard concentration fields over a corresponding two-dimensional floor plan. With appropriate sampling plans, the sources and extent of hazardous exposures can be determined with a high degree of spatial resolution. These maps provide a great deal of visual information in a format that is easily understood. Well-designed maps serve as powerful tools for communicating risk to colleagues, management, and employees for informed decision making on exposure control and prevention strategies.

Hazard mapping suffers from three forms of measurement error: instrumental, completeness, and representativeness. Instrumental error, which will only be addressed briefly here, results from various issues including instrument bias, accuracy, precision, and sensitivity. The completeness of a hazard map is a measure of error based on the fact that one cannot simultaneously monitor a hazard at all locations and times. This implies that interpolation will be required to produce a hazard map. In general, maps with higher spatial and temporal sampling resolutions will have higher completeness. The representativeness of a hazard map is based on the fact that interpolation of spatially and temporally resolved measurements can result in errors of estimation, misrepresenting actual sample variance. Interpolations with better fitting spatial statistical models generally result in maps with higher representativeness (Koehler and Volckens, 2011; Koehler and Peters, 2013).

Numerous instances of hazard mapping were uncovered during literature reviews in the fields of public and occupational health. Concerning public health, noise hazard mapping is used in the EU by law (Murphy and King, 2010) and the US (Seong *et al.*, 2011) to inform decision

makers on the protection of the public from noise hazards around roadways. To better understand asphyxiation and explosion hazards indoor from methane, gas hazard mapping was used by Fischer *et al.* (2001) to elucidate the behavior of methane in a large interior space with high spatial (0.5 m) and temporal resolution (7 s). In Taranto, Italy, aerosol hazard mapping with environmental monitoring for PM_{10} was utilized by Pollice and Locinio (2010) to assess public aerosol exposure and inform decision makers to protect human health.

Concerning occupational health, hazard mapping has been used extensively to assess, communicate, and prevent or control hazardous exposures in the workplace. In a machining plant with multiple cases of Hypersensitivity Pneumonitis (HP) caused by mycobacteria from water based metal working fluids (MWF), O'Brien (2003) used aerosol mapping to identify the sources and spatial nature of exposures. Sources were controlled and prevented with a combination of mist collectors, new ventilation systems, and the addition of biocides to reduce mycobacteria concentrations in MWF. Subsequent aerosol mapping revealed that controls resulted in a significant reduction in aerosol concentrations and follow-up with the workers showed no new incidence of HP. Thus, this method was sufficient to improve worker health. Dasch *et al.* (2005) used aerosol mapping to characterize airborne particles generated from metalworking fluids around five machining processes at General Motor Plants. Spatial coarse (PM_{10}) and fine ($PM_{1.0}$) particle mass concentrations were mapped for dry, wet, retrofitted (mist cover), and new (enclosed or vented) emission control technologies. The mapped concentrations showed that the new vented and enclosed machines were most effective at decreasing particle emissions for coarse particle control. Fine particle control with the new technology was also improved but to a comparatively lesser degree.

Noise hazard mapping has also been used extensively in the field of occupational health. In a study from Nigeria, hazardous noise exposure and hearing loss were identified for steel mill workers by Ologe *et al.* (2006). In the study, workers were screened with structured questionnaires and hearing tests, including otoacoustic emissions, typanometry, and pure-tone audiometry. Noise mapping was then conducted in respective work places, finding exposures ranging from 49 to 93 dBA. The study identified a high prevalence of sensorineural hearing loss in the study population and recommended pre-employment and regular audiometry testing at these work places.

1.5 Current Hazard Mapping with Direct Reading Instruments

The current state of the art for regulatory assessment of occupational hazard exposure is the use of employee personal dosimetry (e.g. noise and particulates) for comparison of TWA (8 hr) with OELs. While these common and lower cost personal dosimeters are effective at determining TWA (8hr) for regulatory compliance, they cannot assess the temporal or spatial variability experienced by a worker. DRIs, such as sound level meters and optical particle counters/sizers that measure hazard intensities and characteristics (octave band levels, particle number and size distributions) at near real-time resolution are typically only used for area survey exposure assessment and hazard control due to their high cost, bulk, and weight. Thus, one of the main objectives of the research was to develop roving sampling methodologies employing personal dosimeter DRIs for area survey (Koehler and Volckens, 2011). Procedures were developed for simultaneous collection of individual sample times, relative spatial locations, and sampling durations for each measurement during sample collection. Location- and time- specific exposure measurements (equivalent sound pressure (dBA) and/or particle mass concentration (mg/m^3)) were then combined to produce hazard maps.

2 Experimental

2.1 Facilities

Our first opportunity to conduct these novel techniques originated from the request of a Colorado Front Range Plastic Manufacturing facility (PMF) for help in investigating occupational hazards from noise in three areas (PMF Production, office, and Plastic Recycling (PR)) and from vibration hazards in one area (office). The next sampling opportunity was found at Colorado State University's EECL, where we applied our new sampling techniques for noise and/or aerosol hazards at two engines on two days. Floor plans for these study locations are displayed in Figure 2.1.

2.1.1 Plastic Manufacturing Facility (PMF) Area

Noise hazard mapping was conducted in PMF Production with personal noise dosimeter DRIs (see Figure 2.2). Occupational noise exposure was also assessed with personal dosimetry of employees and SLM area surveys. PMF Production was rectangular in shape (149 m by 10 m to 14 m) and encompassed an area of about 1950 m^2. This area contained a long, rectangular machine, which ran the length of the room (143 m by 1.5 m). This machine was the only significant source of noise and vibration in the room. The southern side of the room contained three sound dampening enclosure workspaces for employee protection.

2.1.2 PMF Office

Occupational noise exposure and WBV analysis was conducted in the PMF office with SLM and accelerometer area surveys. Employees had complained about noise and vibration in this region with symptoms including headaches, increased distractibility, and

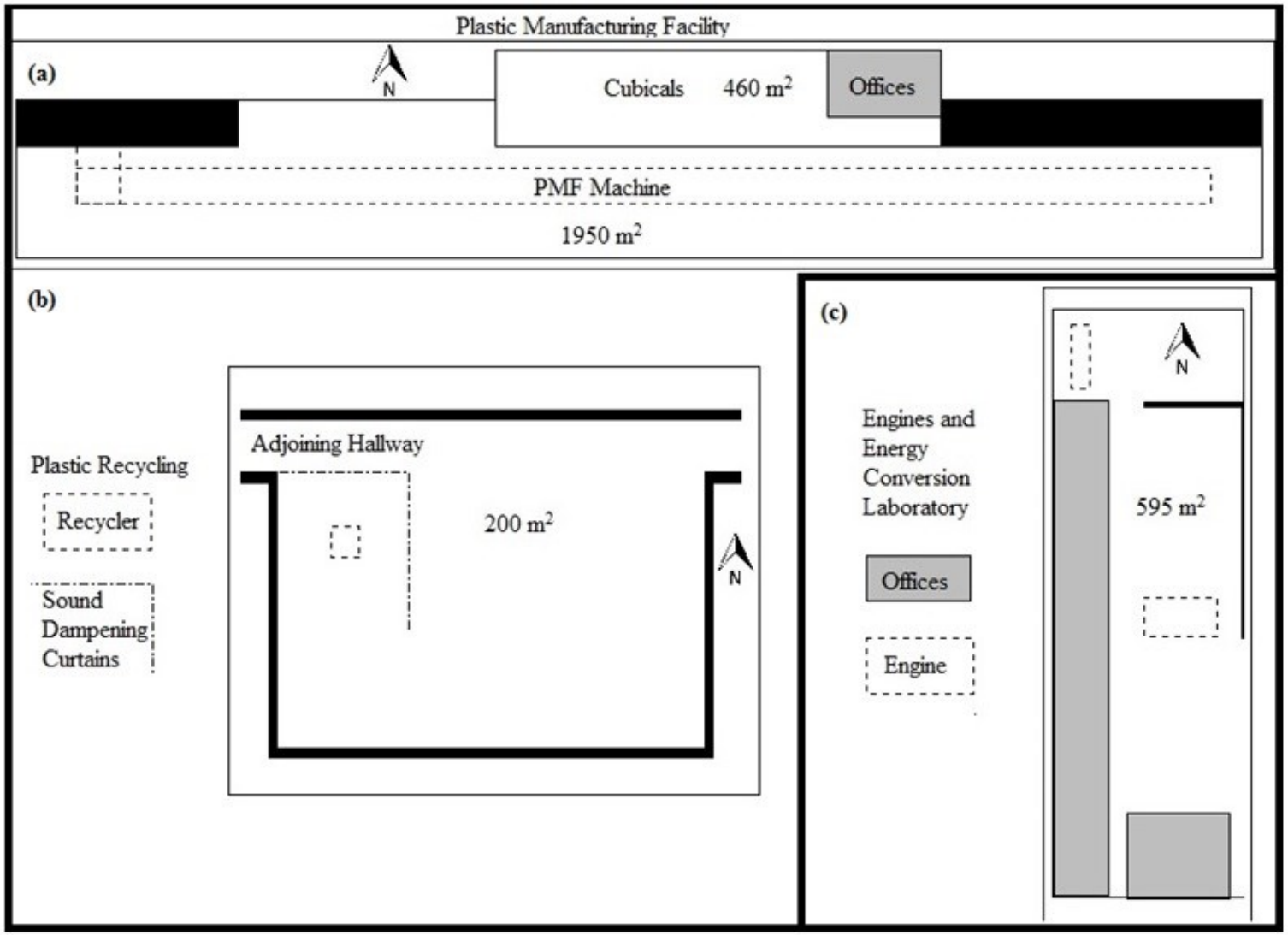

Figure 2.1: PMF Production and offices (a), Plastic Recycling (b), and EECL (c) are displayed.

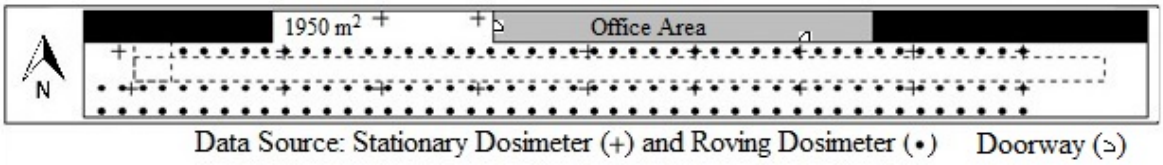

Figure 2.2: The PMF Production floor plan displays sampling positions for personal DRIs.

tingling of extremities. Employees in the office may be exposed to hazardous noise and vibration, originating from the machine in the southern PMF Production area. The office was rectangular in shape (51 m by 10 m) and encompassed an area of about 460 m^2. Private offices (not sampled) were located to the east and open space cubicles were located in the central and western portions of the room, as shown in Figure 2.1a.

2.1.3 PMF Plastic Recycling (PR) Area

Occupational noise exposure was assessed in the Plastic Recycling (PR) area, as shown in Figure 2.1b, with SLM area surveys and octave band analysis to determine the effectiveness of existing engineering controls (partial barrier modular acoustic screens) and resultant exposure levels. The PR area was located one floor directly below PMF Production. The PR area contained a machine (1 m^2) in the southwest corner of the room, which extended up into the ceiling. An adjoining hallway to the north ran east to west in direction. The machine emitted noise above 90 dBA in surrounding areas, and the hierarchy of controls had been implemented to control and prevent exposure to the noise hazard in this area. Hearing protection was required, and protective earmuffs were provided for dual-protection on a nearby wall. Administrative controls were in place in the form of warning signage and detour pathways for general foot traffic. Employees did not have work areas or responsibilities, requiring them to spend time in this area on a regular basis. Engineering controls in the form of modular acoustic screens had been installed on the northern and eastern sides of the machine to reduce noise levels in the adjoining northern hallway.

2.1.4 Engine and Energy Conversion Laboratory (EECL)

Aerosol and noise hazard mapping was conducted at Colorado State University's EECL with personal noise dosimeters and aerosol photometers (see Figure 2.1c and 2.3). Occupational noise exposure was also assessed with SLM area surveys. The area selected for sampling in the EECL consisted of two rooms, connected lengthwise from the north to south by a sliding door. The northern and southern rooms were both rectangular in shape (14.8 m by 6.5 m and 14.8 m by 33.7 m, respectively) and encompassed a combined an area of about 595 m^2. The northern

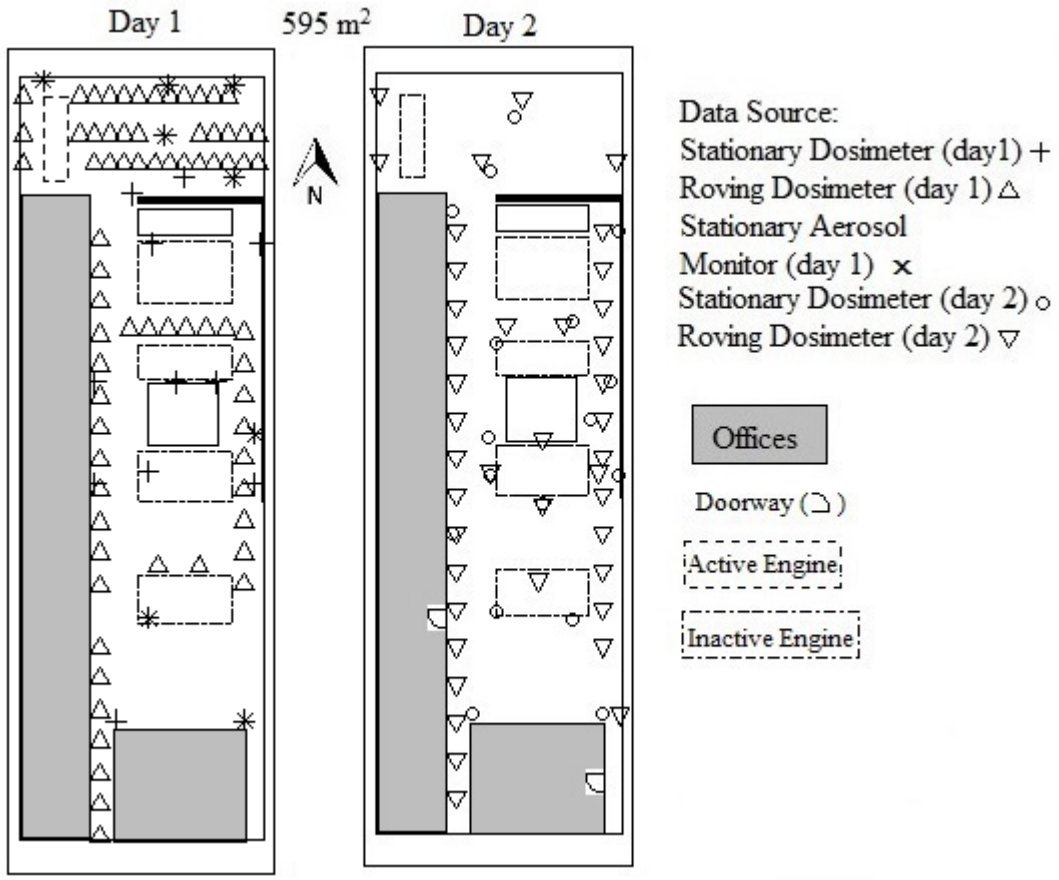

Figure 2.3: The EECL floor plans display day 1 and 2 DRI sampling positions for hazard mapping.

room consisted of an engine on the far west side and a sliding door to the south. The sliding door between rooms remained in a constant open position throughout all sampling activities. Workbenches, storage space, and tool boxes filled most of the available wall and floor space.

The southern room consisted of four engines stacked lengthwise, occupying most of the central floor space in the room. Workbenches, storage space, and tool boxes filled most of the available wall and floor space. In both rooms, engines and several storage containers were of sufficient width and height to act as partial barriers, interfering with the propagation of noise throughout the workspace. These partial barriers may have significant effects on personal noise exposures and measurements for area surveys and hazard mapping. Exhaust was vented from the engines to the exterior of the building, but staff believed that significant leaks existed. Open windows on the northern side of the building and commercial heating and cooling systems were the only other sources ventilation in the EECL. Two sets of offices (not sampled) covered the western and southern sides of the room. The southeastern part of the room contained a corridor, connecting to unsampled portions of the EECL building. This corridor could have represented additional sources of aerosol and noise hazards. Major construction activities were occurring directly outside the building, and brief, intermittent welding activities were observed in the southern room between the 3rd and 4th engines throughout the sampling period. Those activities could not be ruled out as potential sources of noise and aerosol exposure.

2.2 Noise Monitoring Equipment

Monitoring for noise hazard mapping with our novel techniques was conducted by stationary and roving (for more details see Sections 2.51-2.52) sampling strategies with personal noise dosimeters in the PMF and EECL facilities. Occupational noise exposure was assessed for dose and TWA (8 hr) during full and partial work shifts by personal noise dosimetry of employees in PMF Production and by area surveys with a SLM in the PMF and EECL. All instruments are able to internally log data and were synchronized with a timepiece.

2.2.1 Personal Noise Dosimeters

Noise exposures were measured at the PMF and EECL facilities with Spark personal dosimeters (Model 706RC and 703, Larson Davis Inc, Provo, Utah). All dosimeters were set to log measurements at 1-second resolution with the following OSHA required measurement settings: A -weighted, slow response, 5 dB exchange rate, 80 dB threshold, and 90 dB criterion level (CL). The criterion level refers to the sound pressure for the occupational exposure limit (PEL, REL, TLV, etc.). The threshold value sets a limit below which all sound pressure values are equal to zero for TWA calculation. Each dosimeter was calibrated within 24 hr of use with a SparkCal (Model 150, Larson Davis Inc, Provo, Utah) at 94 dBA and 114 dBA. Post-calibration revealed no values greater or less than 0.5 dBA from pre-calibration values. Instrumental accuracy for these instruments varies by $\pm$ 2 dB.

When using 3 dB exchange rates, the produced value is referred to as an equivalent steady state sound pressure level (Leq). Dosimeters produce level averaged sound pressure (L_{avg}) values when using 4, 5, or 6 dB exchange rates. For all practical purposes, these terms are the same and are defined as average sound pressure level for the measurement period based on an exchange rate. By industry convention, all of these values will be referred to as Leq (L_{avg} will not be used) and the ER is assumed to be 5 dB unless otherwise specified.

For occupational noise exposure, Equations 1-3 below were used to estimate noise exposure based on Leq values. Dose (8 hr) is a measure of exposure over 8 hr expressed as a percentage of maximum permissible exposure for a full shift (T hr). Dose (8 hr) is calculated from a unitless constant value (q) that varies by ER and Leq or TWA (8 hr) for 8 or 12 hr shifts by Equation 1. The time allowed for a full dose is calculated by Equation 2 from Leq or TWA. TWA (8 hr) can be estimated from dose (8 hr) by Equation 3. OSHA criteria are necessary for

regulatory compliance for occupation noise exposure with a PEL of 90 dBA TWA (8 hr), CL 90 dBA, ER 5 dB, and q 16.61, while ACGIH conditions are protective against increased risk of NIHL with a TLV of 85 dBA TWA (8 hr), CL 85 dBA, ER 3 dB, and q 10. Dose will be reported using both the OSHA and the more protective ACGIH specifications.

When dosimeters measure noise over an entire 8-hour work shift, the resultant Leq value is equal to TWA (8 hr). When dosimeters sample for less or more than the full work shift, the assumption may be made that if the Leq value is representative of the full work shift, then Leq equals TWA (8 hr). In this investigation, static and roving dosimeters and a SLM sampled noise for less than 8 hr work shifts at the PMF and EECL. For our purposes the assumption was made that Leq values approximately equal TWA (8 hr). This assumption allows the use of Leq rather than TWA (8hr) in the calculation of estimated noise exposure.

$$\text{Dose (8 hr)} = 100 \times \left(\frac{T}{8\ hr}\right) \times 10^{[\text{Leq or TWA (8 hr)}]-\text{CL}/q} \quad [\%] \quad \text{Equation 1}$$

[q=16.61 for 5 dB ER and q=10 for 3 dB ER]

$$\text{Time Allowed} = 8/2^{[\text{Leq or TWA (8 hr)}]-\text{CL}/\text{ER}} \quad [\text{hr}] \quad \text{Equation 2}$$

$$\text{TWA (8 hr)} = q \times \text{Log}_{10}\left(\frac{\text{Dose (8 hr)}}{100}\right) + \text{CL} \quad [\text{dBA}] \quad \text{Equation 3}$$

2.2.2 Sound Level Meter and Octave Band Analyzer

Area survey noise samples were measured at the PMF and EECL facilities with a type 1 SLM and octave band analyzer (System 824A, Larson Davis, Provo, Utah). The SLM was set to record Leq and third octave band measurements between 12.5 and 20,000 Hz. The SLM was calibrated within 4 hr of use with a SparkCal (Model 200, Larson Davis Inc, Provo, Utah) at 94 dBA and 114 dBA. Post-calibration revealed no values greater or less than 0.5 dBA from pre-calibration values. Instrumental accuracy for this type 1 SLM varies by $\pm$ 1 dB.

2.3 Aerosol Monitoring Equipment

Monitoring for aerosol hazard mapping of $PM_{2.5}$ from diesel exhaust (DE) was conducted by stationary and roving sampling strategies with aerosol photometers in the EECL facility. Additionally, the particle size distribution was determined at 5 m from the active engine. Aerosol photometers were paired with TWA gravimetric filters to estimate total mass to determine a calibration value and a monitor inter-comparison was completed in an aerosol chamber with urban dust mist to determine accurate calibration coefficients for optical measurements (Benton-Vitz and Volckens, 2008). For time keeping purposes, the instruments were synchronized with a timepiece.

2.3.1 Filter Papers for Particulate Collection

Airborne particulates were collected on Pallflex Air Monitoring Filters (T60A20 Fiberfilm membrane filters, Pall Corp., Putnam, CT). Prior to sampling and after sample collection, filters were placed in petri dishes (Brand Falcon, 60x15 mm, polystyrene, Becton Dickinson Labware, Franklin Lakes, NJ) and stored in an equilibration chamber (a vented plastic Tupperware container in a low humidity environment) for 6-24 hours prior to weighing. Filters were statically discharged and weighed with a microbalance (Model MX5, Mettler Toledo, Columbus, OH). Room temperature and humidity were recorded for each weighing session and relative humidity was maintained below 35% to prevent a humidity bias. The gravimetric limit of detection (LOD) for the filters was calculated as 3 times the standard deviation of repeated blank filter weighing. All sample masses were above the LOD (18 μg).

2.3.2 DustTrak (DT) I and II

A DT I (Model 5820 Aerosol Monitor, TSI Inc., Shoreview, MN) and DT IIs (Model 8530 Aerosol Monitor, TSI Inc., Shoreview, MN) were used to monitor fine particle exposure

from DPM at stationary positions at the EECL. These instruments are battery powered, portable laser photometers with real time data logging. The main difference with these models is that DustTrak I requires an external filter and DustTrak II has an internal filter for gravimetric calibration. The instruments were zeroed with a zero filter inlet and flow calibrated for 4 (DT I) and 3 (DT II) L/min, within 1 hr of use and logged mass concentration at 1-second resolution. The DustTrak was operated with a $PM_{2.5}$ impaction inlet for size-selective sampling. A Personal Environmental Monitor (PEM Monitor, 2.5 μm, 4 L/min, Indoor Air, SKC Corp., Eighty Four, PA) was fitted with a pre-weighed filter and co-located with the DustTrak I to provide a time-integrated sample for calibration of the direct-reading concentrations. After aerosol monitoring, the pumps were post-calibrated, the filter was removed for weighing, and logged real-time data were downloaded as mass concentration.

2.3.3 Personal Dataram (PDR)

PDRs (Model 1200 Aerosol Monitors, Thermo Electron Corp., Franklin, MA) were used to monitor fine particle exposure from DPM on roving pathways and at stationary positions. This instrument is a battery powered, portable photometer with real time data logging (1-second resolution). The instruments were fitted with an external personal sampling pump (Model 400, BGI Inc., Waltham, MA) and $PM_{2.5}$ impaction inlets. The pumps were pre-calibrated at 4 L/min within 2 hrs of use. They were loaded with pre-weighed filter papers behind the aerosol sensing region for time integrated sampling. Filters were removed for weighing, the pumps were post-calibrated, and logged real-time data were downloaded as mass concentration.

2.3.4 Particle Size Distribution

Particle size distribution for DPM was determined at approximately 5 m from the particle source at the EECL with two instruments, an Optical Particle Sizer (OPS) and a Nanoscan

Scanning Mobility Particle Sizer (SMPS). First, the OPS (Model 3330, TSI Inc., Shoreview, MN) is a battery powered and portable unit measuring size distribution over the particle diameter range of 0.3-10 μm in up to 16 channels and for concentrations up to 3000 particles/cm^3. Second, the SMPS (Model 3910, Nanoscan SMPS Nanoparticle Sizer, TSI Inc., Shoreview, MN) is also battery powered and portable, estimating size distribution for particle diameters between 10 nm and 400 nm at maximum concentrations at 1,000,000 particles/cm^3. Both instrument pumps were auto-calibrated and the flow rate was verified within 2 hours of use.

2.3.5 Aerosol Photometer Calibrations

Individual PDR and DustTrak calibration factors (CF) were tested and refined in an aerosol chamber with a particle source, having a similar refractive index to elemental carbon (EC), (Urban Dust Mist SRM1649B, National Institute of Standards and Technology (NIST), Gaithersburg, MD) on two occasions, March 22th and May 1st of 2013. The aerosol chamber was a cube constructed of sealed Plexiglas, enclosing a space of 1 m^3 with flow-regulated gas inlets and ventilation. A small fan was used to spatially homogenize particle concentrations in the chamber. The PDRs and DustTraks were operated in the aerosol chamber. A nebulizer was used to disperse urban dust mist for approximately 4 hrs and aerosol concentrations were changed in a step-wise manner covering the range of measured values. After aerosol monitoring the filters were removed for weighing and logged real-time data were downloaded.

At the EECL, all particle-monitoring instruments were collocated for 20 minutes at the end of the sampling period. Because the PDR and DustTrak instruments have different responses, we calibrated these units by first normalizing each unit's mass concentration by the TWA filter mass. The gravimetric adjustment substantially improved agreement between the

units. Next, a daily calibration factor was added to all units such that each measured the same average concentration during the 20 minutes the instruments were collocated at the EECL.

2.4 Vibration Monitoring Equipment

Vibration samples were obtained in the PMF office with an accelerometer (Model - 353B03 ICP®, PCB Piezotronics, Depew, NY) and pre-amplifier connected to the SLM base instrument (System 824A, Larson Davis, Provo, Utah). The accelerometer-SLM system was set to record absolute vibration at third octave band frequencies at 1-second resolution. Building vibration and WBV analysis typically considers the frequencies between 1-80 Hz by third octave bands, because these frequencies include those to which human beings are the most susceptible. However, this instrumentation was limited to measuring frequencies between 12.5-80 Hz. Acceleration was measured in dB and then converted to units of m/s^2 with method variability of $\pm$ 2 dB using Equation 4 (Larson Davis, 2004):

$$\text{RMS Acceleration } (m/s^2) = 9.806 \times 10^{((\text{Leq}-(-4.577)-167)+40)/20} \qquad \text{Equation 4}$$

For each axis orientation, if third octave band (1-80Hz) RMS acceleration is greater than or equal to the TLV, the TLV is exceeded for that exposure. The axis orientation with the greatest third octave spectral peak determines the permissible exposure. Crest factor (CF) is defined by the ratio of peak to root mean squared (RMS) acceleration in a single direction for any axis. CFs with values greater than 6 should be used with caution based on their tendency to underestimate impinging vibration (ACGIH, 2001b).

2.5 Hazard Mapping with Measurements from Direct Reading Instruments

In this section, techniques for sampling at stationary positions and on roving pathways with personal dosimeters will be discussed. Methodologies for extraction for individual roving

samples from logged concentrations will be related. Spatial geostatistical techniques (universal Kriging) for creating hazard maps with high representativeness will be summarized.

2.5.1 Roving Sampling with Personal Noise Dosimeters

Before the commencement of roving sampling for area survey, an irregular sampling grid was established along accessible areas of the facility. Personal dosimeter microphones and/or PDR inlets were mounted at shoulder height in the sampler's hearing and/or respiratory zones. Relative location was monitored in the PMF facility with a Lufkin 4 inch ABS Plastic and Aluminum Measuring Wheel and in the EECL with premeasured tape indicators and a measuring wheel. Along these predetermined pathways, roving sampling data were collected by a three step process as follows: first, the sampler stops at a location, recording the sample start time on the spreadsheet at the corresponding predetermined location entry; second, the sampler waits the allotted sampling duration; and third, the sampler moves to the next location, repeating the steps from the beginning until the sampling is finished.

2.5.2 Stationary Sampling with Personal Noise Dosimeters

Area noise surveys were also conducted with personal dosimeters and particle photometers at constant, static positions for partial work shifts. In PMF Production, personal noise dosimeters were mounted on music stands at hearing zone height (approximately 1.5 m). In the EECL, noise and particle meters were mounted at variable, recorded heights, as dictated by available space. Start and stop times were recorded with dosimeter-synchronized time pieces.

2.5.3 Roving Pathway and Stationary Position Selection Criteria

Stationary position selection was based primarily on the amount of available monitoring equipment, accessibility (spatial and work interference), and judgment decisions based on known or prediction of hazard sources, i.e., increased sampling resolution with increasing proximity to

expected hazard sources. Roving pathways were predetermined according to specified spatial resolution, accessibility (spatial and work interference), and judgment decisions based on prediction of hazard sources and extent. Under best conditions these measurements would be collected randomly with a statistically significant number of samples. In practice this is difficult due to the constraints of time, money, equipment, and accessibility. As such, all of our hazard data sets were collected as irregularly gridded data, requiring subsequent interpolation to a regular grid for hazard mapping.

Measurement error for completeness of the hazard measurements was an issue during pathway and position selection for data hazard mapping. In terms of completeness, roving data may only have high completeness for the sampled period (low temporal resolution), which is misrepresentative of full exposures (low completeness for the whole exposure period). To increase completeness, roving pathways should be sampled on multiple occasions during exposure periods (higher temporal resolution). Pre-survey interviews with employees may be useful for scheduling sampling times to capture anticipated exposure events. For stationary measurement, completeness is much higher for exposures in the vicinity of the sample location (high temporal resolution) but is likely to decrease with distance from sampled locations (low spatial resolution). The only way to increase completeness for stationary data is to increase the spatial resolution (more stationary sampling positions). For exposures that vary considerably in time and space, sampling over multiple sessions at new, unsampled positions will increase completeness (Koehler and Volckens, 2011).

2.5.4 Spatial Data Extraction from Roving Sampling

Logged roving measurements were downloaded from the dosimeters as time series CSV files. The MATLAB script was used to extract individual measurements from these files based

on recorded start times and known sample durations. An example of the script is listed in Section 7.1 of the Appendix. Spatially resolved measurements were produced by combining the extracted measurements with time-specific location coordinates for hazard mapping.

2.5.5 Hazard Mapping

In the present study universal Kriging (UK) was utilized to create interpolated hazard maps, increasing accuracy and reducing errors of representiveness, which may lead to mischaracterization of hazards. Kriging is a geostatistical estimator for predicting (interpolating) values at unobserved locations based on a weighted combination of observed values at nearby locations. For UK, a trend surface model is applied based on observed, spatially-resolved values with the difference between the trend surface and observed values resulting in residual values. The goal of UK is to estimate values that are the best linear unbiased predictions of the residual values at observed locations. UK is accomplished by fitting experimental variograms to the residual values to capture the spatial dependence in the data and estimating optimized weights for subsequent interpolation (Reich and Davis, 2008).

Variograms are used to describe spatial dependence as a function of distance and direction between points. The plotting of the squared difference of the values between two points versus the distance that separates them results in an experimental variogram. Experimental variogram plots of spatially correlated data tend to have a number of features in common. They tend to originate from the origin with variogram values generally increasing with distance (i.e., points that are closer together are more similar than points that are further apart). Typically, a variogram value plateau will be reached with increasing distance. The variogram value of the plateau is called the sill and the corresponding distance is called the range parameter (limit of spatial dependence). If the variogram value is not equal to zero at distance zero (i.e., two values

measured at the same location are not identical), this value is called a nugget effect parameter and is often interpreted as measurement error. Nugget effect, sill and range parameters can be estimated visually or automatically with iterative fitting from the experimental variograms (Reich and Davis, 2008 and Li and Heap, 2008). These optimized model parameters are used to describe spatial dependence of residual error for selection of the best trend surface model by lowest Akaike information criterion with correction (AICC) value. The AICC value denotes the relative quality of statistical models, penalizing for additional parameters. Automatic contouring is then utilized to create a hazard concentration field that is overlaid on a floor plan to create a hazard map (Reich and Davis, 2008 and Koehler and Volckens, 2011).

Interpolated values are usually less variable than sampled values because the interpolated values are a function of nearby weighted measurements. This may result in underestimation of variability and misleading quantitative values (errors of representativeness). Hazard mapping from roving pathways tends to only have high spatial representativeness for the sampled periods, which may not be representative for whole exposures, resulting in misleading information. Hazard mapping for stationary positions only have high temporal representativeness in the vicinity of sampled positions. Representativeness tends to decrease with increasing distance from sampled positions. All hazard maps were produced using the free statistical package R ("The R Project for Statistical Computing", 2013). An example of R codes utilized for creating the hazard maps is listed in Section 7.2 in the Appendix.

2.6 Hazard Mapping in the PMF Production

Two unique film production processes with different noise characteristics were sampled in PMF Production. The first process (Process I) was sampled on June 27th (day 1), June 29th (day 2), and December 10th (day 3) of 2012. The second process (Process II) was sampled on

July 13th (day 1) and July 30th (day 2) of 2012. Hazard mapping was conducted in PMF Production with 2 roving and 18 static dosimeters. Roving measurements were collected along three predetermined pathways in PMF Production (Figure 2.2). Samples were collected at approximately 1-meter resolution for 10-seconds per location. We expect that 10 seconds is sufficient to capture current noise levels as Royster *et al.* (2003) recommended sampling for a minimum of 5 seconds to capturing steady state noise levels at least 10 times for each work area throughout the day. The first pathway started in the south-eastern corner of the room and then followed a western course staying approximately 0.5 m from the southern wall. The second pathway started in the south-eastern corner of the room and then followed a western course staying approximately 0.5 m from the southern side of the machine. The third pathway started in the north-eastern corner of the room and then followed a western course staying approximately 0.5 m from the northern side of the machine. Start times for each 10-second sampling period were noted on a spreadsheet with dosimeter-synchronized time pieces.

Stationary sampling was conducted in PMF Production for noise hazard mapping with noise dosimeters mounted on music stands at a height of 1.5 m. Eighteen personal noise dosimeter DRIs were placed at corresponding positions to the north and south at 1 m distance from the machine with spatial resolutions of 15-meters. Start and stop times were recorded on a spreadsheet with dosimeter-synchronized time pieces. Sampling durations exceeded half shifts but did not cover full shifts. Preliminary tests showed that floor vibration through the music stand did not influence sound pressure levels measured by the dosimeters.

2.7 Occupational Hazard Exposure Monitoring at the PMF

Due to limited access to noise and vibration monitoring instruments, PMF representatives requested that we conduct an occupational assessment for hazardous exposures to workers in

three areas of the PSM facility. First, we conducted an occupational noise assessment around the PMF machine with personal dosimetry and noise hazard mapping. Dose and TWA (8 hr), under ACGIH and OHSA noise exposure criteria, were calculated in PMF Production to determine regulatory compliance with OSHA and the risk for workers developing NIHL. Second, we monitored noise and vibration levels in the PMF office to characterize potential hazards for workers. Third, we evaluated the effectiveness of current noise reduction engineering controls in the PR area with SLM area surveys. Based on our measurements we offered recommendations to control or prevent hazardous exposures to workers at the PMF.

2.7.1 Personal Noise Exposure PMF Production

Employee personal noise surveys were conducted by the PMF industrial hygiene staff for Process I on June 27th (day 1) and 29th (day 2) and for Process II on July 15th (day 1) and 30th (day 2) of 2012. Employees working in PMF Production with five different job titles (Leader, Casting, Finishing, Windup, and Quality) wore Larson Davis Spark Model 703 dosimeters for full and partial 12 hr shifts to determine noise exposure. De-identified data were then shared for use in this investigation. Excel was used to create exposure time series graphs for each worker dose, as shown in Appendix 7.3 with Figures 7.1-7.20.

An area noise survey was conducted for Process I in PMF Production with a SLM on day 3. Measurements were taken on all sides of the machine at a distance of 1 m. Two measurements were obtained on the eastern and western sides of the machine. Measurements were taken on the northern and southern sides of the machine at 10-meter intervals moving from east to west. Noise exposure was evaluated in three protective noise enclosures around PMF Production. Sampling duration was at least 10-seconds for all measurements. Hazard mapping was conducted to identify sources and areas of concern in PMF Production.

2.7.2 Occupational Noise and Vibration Exposure in the PMF Office

Office noise area survey measurements were taken strategically at multiple positions with a SLM instrument. Sampling duration was at least 60-seconds for all measurements in the office area.

PMF Production is a high vibration environment. Vibration originates from the machine in the center of the room. Employees in the northern office area are also exposed to the vibration. A vibration survey was conducted in the office area with an accelerometer-SLM system instrument to estimate the levels of WBV, where vibration was perceived to be strongest from worker complaints. The accelerometer was securely affixed to vibrating surfaces (tiles or walls) with wax. For floor samples on carpet, a thin plastic tile was affixed with tape to the carpet and the accelerometer was secured to the tile with wax. Measurements from carpet taken in this manner may be subject to higher error than those from tile and walls. Samples were taken for at least 1 min at each position. Measurements were downloaded with Larson Davis 824 Utility software as CSV files. Third octave band measurements were converted to vibration acceleration measurements by Equation 4.

2.7.3 Occupational Noise Exposure in the PMF PR Area

Three measurements were obtained with a SLM to determine the effectiveness of noise engineering controls in the PR area. Leq values and third octave band intensities were collected for at least 30-seconds at each position. Larson Davis 824 Utility software was used to obtain Leq values and third octave bands in the form of CSV files for evaluation of noise controls.

2.8 Hazard Mapping at EECL

Noise and fine aerosol monitoring was conducted in the EECL on March 21st (day 1) of 2013. On July 12th (day 2), only noise monitoring was possible due to scheduled engine run-

times below the gravimetric LOD for the filters. On day 1, the only major identifiable sources of DPM and noise were emitted from the engine on the west side of the northern room. The DT I, four DT IIs, a PDR, the OPS, the SMPS, and seven noise dosimeter DRIs were placed around the northern room at stationary positions (Figure 2.3). A DT II, three PDRs, and thirteen noise dosimeter DRIs were placed around the Southern room at stationary positions. Stationary sampling heights varied by necessity and were recorded. Sampling durations exceeded half shift but were not full 8 hr shifts.

On day 1, roving samplers were fitted with a noise dosimeter microphone affixed to a collar in the hearing zone and a PDR aerosol monitor inlet held near the respiratory zone. Distances were monitored with pre-measured tape labels and individual roving samples were taken for 15-seconds at each pathway position for noise and aerosol measurements. Start times for each position were noted on a spreadsheet. In the northern room, three separate roving pathways were selected running from west to east at 1-meter resolution. In the southern room three roving pathways were selected. Two roving pathways ran north to south with 1.6-meter resolutions on both sides of the engines, while a single path ran from west to east at 1.2-meter resolution between the 1st and 2nd engines from the top. Two samples were also obtained between the 3rd and 4th engines.

On day 2, the only major identifiable source of noise was emitted from the third engine from the top in the southern room. Sixteen noise dosimeter DRIs were placed at stationary positions in the southern room, and two noise dosimeters were placed in the northern room at stationary positions. These positions were sampled for 2.5-3 hrs (almost full engine run times). Roving samplers were fitted with a noise dosimeter with the microphone clipped to the collar in the hearing zones. Distances were monitored with pre-measured tape indicators and a rolling

distance wheel. Two roving pathways were established in the southern room running from north to south at 2-meter resolutions at approximately 1.5 m from the western and eastern side of the four engines. Random roving samples were obtained throughout the northern room and between engines in the southern room. The roving pathway traverses were sampled during engine run time three times at 1-minute durations and finally once at 15-second durations. Stationary and roving sampling positions for day 1 and 2 are displayed in Figure 2.3. Measurements with a SLM were taken simultaneously on the last roving noise dosimeter traverse at 15-second intervals for comparison of instrumental accuracy between SLM, roving noise dosimeter, and stationary noise dosimeter DRI measurements with close proximity.

2.9 Statistical Analysis

Summary statistics and side-by-side boxplots allowed relative comparison of measurements from the PMF and EECL. Tests of normality were conducted on these measurements and log-transformed measurements with QQ plots and Shapiro-Wilk (SW) normality tests. Temporal and spatial hazard variability was assessed by examination of Leq time series and cumulative frequency distributions (CFD) from stationary (static) noise dosimeter locations. Occupational noise exposure was explored with noise hazard mapping to locate noise sources and areas of concern for noise hazards. Relative similarity of hazard maps by sampling technique was determined by comparison of overall mean Leq for hazard maps, pairwise mean squared difference (MSD) between maps, and plots of the percentage of location-paired interpolated values with differences greater than the indicated values between maps. Overall mean Leq was calculated by summing all interpolated map values and dividing by the number of values for each map. MSD was calculated by location-pairing corresponding interpolated values from maps and subtracting them. Subtracted values were squared and divided by the number of

location-paired values. This average of squared differences gave an estimator of overall difference between maps to compare relative similarity. Percent differences were calculated by dividing the absolute value of subtracted location-pairs between hazard maps by the largest value of the pair to yield a percent difference for each interpolated location pair. The percentage of location paired interpolated values with percent differences greater than indicated values from 1-15 % were calculated and plotted to show how the percentages changed between hazard maps. To validity the novel sampling technique, differences in instrumental accuracy between personal noise dosimeters ($\pm$ 2 dBA) and the SLM ($\pm$ 3 dBA) were determined by comparing measurements taken at the same time in close spatial proximity from a pilot study in the EECL.

3 Results

This section will describe measurements collected during noise, aerosol, and/or vibration exposure assessment with DRIs at the PMF and/or EECL.

3.1 Area Survey Measurements

Equivalent sound pressure level (Leq) noise and mass concentration aerosol measurements from area surveys were listed as summary statistics (Table 3.1) and side-by-side boxplots for comparison of relative noise intensity levels and measurement distributions in the PMF and EECL. Leq values for PMF Production Process I were taken with stationary dosimeters, roving dosimeters, and a SLM instrument. Means (83-86 dBA) and median (84-86 dBA) values were nearly identical with similar spreads and approximate symmetry, as shown in the boxplots of Figure 3.1, indicating normal distribution. Normality was also observed in QQ plots and Shapiro-Wilks (SW) test before and after log-transformation. For PMF Process I, Leq measurements were also collected with a SLM in the office and PR areas. Relative noise intensity levels were highest in the PR area (mean 95 dBA) with heavy right skew, corresponding to the measurement at 1 m from the PR machine. Noise intensity levels were lowest in the office area (mean 69 dBA) with left skew from a mild outlier, corresponding to one of the samples farthest from the southern wall (noise source).

Leq measurements for PMF Production Process II were only taken with stationary dosimeters and roving dosimeters. Mean (83-84 dBA) and median (83-83 dBA) values were similar with approximate symmetry, as shown in the boxplots of Figure 3.1, indicating normal distributions. Normality was also observed in QQ plots and SW test before log-transformation.

Table 3.1: Summary statistics for noise and aerosol measurements from the PMF and EECL are displayed.

Location	Type or Day	Data Source	Mean Leq dBA	Standard Deviation	Median Leq dBA	Samples (n)
PMF	Process I	Stationary Production	83	4.4	84	18
		Roving Production	86	3.2	86	134
		SLM Production	83	3.3	84	28
		SLM Office	69	2.8	70	10
		SLM PR	95	6.9	92	4
	Process II	Stationary Production	83	4.9	83	18
		Roving Production	84	4.6	85	134
EECL	Day 1	Stationary	78	5.8	76	19
		Roving	81	8.5	85	108
	Day 2	Stationary	94	3.6	94	17
		Roving	94	4.7	96	41
		SLM	96	4.9	94	40

Location	Day	Data Source	$PM_{2.5}$ Mean Mass Concentration mg/m^3	Standard Deviation	$PM_{2.5}$ Median Mass Concentration mg/m^3	Samples (n)
EECL	1	Stationary Aerosol	0.08	0.011	0.079	8
		Roving Aerosol	0.095	0.025	0.072	73

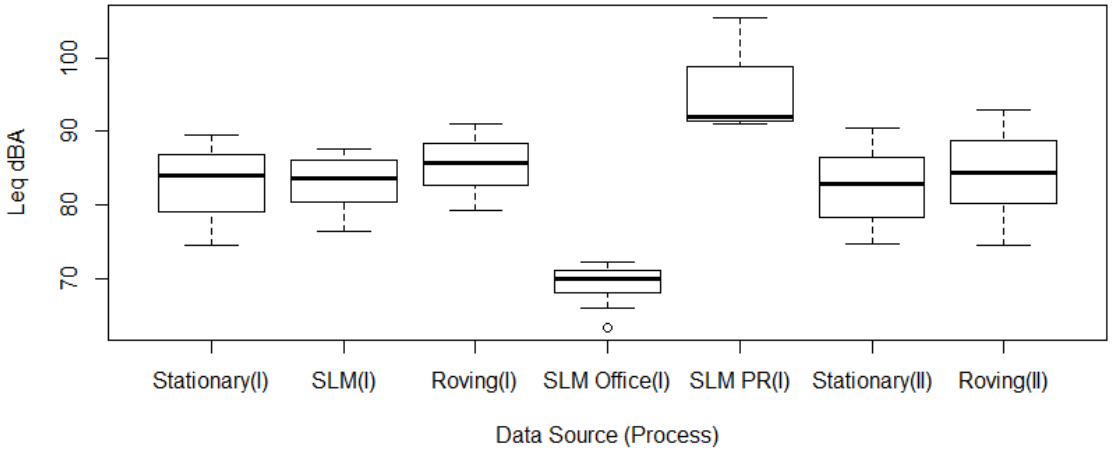

Figure 3.1: Boxplots of Leq values for noise measurement at the PMF are displayed. On the x-axis, Stationary (I) refers to stationary noise dosimeter Leq measurements around the PMF machine for Process I, SLM (I) refers to SLM Leq measurements around the PMF machine for Process I, Roving (I) refers to roving Leq measurements around the PMF machine for Process I, SLM Office (I) refers to SLM Leq measurements in the office for Process I, SLM PR (I) refers to SLM Leq measurements around the PR machine for Process I, Stationary (II) refers to stationary noise dosimeter measurements around the PMF machine for Process II, and Roving (II) refers to roving noise dosimeter measurements around the PMF machine for Process II.

Leq measurements for EECL day 1 were taken from noise area surveys with stationary and roving dosimeter instruments and from fine particulate matter ($PM_{2.5}$) area surveys with stationary and roving aerosol photometers. For noise sampling, Leq measurement means (78-81

dBA) and medians (76-85 dBA) were similar but less symmetrical with widely varying spreads, as displayed by Figure 3.2. Different Leq ranges were caused by differences in spatial sampling resolution. Roving sampling was completed at high spatial resolution so a wider array of maximum and minimum measurements were observed; whereas, only the limited number of personal noise dosimeters were available for stationary positions, resulting in more limited observation of high and low noise intensity levels. QQ plots and SW tests failed to indicate normality even after log-transformation. Although, noise measurements were expected to have normal (or log-normal) distributions, high variability in noise intensity levels over time (see Section 3.3 for more details) may have resulted in sampling from many different non-overlapping normal distributions that did not cumulatively exhibit normality even after log-transformation of collected measurements.

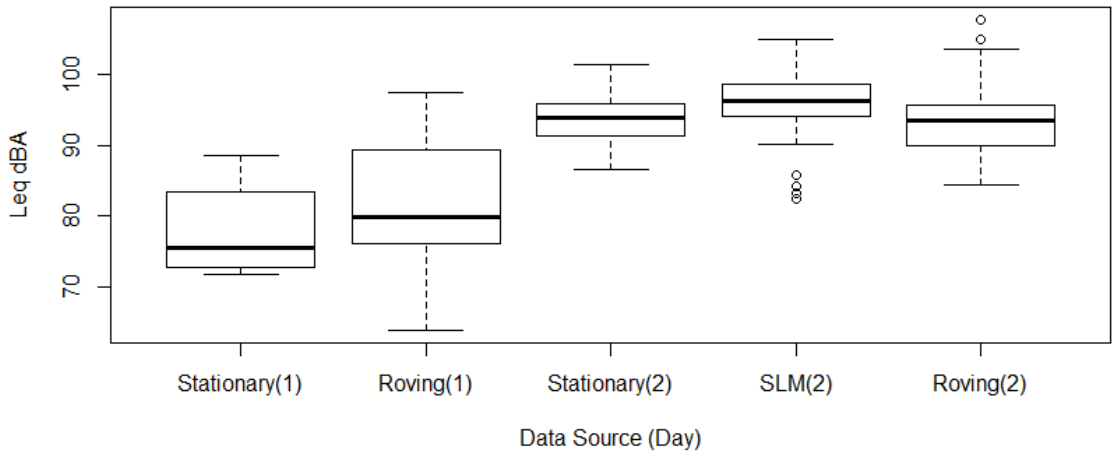

Figure 3.2: Figure 3.2: Boxplots of Leq values for noise measurements in the EECL are displayed. On the x-axis, Stationary (1) refers to stationary noise dosimeter Leq measurements at the EECL on day 1, Roving (1) refers to roving noise dosimeter Leq measurements at the EECL on day 1, Stationary (2) refers to stationary noise dosimeter Leq measurements at the EECL on day 2, SLM (2) refers to SLM Leq measurements at the EECL for day 2, and Roving (2) refers to roving noise dosimeter Leq measurements at the EECL on day 2.

For $PM_{2.5}$ aerosol sampling at the EECL for day 1, stationary and roving measurement means (0.08-0.095 mg/m^3) and medians (0.072-0.079 mg/m^3) were similar but had widely varying spreads, as shown in Figure 3.3. As was the case for noise data, differences in variability

were likely dependent on spatial resolutions between numerous roving and limited quantity stationary measurements. QQ plots and SW tests did not exhibit normal distributions until after log-transformation.

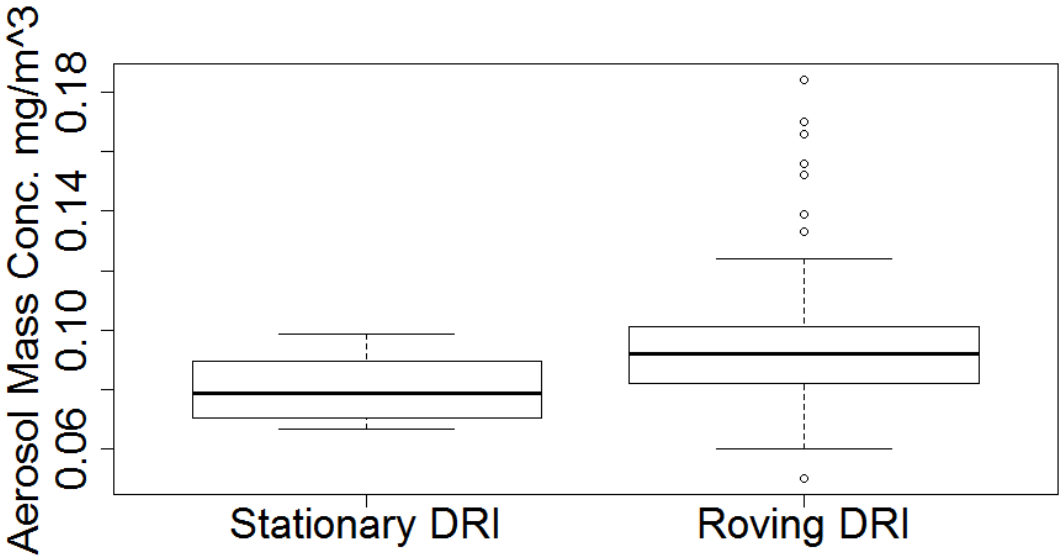

Figure 3.3: Boxplots of mass concentrations values for PM2.5 measurements in the EECL are displayed. On the x-axis, Stationary DRI refers to stationary aerosol monitor measurements at the EECL for day 1, and Roving DRI refers to roving aerosol monitor measurements at the EECL for day 1.

Only noise sampling was conducted for EECL day 2 with stationary dosimeter, roving dosimeter, and SLM instruments. Leq measurement means (94-94 dBA) and medians (94-96 dBA) (Figure 3.2) were similar with symmetric spreads from stationary dosimeters exhibiting normal distributions by QQ plots and SW testing and with non-symmetric spreads from roving dosimeters and SLMs not exhibiting normal distributions even after log-transformation.

3.2 Temporal and Spatial Variability from Stationary Monitors

Leq time series and cumulative frequency distributions (CFD) from stationary dosimeters were plotted to assess temporal and spatial variability of noise intensity levels for PMF Production Process I and II and EECL day 1 and 2 in Figures 3.4 and 3.5. Based on analysis of

CFD plots, it was determined that strong variability with location but very little temporal variability at any given location (steeply sloped curves) was present for PMF Production Process I and II. Plotted lines were offset from each other, representing conserved spatial variability in average Leq throughout the facility. Thus for measurements at the PMF, it appears reasonable that even Leq values with low temporal resolution (short sampling duration) would still be representative of full work shifts, providing maps with high completeness.

For EECL day 1 and 2, researcher analysis of time series indicated strong variability both temporally and spatially. For EECL day 1, there was likely more than one distinct noise source because the CFD lines, representing different sampling locations, crossed one another. There was also high temporal variability because the CFD curves had shallow slopes. For EECL day 2 CFDs, lines were offset from one another but had shallowly sloped curves, indicating high temporal variability from a single source. At the EECL, Leq values with decreasing temporal resolution may be less representative of whole exposures. Thus stationary noise dosimeter measurements with high temporal resolution would likely result in maps with high temporal completeness in close proximity to sampled locations, and roving noise dosimeter and SLM measurements with lesser temporal resolution would likely result in maps with less temporal completeness, as they were misrepresentative of whole exposures.

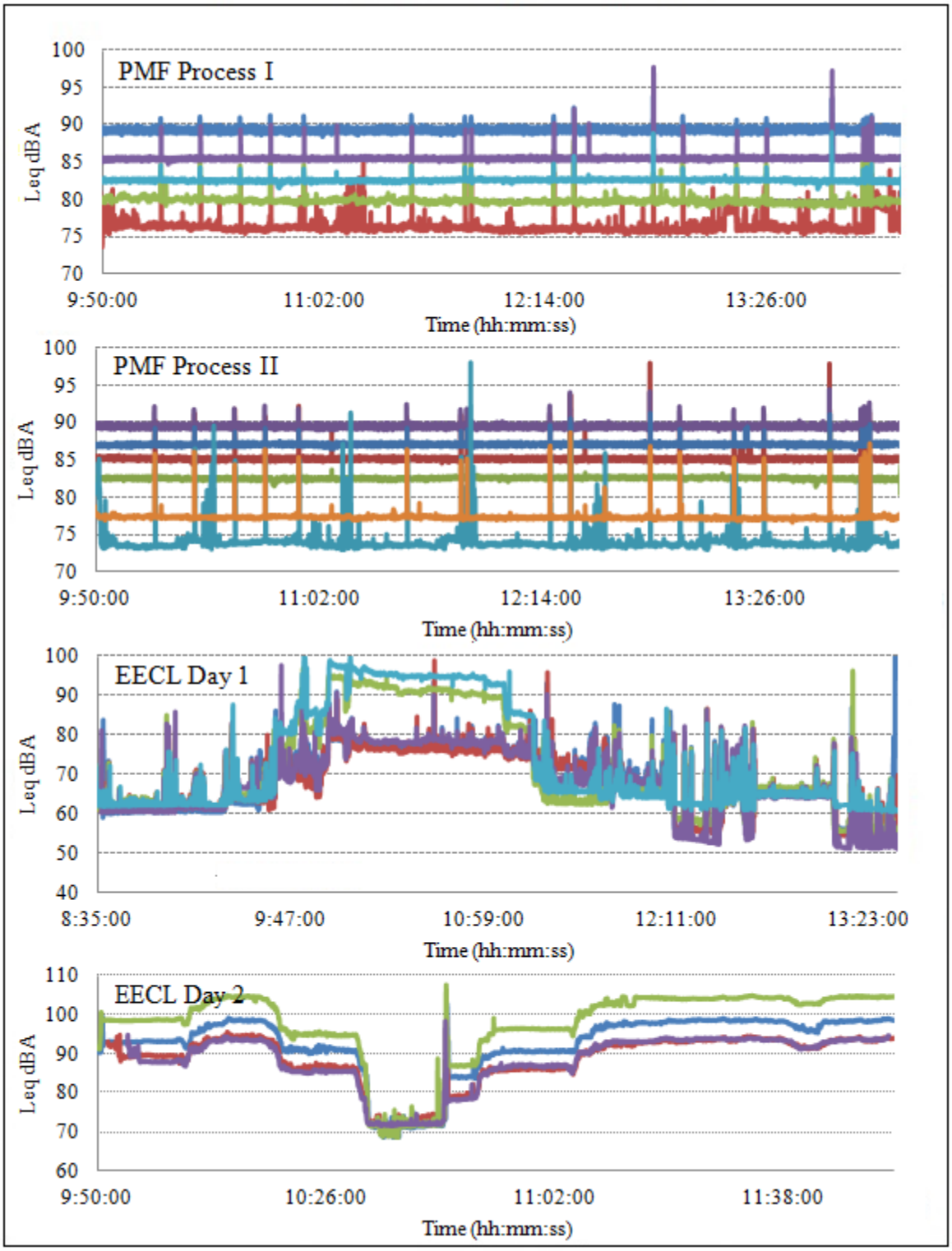

Figure 3.4: Representative Leq time series from several stationary dosimeter positions are displayed from top to bottom for PMF Production on Process I, PMF Production on Process II, the EECL on day1, and the EECL on day 2.

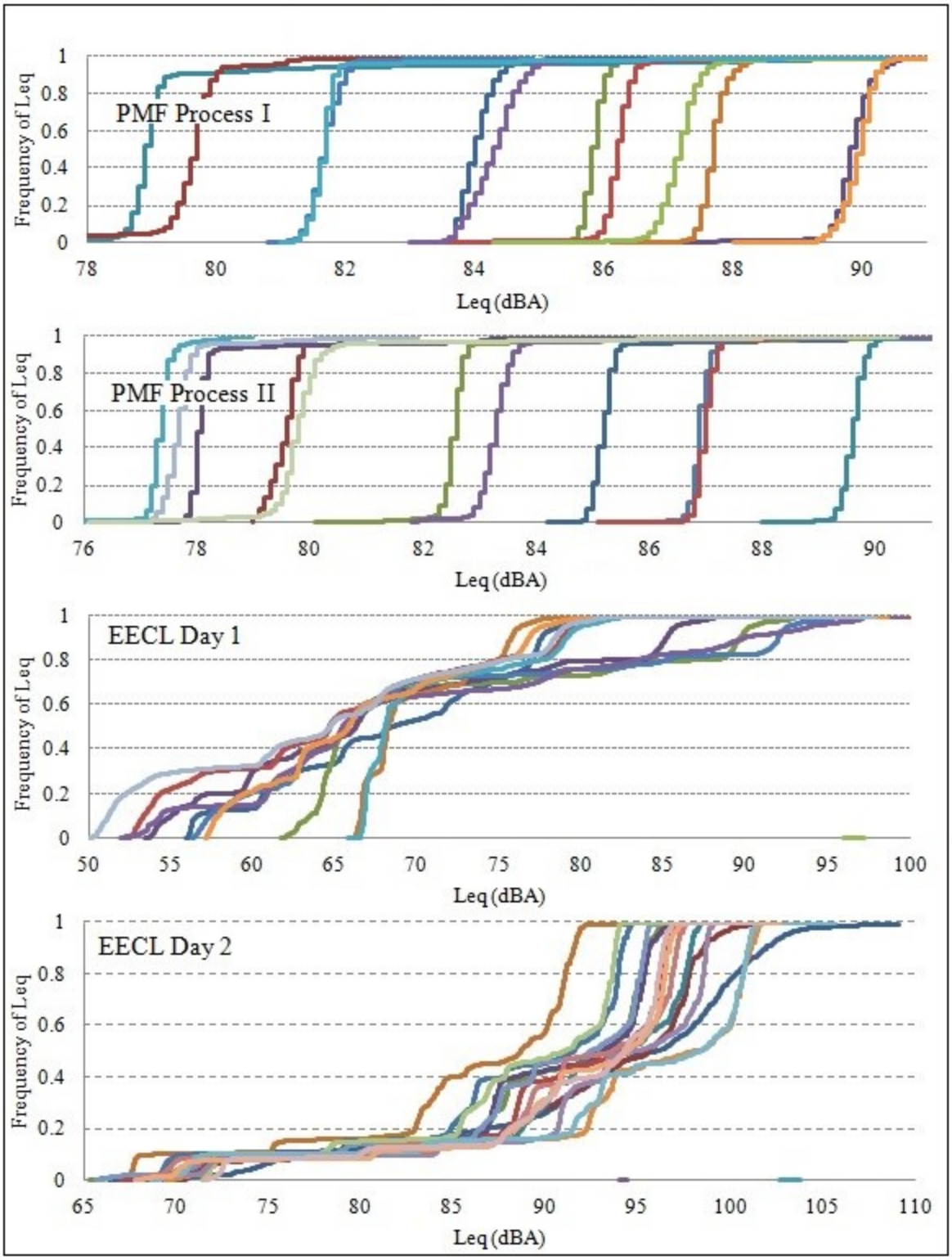

Figure 3.5: CFDs for Leq data from representative stationary dosimeter positions are displayed from top to bottom for PMF Production on Process I, PMF Production on Process II, the EECL on day 1, and the EECL on day 2.

3.3 Noise Hazard Mapping

After noise sampling in PMF Production over several days, spatially resolved Leq measurements were created for hazard mapping of noise intensity to identify noise sources and the spatial extent of exposures. For PMF Process I, hazard mapping of noise intensity levels was conducted with SLM, stationary and roving dosimeter instruments, as displayed in Figure 3.6 following the Kriging methods outline in Section 2.6. Roving noise dosimeter measurements were observed with the highest spatial resolution at 1 m sampling intervals. This resolution was reduced to 3 m by selecting every 3rd point while mapping due to computational limitations. Replicate roving Leq measurements over day 1 and 2 in PMF Process I were averaged as mean Leq values for roving maps. SLM noise samples were recorded with 10-m spatial resolution over a single-traverse and mapped as Leq values for SLM maps. Replicate stationary dosimetry noise samples were averaged over day 1 and 2 as mean Leq values and recorded with 15-m spatial resolution for stationary maps. Hazard concentration gradients from all three maps were qualitatively similar in identifying two areas, west and central, in PMF Production with relatively higher sound pressure levels (SPL). Leq measurements from stationary, SLM, and roving methods resulted in hazard maps with maximum values of 88, 87, and 88 dBA in the west area and 90, 88, 92 dBA in the central area respectively.

For PMF Production Process II, hazard mapping of noise intensity was conducted with stationary and roving dosimeter measurements, as displayed in Figure 3.7. Replicate roving dosimeter Leq values were averaged over day 1 and 2 and spatial resolution was again reduced from 1- to 3-m for mapping by selecting every 3rd measurement. Replicate stationary dosimetry noise samples were averaged over day 1 and 2 was mean Leq values and recorded with 15-m spatial resolution

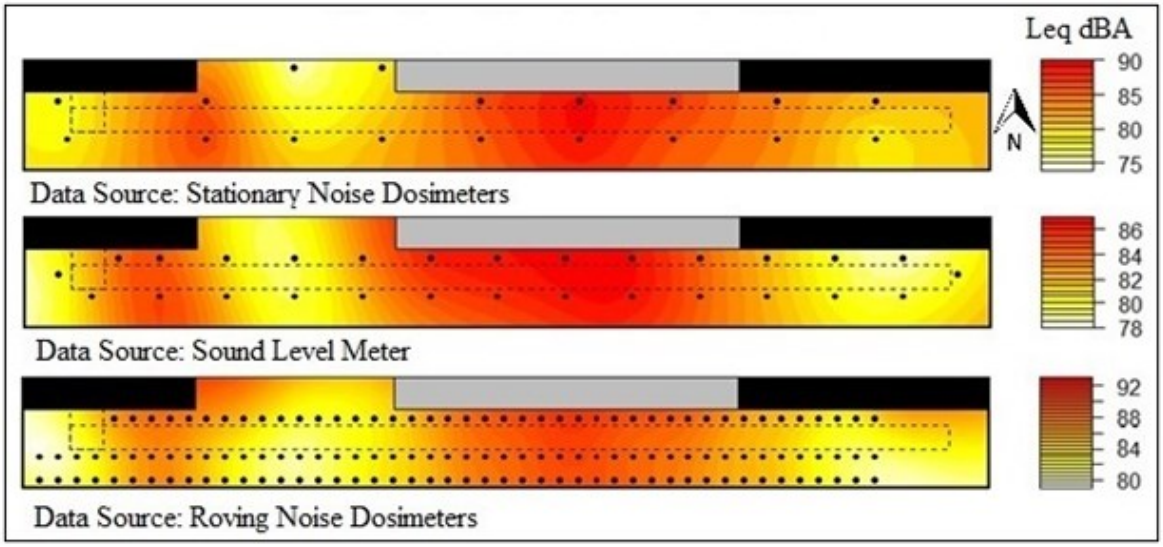

Figure 3.6: Noise hazard maps of PMF Production for Process I display sampling positions with dot symbols from top to bottom for stationary dosimeter, SLM, and roving dosimeter data.

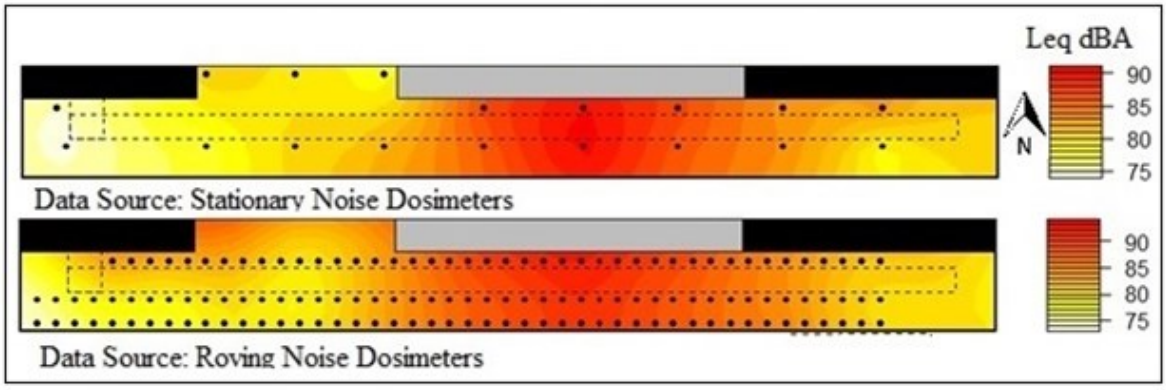

Figure 3.7: Noise hazard maps of PMF Production for Process II display sampling positions with dot symbols from top to bottom for stationary dosimeter and roving dosimeter data.

for stationary mapping. Only a single area near the center was revealed with a relatively higher noise intensity level (90 dBA) from the stationary map. The western area, where high noise intensity levels were observed for Process I, only had noise intensity levels around 80 dBA. For Process II, two areas, western (86 dBA) and central (92 dBA), were revealed from the roving map with relatively higher noise intensity levels.

Researcher analysis of all hazard maps for Process I and II with the exception of the stationary map for Process II indicated similar spatial distributions of noise, identifying west and central areas in exceedance of OSHA's action level (≥ 85 dBA), if employees were exposed for 8

hrs, and represented high risk noise hazards for NIHL over time. Process II Leq measurements from the west area had noise intensity levels 2-6 dBA lower than maps for Process I.

For EECL day 1, noise hazard mapping was conducted with stationary and roving dosimeter data, as displayed in Figure 3.8. Replicate measurements from roving pathways (four traverses) were averaged and mapped as mean Leq values. Two areas, the Northwestern Engine and Southwestern Corner, were identified with relatively higher noise intensity levels. Direct comparison of Leq time series with stationary dosimeters in close proximity to the two noise sources, as displayed in Figure 3.9, revealed that they had distinctly different noise patterns. Maximum Leq values were estimated from stationary and roving maps around 90 dBA by the Northeastern Engine and around the low 80 dBA range by the Southeastern corner. The noise source in the Southeastern corner was later identified as originating from a crane conducting construction activities directly outside the building.

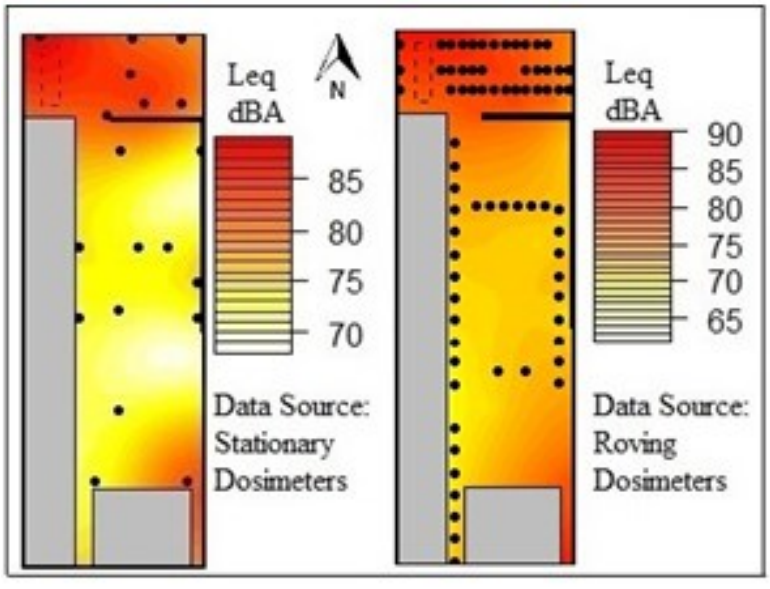

Figure 3.8: Noise hazard maps of the EECL for day 1 display sampling positions from stationary and roving dosimeter data from left to right with dot symbols. The dashed box indicates the location of the active engine.

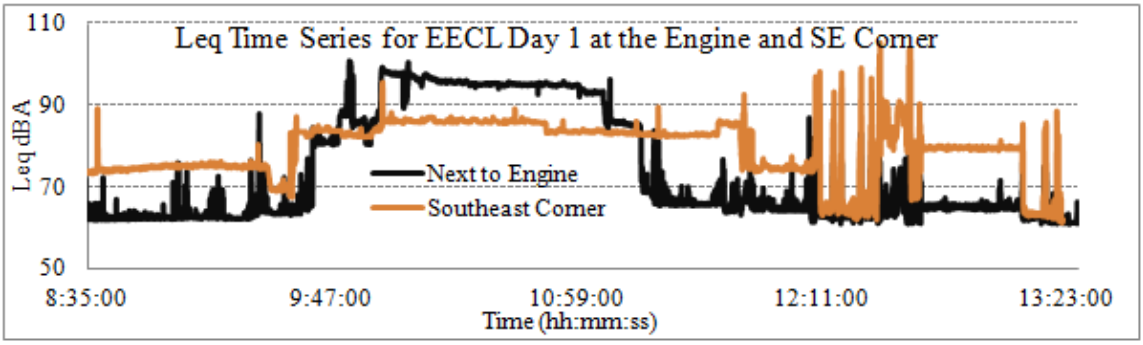

Figure 3.9: Leq time series from stationary dosimeter positions comparing noise sources at the active engine and southeastern corner of the EECL.

Two errors of representativeness were observed while hazard mapping of noise intensity levels at the EECL for day 1. Rather than displaying smooth noise intensity level gradients, two low noise intensity areas (two white patches, ‹ 70 dBA) were created during mapping in the eastern upper and middle parts of the southern room. These low intensity areas were likely artifacts of universal Kriging in regions far from measurements and are unlikely to be representative of the actual noise intensity levels.

For EECL day 2, noise hazard mapping was conducted with SLM, stationary and roving noise dosimeters. Replicate measurements from roving pathways (four traverses) were averaged and mapped as mean Leq values. These maps are displayed in Figure 3.10. Observations from all three maps were qualitatively similar in identifying the region around the southern active engine in the EECL with a relatively higher noise concentration. Maximum Leq measurements of 101, 105, and 108 dBA were identified next to the Southern Engine from stationary dosimeter, SLM, and roving dosimeter maps, respectively. Leq measurements for all positions in the northern and southern rooms exceeded OSHA's action level (≥ 85 dBA), if employees were exposed for 8 hrs, and represented high risk noise hazards for NIHL overtime.

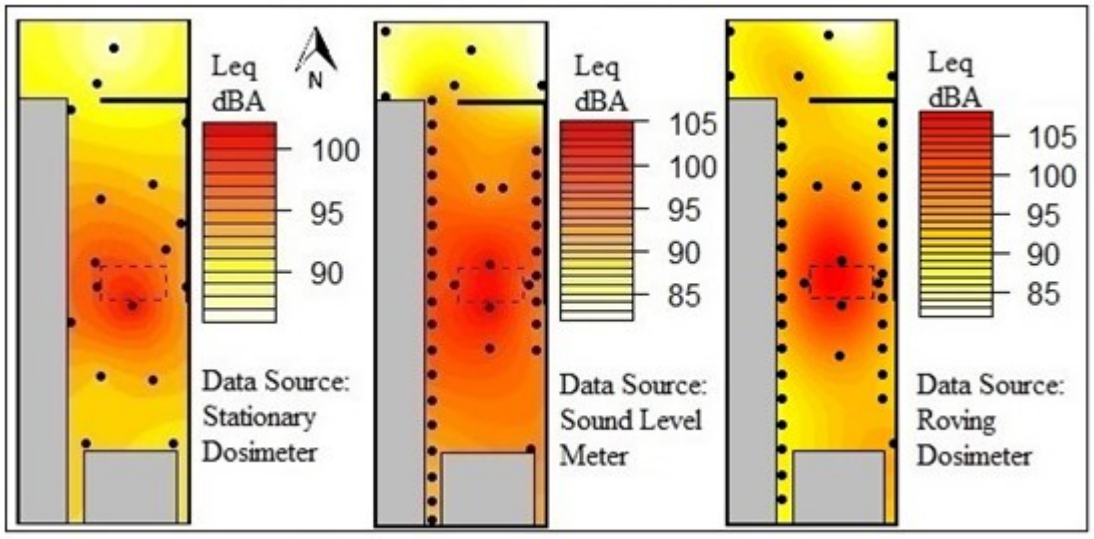

Figure 3.10: Noise hazard maps of the EECL day 2 display sampling positions from stationary dosimeter, SLM and roving dosimeter data from left to right with dot symbols. The dashed box indicates the location of the active engine.

3.4 Noise Area Surveys

Area surveys were conducted at PMF Production for Process I and II (see Appendix 7.4, Figures 7.21-7.23 and Tables 7.1-7.3), the Production protective noise enclosures and the office for Process I (Figure 7.24 and Table 7.4), the PR area for Process I, and the EECL for day 1 and 2 (Figures 7.25-7.27 and Tables 7.5-7.7). Considering the large sample sizes with roving data sets for PMF Production Process I and II and EECL days 1 and 2, noise area surveys were not listed. In general for measurement sets with Leq values exceeding the OSHA action limit, time allowed to full dose was calculated by Equation 2.

Noise area surveys were conducted in PMF Production at noise protective enclosures to determine their effectiveness and the office area to characterize noise intensity levels with a SLM on day 3. None of the samples from the PMF enclosures or office were observed to exceed the OSHA action level (85 dBA) for Leq values (Figure 7.24 and Table 7.4), resulting in low-medium risk for hearing loss if employees were exposed for 8 hrs.

A noise area survey and octave band analysis was conducted in the PMF PR area with a SLM on day 3 to determine the effectiveness of existing engineering controls (partial barrier). The partial barrier was constructed with Sound Stopper Modular Acoustic Screens (Singer Safety Company, part # 22-310148) in a sealed continuous series. The partial barrier enclosed the PR machine on the northern and eastern sides. The partial barrier was approximately 3.6 m from the floor with an approximate 1 m opening on top filled with a network of wires and piping. The screens were rated by sound transmission class with an overall SPL reduction of 25 dB and by noise transmission loss for a SPL reduction by frequency of 10 dB at 500 Hz, 16 dB at 250 Hz, 23 dB at 500 Hz, 28 dB at 1000 Hz, 31 dB at 2000 Hz, and 37 dB at 4000 Hz (Singer, 2013). A noise sample was first obtained at 1 m (106 dBA) distance south from the PR machine (the only accessible side), two samples were obtained in the northern hallway with the screens closed (91 dBA), and then another sample was obtained with the screens open (92 dBA) to determine if there was a difference between overall and individual frequency Leq values. Considering instrumental accuracy of $\pm$ 1 dB, an overall noise reduction from the acoustic screen on the other side of the barrier was not observed. All Leq values exceeded the OSHA action limit ($\geq$85dBA), if employees were exposed for 8 hrs, requiring the implementation of an HCP. Third octave band analysis was performed as displayed in Figure 7.30. Expected individual frequency noise reductions were not observed. Differences between closed and open screens frequency bands outside the enclosure were not observed to differ except at 160 Hz, where a 3.6 dB reduction was observed.

3.5 Personal Noise Dosimetry in PMF Production for Process I and II

Personal noise dosimetry samples were collected for five job titles (Leader, Casting, Finishing, Windup, and Quality) during PMF Production Process I (day 1 and 2) and II (day 1

and 2) by the industrial hygiene staff. A representative personal noise Leq time series is displayed in Figure 3.11. The remaining personal dosimetry figures are displayed in the Appendix as Figures 7.1-7.20. While no TWA (8 hrs) exceeded the OSHA PEL, the ACGIH TLV was exceeded by 80 % of TWA (8 hr) for Process I and 30% for Process II, as displayed with boxplots in Figure 3.12. Dosimeter calculated exposure results are listed in Table 3.2.

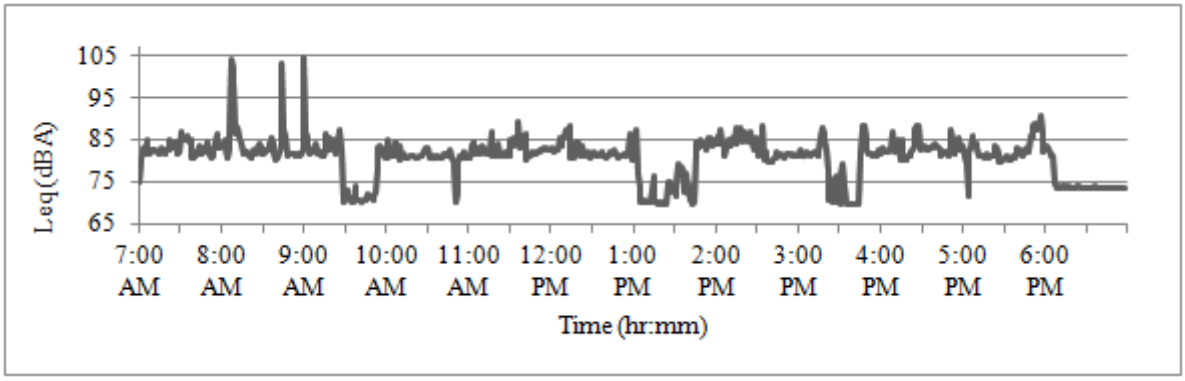

Figure 3.11: A representative Leq time series from the personal dosimetry of Casting worker is displayed for PMF Process I (Day 1).

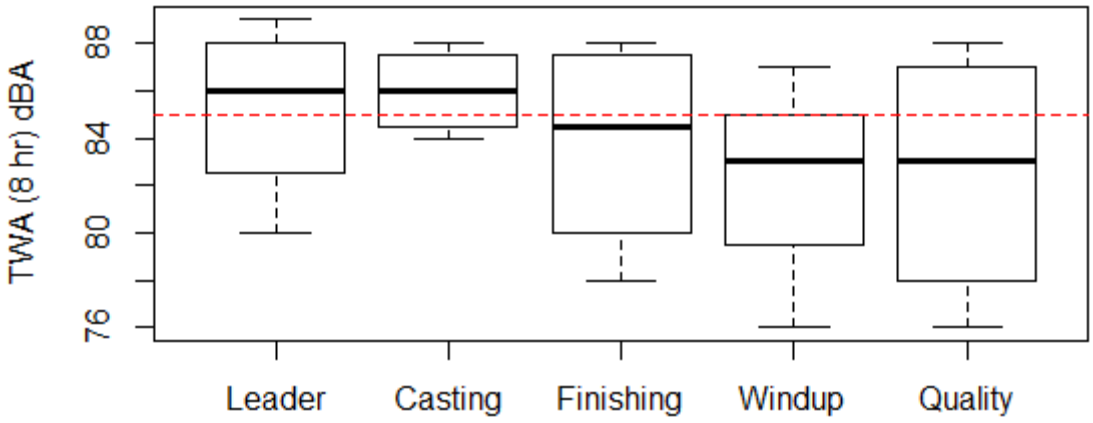

Figure 3.12: Boxplots of personal noise dosimetry under ACGIH criteria for PMF Production workers from Process I and II are displayed by job title. The ACGIH TLV (85 dBA) is displayed as a dotted red line in the figure.

Table 3.2: Personal noise exposure for PMF Production workers was determined with personal noise dosimeters over two days each for Process I and II under OSHA and ACGIH noise exposure criteria.

				OSHA Criteria		ACGIH Criteria	
Entry	Job Title	Process (Day)	Sampling Time hr	Dose (8hr) %	TWA (8 hr) dBA	Dose (8hr) %	TWA (8 hr) dBA
1	Leader	I (1)	12	26.3	80	99.7	85
2	Leader	I (2)	7	51.8	85	241.8	89
3	Leader	II (1)	9.1	28.1	81	35.2	81
4	Leader	II (2)	12	33.1	82	146.5	87
5	Casting	I (1)	12	47.3	85	141.8	87
6	Casting	I (2)	10.9	54.6	86	209.1	88
7	Casting	II (1)	9	43.4	84	73.1	84
8	Casting	II (2)	12	44.9	84	96.4	85
9	Finishing	I (1)	12	56.1	86	210.8	88
10	Finishing	I (2)	12	49.3	85	160.3	87
11	Finishing	II (1)	9	23.8	80	26.8	80
12	Finishing	II (2)	12	17.1	77	52.9	82
13	Windup	I (1)	12	50.3	85	151.3	87
14	Windup	I (2)	12	32.1	82	60.1	83
15	Windup	II (1)	9	23	79	25.5	79
16	Windup	II (2)	6.8	21.6	79	60.2	83
17	Quality	I (1)	12	6.6	70	13	76
18	Quality	I (2)	12	49.6	85	189.5	88
19	Quality	II (1)	8.6	28.7	81	37.8	81
20	Quality	II (2)	12	18.4	78	121.2	86

TWA (8 hr) values exceeding the TLV (85 dBA) under ACGIH criteria are shaded.

3.6 Third Octave Bands Analysis

A SLM was used to conduct third octave band analysis in PMF Production for Process I, the PMF office area, the PMF PR area (refer back to Section 3.4 for details), and the EECL day 2. Third octave bands for PMF Production during Process I were obtained by averaging individual bands for all SLM positions in the area (Figure 7.29). Noise in this area was broadband in the high 70 dBA region for low and middle frequency bands, which are less hazardous than high frequency (Ward *et al.*, 2003). High frequency bands dropped gradually with increasing frequency. For the PMF office during Process I, third octave bands were

obtained by averaging individual bands for all SLM positions in the office (Figure 7.30). Noise in this area was broadband in the low 70 dBA region for low frequency bands. Medium and high frequency bands dropped sharply with increasing frequency. Third octave bands for EECL day 2 were obtained by averaging individual bands surrounding the engine at 1 m distance on all four sides (Figure 7.32). Noise in this area was broadband in the high 90 dBA region for middle and high frequency bands. For very high and low frequencies SPLs dropped off gradually.

3.7 Whole Body Vibration (WBV) Area Survey for the PMF Office

An area survey for the PMF office was conducted for WBV with an accelerometer-SLM base system as displayed in Figure 3.13. One sample (position 1) was collected in PMF Production for comparison with the nine samples (positions 2-10) taken in the PMF office area. Leq values were converted to Peak Acceleration and RMS Acceleration values with crest factors (CF). The highest third octave band frequency was selected for comparison with the WBV ACGIH TLV as listed in Table 3.3. While the sample from PMF Production was close to exceeding the ACGIH TLV, none of the samples from the PMF office directly exceeded the TLV. However, three of the samples (positions 2, 6, and 8) had CF much greater than 6, which may still have the potential to exceed the TLV due to underestimation of WBV exposure (ACGIH, 2001b).

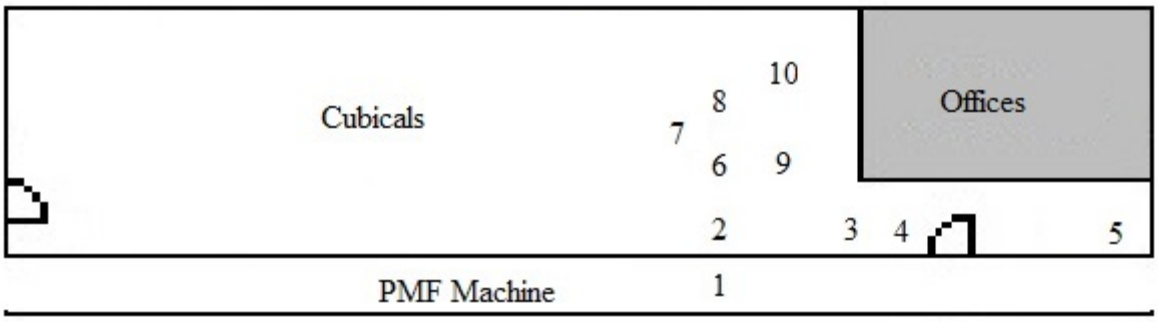

Figure 3.13: The WBV area survey of the PMF office for Process I from accelerometer data is displayed.

Table 3.3: WBV exposure from area survey for the PMF office during Process I is listed. Axis X, Y, and Z refer to wall, support beam, and floor mounts, respectively.

		Highest Third Octave Band				ACGIH	
Position	Axis	Leq dBA	Frequency hz	Peak Acceleration m/s^2	RMS Acceleration m/s^2	TLV WBV m/s^2	Crest Factor (Peak/RMS Acceleration)
1	X	79.7	12.5	62.37	8.22	12.5	7.6
2	X	33.1	63	55.59	0.038	63	1445
3	X	36.8	63	0.076	0.059	63	1.3
4	X	32.4	63	0.04	0.035	63	1.1
5	X	26.2	63	0.025	0.017	12.5	1.5
6	Y	38.9	31.5	21.88	0.075	31.5	291
7	Z	28.3	63	0.028	0.022	22.4	1.3
8	Z	34.7	63	18.84	0.046	22.4	407
9	Z	33.3	31.5	0.042	0.039	11.2	1.1
10	Z	36	31.5	0.058	0.054	11.2	1.1

3.8 Occupational Exposure to DPM at the EECL

3.8.1 DPM Hazard Mapping

$PM_{2.5}$ mass concentration measurements were collected with one roving and nine stationary aerosol photometers at the EECL on day 1 to approximate DPM exposure. Roving samples were collected for 15 s. $PM_{2.5}$ concentrations from stationary and roving aerosol photometers were interpolated for hazard mapping as displayed in Figure 3.14. For stationary measurements, highest particle mass concentrations were observed in the northwestern corner of the northern room near the active diesel engine. Concentrations decreased in the eastern direction perhaps due to ventilation from the open windows along the northern side of the room. Concentrations remained high in the northern half of the northern room, decreasing in the eastern and southern directions. Brief welding activities in the southern room were not detected. For roving measurements, the highest particle mass concentrations were detected in the northern room to the east of the active engine. Concentrations decreased to the north toward ventilation provided by open windows. In the southern room, concentrations were highest on the northern

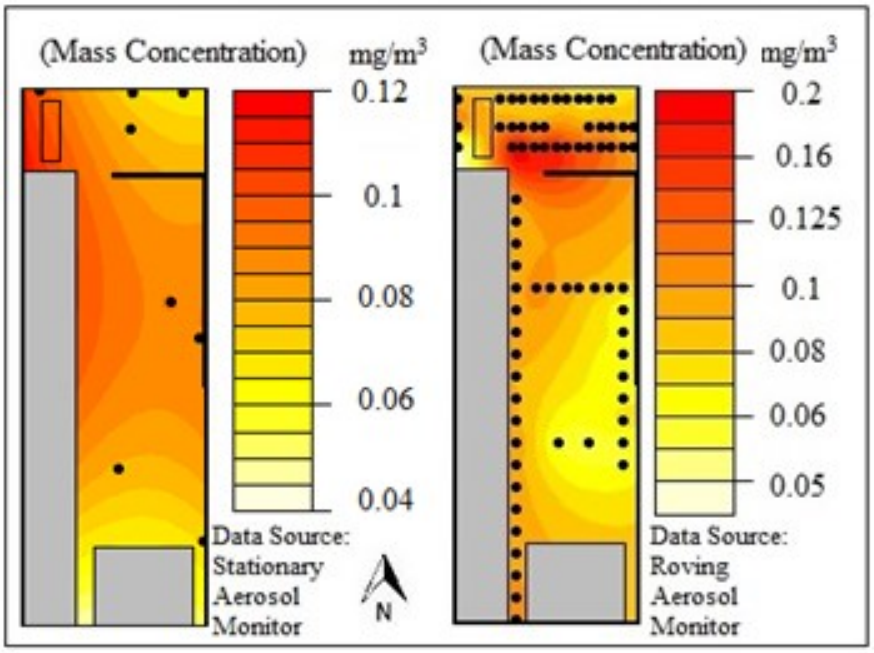

Figure 3.14: Diesel Particulate Matter (PM2.5) Hazard Map of EECL for day 1 displays Stationary and Roving aerosol monitor data with dot symbols.

and western sides of the room. Concentrations decreased in the middle of the room on the east side and then increased again moving south. It was unknown, if increased concentrations in the south of the southern room was being caused by brief welding activities, ventilation air currents, or errors of representativeness from universal Kriging.

3.8.2 $PM_{2.5}$ Area Survey

$PM_{2.5}$ Area survey was conducted with nine aerosol photometers as displayed by Figure 7.28. Sampling times and optical mass concentrations are listed in Table 7.8. Considering the large sample size (n=73) for roving aerosol data, area survey results were not listed. For details on this data set, refer to summary statistics in Table 3.1, $PM_{2.5}$ hazard mapping in Figure 3.14, and comparative boxplots in Figure 3.3.

3.8.3 $PM_{2.5}$ Size Distributions

Particle size distributions were monitored at approximately 5 m distance from the active engine in the northwest corner of the EECL on day 1. A Nanoscan SMPS was used to monitor

particle sizes from 10 to 350 nm. These data are displayed in Figure 3.15 as a bar graph with mean concentration and standard error bars. An OPS was used to monitor particle sizes from 0.3 to 10 µm. These data are displayed in Figure 3.16 as a bar graph with mean concentration and standard error bars. For combined measurements from both instruments count median diameter (CMD) was 31.6 nm and geometric standard deviation (GSD) was 2.1 nm calculated from an aerosol size distributions cumulative probability plot (not displayed).

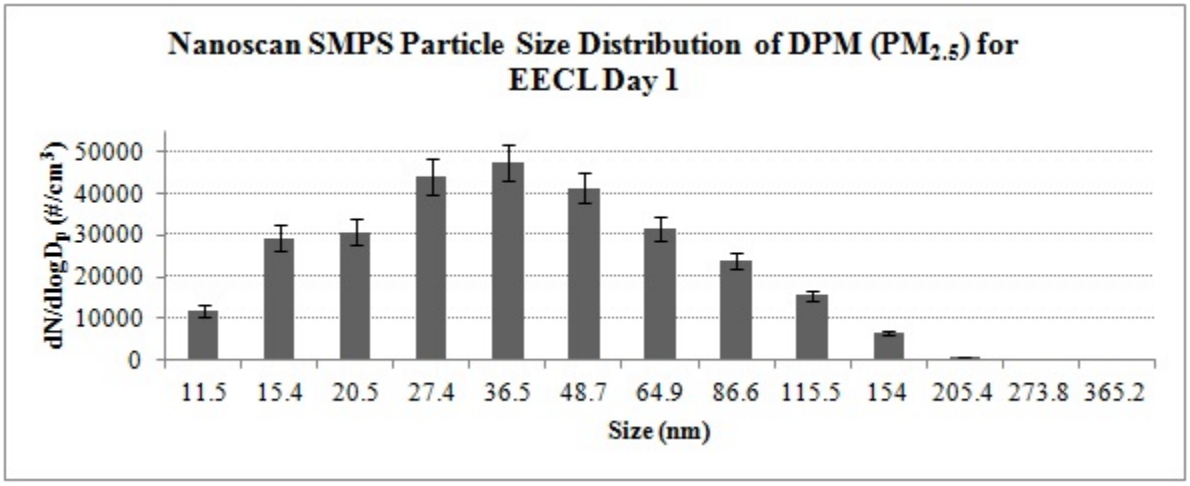

Figure 3.15: Bin normalized particle size distributions (dN/dlogDp) from 9.6 nm to 411 nm with standard error bars from Nanoscan SMPS data are displayed for PM2.5 at 5 m from diesel engine on day 1 in the EECL.

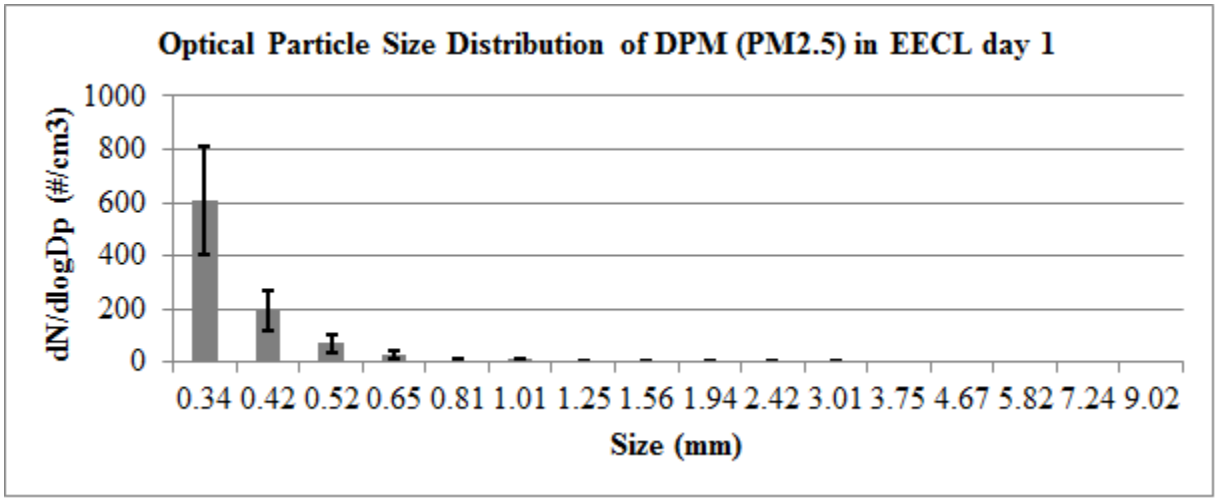

Figure 3.16: Bin normalized particle size distributions (dN/dlogDp) from 300 nm to 10 µm with standard error bars from OPS data are displayed for PM2.5 at 5 m from diesel engine on day 1 in the EECL.

4 Discussion

4.1 Hazard Mapping with Direct Reading Instruments

Hazard maps have been demonstrated as a powerful tool for identifying and communicating environmental and occupational hazard sources (Fischer *et al*., 200; Peters *et al*., 2006) and the spatial extent of hazards to evaluate engineering controls and protect human health (Dasch *et* al., 2005; Murphy and King, 2010; O'Brien, 2003; Ologe *et al*., 2006; Pollice and Locinio, 2010; Seong *et al.*, 2011). Novel sampling techniques were developed with common, lower cost direct reading instruments (DRIs) to generate hazard maps. The representativeness and similarity of the maps generated with different sampling techniques will be discussed with qualitative and quantitative comparisons at locations with low (PMF) and high (EECL) temporal variability.

The DRIs utilized in the development of these novel techniques are generally associated with determination of personal worker exposures to hazards (personal noise dosimeters, personal aerosol photometers) for comparison with regulatory occupational exposure limits (OELs). These instruments had the advantages of being low in cost, size and weight. Stationary (static) positions had the advantage of enabling sampling for whole work shifts, offering high completeness for mapping at the sampling location. Comparison of time series and cumulative frequency distributions among stationary positions facilitated understanding of how these exposures change over space and time (Figures 3.4 and 3.5). Sampling methodologies on roving pathways had the advantages of providing measurements with both high spatial and moderate temporal resolutions, when sampling was conducted frequently over pathway traverses all throughout work shifts.

Based on analysis of measurements from novel personal DRI techniques and single-traverse SLM, it was determined that similar results were obtained between the instruments, when personal DRIs were temporally averaged over the process type (PMF) or day (EECL). This conclusion was in agreement with the work of Valoski *et al.* (1995), which found no significant differences between type II or better personal noise dosimeter and SLM measurements. While measurements from single-traverse SLM measurements techniques did not offer information on how noise intensity levels changed over time, comparison of stationary positions and measurement time series revealed a high level of homogeneity for noise intensity levels over time at any given position in the PMF. At the EECL, researcher analysis of stationary measurements indicated high variability in noise intensity levels over both time and space. In other words, Leq not only varied with respect to distance but also over time corresponding to engine acceleration gradients and unexpected mechanical failures at the EECL. This knowledge was useful in rationalizing departures from normal distributions for noise measurement in the EECL due to high noise variability over time.

While some variation was observed in maps concerning quantitative spatial extents of hazard concentrations, maps based on each data collection method allowed successful qualitative identification of major sources of hazards and general areas of concern. These hazard maps yielded similar results for both novel personal DRI techniques and single-traverse SLM measurements. For EECL day 1 with stationary measurements, patchy areas of uncharacteristically low noise intensity levels could be attributed to issues with universal Kriging (errors of representativeness) and a lack of measurements in the area (errors of completeness). The only map that failed to identify a hazard source and area of concern occurred with stationary dosimeter measurements on the western side of the PMF Production area for Process II (Figure

3.7, top display). This identification failure occurred for two reasons. The first reason was an error of completeness based on a sampling position location. When comparing position 2 from area surveys for Process I (see Figure 7.21) and Process II (see Figure 7.22), the sampling location for Process II position 2 was shifted to the northernmost boundary around a corner, decreasing its ability to detected hazardous noise intensity levels in the west area. The second reason was an overall reduction in noise intensity around the west area between Process I and II. Comparison of overlapping west positions resulted in a 2 to 6 dBA reduction for Process II, resulting in decreased ability of positions 2 and 11 in Figure 7.22 to detect hazardous noise intensities in the west area.

The relative similarity of noise hazard maps generated with different data collection techniques were assessed to consider completeness based on spatial and temporal sampling resolutions from facilities with noise sources that demonstrated high and low temporal variability. The goal here was to assess exposures to compare against regulatory thresholds; thus, all measurements were temporally averaged. Relative similarity was calculated by comparison of the pairwise mean squared difference (MSD) between whole hazard maps (Table 4.1). Plots of the percentage of location-paired interpolated values with differences greater than the indicated values were displayed for the PMF (Figure 4.1) and EECL (Figure 4.2).

At the PMF, noise intensities were homogeneous over time, so sampling techniques with low temporal resolution were still very representative of whole work shifts. Under these circumstances, techniques with similar sampling plans (spatial resolutions) would be expected to result in more similar hazard maps. This trend was observed with SLM (10 m resolution) and stationary (15 m resolution) sampling techniques being the most similar with a MSD of 4.2 in Table 4.1 and the lowest plotted curve for Process I in Figure 4.1. Stationary to roving (3 m

Table 4.1: MSD results are listed for differences between whole noise hazard maps from sampling techniques at the PMF and EECL.

PMF MSD				
Process I			Process II	
	Roving (86 dBA)	Stationary		Roving (85 dBA)
Stationary (83 dBA)	14.3	-	Stationary (82 dBA)	12.0
SLM (83 dBA)	16.9	4.2		

EECL MSD				
Day 1		Day 2		
	Roving (76 dBA)		Roving (92 dBA)	Stationary
Stationary (76 dBA)	11.5	Stationary (93 dBA)	12.2	-
		SLM (94 dBA)	16.7	8.8

Values in parentheses correspond to overall means for interpolated values over the entire map.

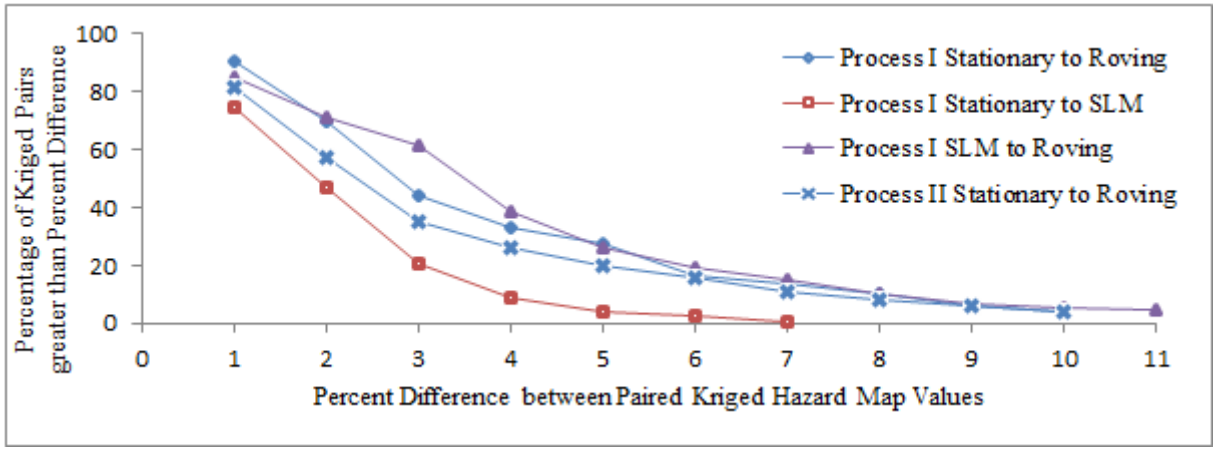

Figure 4.1: The cumulative distribution plots for the percentage of paired Kriged Leq values between PMF noise hazard maps with differences greater that the stated percent difference are plotted for Process I and II.

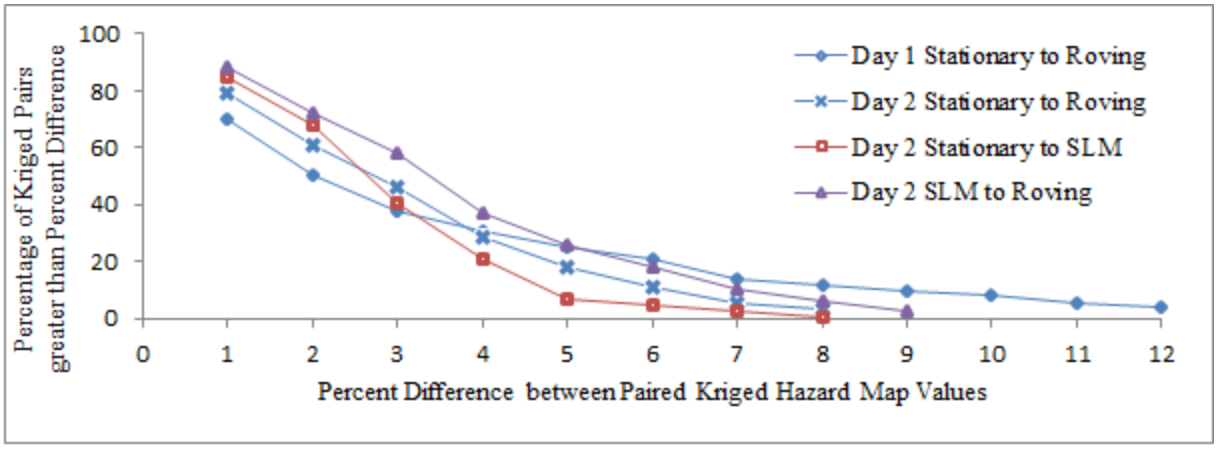

Figure 4.2: The cumulative distribution plots for the percentage of paired Kriged Leq values between EECL noise hazard maps with differences greater that the stated percent difference are plotted for day 1 and 2.

resolution) and SLM to roving sampling techniques for Process I had less similar hazard maps with MSDs of 14.3 and 16.9, respectively. Except for some slight variation in the 2-5 percent difference range, these plotted percent difference curves overlapped closely. Maps from Process II were even more similar between stationary and roving techniques with an MSD of 12. These findings support the trend that under homogenous noise intensities over time, similar spatial sampling techniques tend to result in more similar hazard maps. More complete hazard maps from low temporal variability noise sources can be speculated to result from sampling techniques with higher spatial resolutions.

Unlike the PMF, stationary noise dosimeter time series and CDF curves at EECL for day 1 and 2 revealed noise sources with highly variable noise intensities over time. Under such variable conditions, sampling techniques with similar temporal resolutions, perhaps more so than spatial resolutions, would be expected to yield more similar hazard maps and perhaps more complete maps. Thus, SLM hazard maps (15 sec resolution) would tend to be less similar than roving noise dosimeter hazards maps (3.25 min resolution), which would be in turn less similar than stationary noise dosimeter hazard maps (full engine run time resolution).

At the EECL for day1, hazard maps between stationary and roving dosimeters with a MSD of 11.5 were more similar than the corresponding day 2 maps with a MSD of 12.2. For day 1, the percent difference curve had a distinctly different shape from day 2 curves, which were all similar in shape. At the EECL for day 2, SLM and roving sampling positions with low temporal similarity were almost completely overlapping (similar spatial resolution) but resulted in the least similar hazard maps with a MSD of 16.7. SLM and stationary sampling positions had little spatial or temporal similarity but resulted in the most similar hazard maps with a MSD of 8.8. This effect was caused by high temporal variability in noise intensities over time at the EECL,

random chance concerning when the SLM sampling was conducted, and averaging of stationary measurements over the whole engine time and roving measurements over all traverses.

SLM sampling on day 2 was conducted simultaneously with the final roving noise dosimeter traverse, when noise intensities were at their highest levels. Since single traverse SLM measurements were not averaged with other lower intensity measurements, this resulted in the SLM hazard map having the greatest overall mean of 94 dBA for all interpolated values across the entire map (Table 4.1, values in parenthesis). Therefore, this overall SLM map mean was by chance more similar to the overall stationary map mean of 93 dBA, which collected measurements throughout the entire engine runtime, and least similar to the overall roving mean of 92 dBA, which collected some measurements during both the highest and lowest noise intensity levels before, during, and after the engine mechanical failure time period. If SLM sampling had been conducted before, during, or just after the engine mechanical failure, the resulting hazard maps would have likely been the least similar compared to stationary and roving hazard maps. Thus, these findings would not tend to contradict the stated trend that for environments with high noise intensity variability, sampling techniques with similar temporal resolutions, more so than spatial resolutions, tend to result in more similar hazard maps. More complete hazard maps from high variability noise sources can be speculated to result from sampling techniques with higher temporal and spatial resolutions with a stronger demonstrable effect when accounting for temporal resolution.

4.2 Comparison of Instrumental Accuracy

Since the novel personal DRI techniques had not been validated, we wanted to determine if measurements taken from static personal noise dosimeters, a roving personal noise dosimeter, and a SLM exceeded instrumental accuracy, when sampled at the same time in close spatial

proximity. On EECL day 2, the relative accuracy of these instruments was determined by comparing the variance of six groupings of measurements from SLM, roving, and stationary noise dosimeter instruments at sampling positions with close proximity (≤ 1.5 m) collected at the same time (see Figure 4.3). The SLM was held in the sampler's hand pointed toward the perceived source with a grazing angle (random-incidence microphone), while the roving noise dosimeter was worn at the sampler's collar. Thus, the SLM and roving dosimeter were within 1 m distance for all measurements, but the SLM was slightly closer to the noise source. The distance between the SLM and roving monitors and the stationary dosimeter positions ranged from 0.5 to 1.5 m. In 4 of 6 groupings, the sampler was closer to or between the noise source and stationary position. Stationary noise dosimeters at the EECL were located at variable heights (table tops, inactive engines, cabinets), where space was available without interfering with work activities (music stand usage was not possible as was done at the PMF).

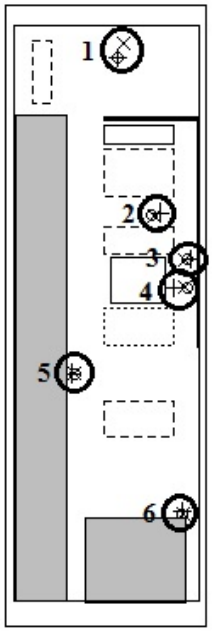

Figure 4.3: Comparison groupings of SLM (o signs), stationary dosimeters (+ signs) and roving dosimeters (x signs) direct reading instruments are displayed for EECL day 2.

Leq values measured by the SLM were greater than measures from the roving dosimeters at all grouped positions with differences ranging from 0 to 4 dBA, and Leq values from roving dosimeters were in turn greater than measurements from stationary dosimeters with differences ranging from 2 to 5 dBA. Measurement distances were least between SLM and roving measurements, so it followed that measurement differences were smallest between them and largest for stationary measurements. SLM measurements were always taken slightly closer to the source than the roving dosimeter with the microphone attached to the sampler's collar so it is unsurprising that SLM measurements were always greater than the roving measurements. Likewise, the sampler was almost always closer to or between the source and the stationary dosimeter so it followed that both the SLM and roving measurements were always greater than the stationary measurements. This was particularly true in close proximity to the noise sources, where distance has the greatest effect on changing sound pressure level.

While SLM to roving and roving to stationary average measurement differences fell within instrumental accuracy (3 dBA range), SLM to stationary average differences were greater than 2 times instrumental accuracy (6 dBA range). A MSHA study by Valoski *et al.* (1995) investigated type 2 SLM and dosimeter measurement based on body positions. When the SLM and dosimeter were separated by up to 1 m, mean differences were calculated as high as 4 dBA. When shoulder mounted dosimeters were blocked by the head from sources (body shadow), mean differences up to 6 dBA were calculated compared to reference measurements (body absent). Byrne and Reeves (2008) observed even higher differences around 8 dBA with microphones at non-standard positions such as the chest or ears. Based on the differences in spatial proximity and existing literature studies, the observed accuracy differences from this study were reasonable between stationary dosimeter, roving dosimeter, and SLM positions.

Investigations at the PMF and EECL had the limitation of only collecting single traverse SLM area surveys in the creation of spatially resolved measurements for noise hazard mapping. As such it was not possible to calculate sample means and standard deviations at individual positions for SLM measurements. Thus, this study was limited to comparing noise intensity levels between the instrumental sampling techniques only on the basis of map differences and instrumental accuracy rather than more rigorous statistical methods such as confidence intervals, t tests and analysis of variances (ANOVA). Future studies should examine hazard map and instrumental comparability further.

4.3 Occupational Noise and Vibration Hazards at the PMF

In this portion of the discussion, appropriate usage of noise protectors in PMF Production will be determined, occupational noise and vibration hazards will be evaluated in the PMF office, the effectiveness of engineering controls in the PMF enclosures and PR area will be determined, and occupational noise and fine particle hazards from diesel engines in the EECL will be evaluated.

4.3.1 Appropriate Noise Protector Usage in PMF Production

One of the most important questions that PMF industrial hygiene (IH) staff wished to answer in the PMF Production area was to determine if "required" hearing protection was necessary for workers in the area (for a floor plan see Figure 2.1a). Similar to the study by Ologe *et al.* (2006), determination of hearing loss and the potential for hearing loss were based on collection of evidence such as hearing loss testing, personal noise dosimetry, and noise hazard mapping of work areas. Prior to this research, the PMF Production area was under the control of a Hearing Conservation Program (HCP). Personal noise dosimetry had been conducted in the past and had not revealed any exceedance of the OSHA PEL by TWA (8 hr) for the workers in

the area. Yearly pure-tone audiometry testing had not revealed any cases of standard (STS) or temporary threshold shifts for permanent or temporary hearing loss with these workers. Hearing protector use at that time was not required for PMF Production workers. Several types of protectors were made readily available by IH staff for workers, and workers were observed using hearing protection regularly based on personal perceived risk.

Personal noise dosimetry was repeated by PMF IH staff with 5 job titles for Production Process I on days 1 and 2 and for Process II on days 1 and 2 during ongoing research sampling activities. The personal monitoring was utilized as part of the company's normal HCP to ensure that conditions had not changed since last tested and to determine the current risk for noise induced hearing loss (NIHL) by ACGIH criteria, which was not required for regulatory compliance and not considered in previous assessments. Workers were only identified by job title to researchers so only a few generalizations could be made about work habits and locations observed during actual worker activities. Most employees in PMF Production worked on the western side of the area near the end of the PMF machine in and around Enclosure position 1, as shown in Figure 7.24, with fewer employees working in and around Enclosure position 3. Employees with the Leader title were observed to work all throughout the area, and based on analysis of personal dosimetry time series plots, it was determined that the facility had high levels of temporal variability.

As was previously reported, none of the workers' TWA (8 hr) exceeded the PEL ($\geq$ 90 dBA) under OSHA noise exposure criteria for which the majority of people are expected to develop hearing loss over time. For Process I and II, 80 % and 30 % of workers' TWA (8 hr), respectively, exceeded the TLV ($\geq$ 85 dBA) under ACGIH noise exposure criteria for the development of NIHL over time (see Figures 3.13 and Tables 3.2). TWA (8 hr) for all job titles

exceeded the TLV for ACGIH criteria on at least one of the four days during personal sampling for Process I and II. Windup workers were least exposed to hazardous noise intensity levels with TWA (8 hr) only exceeding the TLV on one day during Process I. TWA (8 hr) for Quality and Finishing workers exceeded the TLV on two days. TWA (8 hr) for Leader and Casting workers exceeded the TLV on three days. Based on the high variability of these personal dosimetry results and the lack of specific information on work locations and habits, it was impossible to make a "required" hearing protector use decision by individual job title. Based on measured TWA (8 hrs), it was determined that there was a high risk for development of NIHL during Process I and a lesser, but still substantial, medium-high risk during Process II. So irrespective of past pure-tone audiometry results of no permanent STS, the recommendation was offered that noise protector use be "required" at all times while Process I and II were in operation.

4.3.2 Occupational Noise and Vibration Hazards in the PMF Office

The PMF Production machine was a source of high noise and vibration levels, which had the potential to expose workers in an adjoining office to the north. Prompted by worker complaints of headaches, increased stress, increased distractibility and tingling sensations in extremities, the PMF IH staff requested that noise and vibration hazards be identified and characterized in the PMF office. As was observed in PMF Production, noise intensity levels were homogeneous based on stationary time series measurements. Researcher analysis of SLM noise area surveys, as summarized in Section 3.4, and hazard maps (not displayed) indicated the southern wall as the noise source. None of these Leq values exceeded the OSHA action limit ($\geq$85 dBA) for implementation of an HCP, if workers spent full 8 hour shifts in the office.

A whole body vibration (WBV) area survey was conducted around the cubical reported as having the greatest vibrations by office workers, as shown in Figure 3.13 and Table 3.4. This

cubical was physically coupled to a support beam in the middle of the room for added stability. The highest vibration measurement at position 10 in the office was approximately 207 times less than the corresponding WBV TLV value. Although the single vibration measurement from the PMF Production area to the south (position 1) was close to the WBV TLV, PMF Production workers had submitted no complaints so vibrational analysis of hazards in PMF Production was not conducted.

Irregularly high crest factors (RMS peak to average acceleration ratios) were measured for positions 2 (wall mount), 6 (support column mount), and 8 (floor mount) with the potential to exceed the TLVs due to underestimation of exposure (ACGIH, 2001b). All surrounding measurements had reasonable crest factors below 1.5. After the completion of this area survey, these high crest factors could not be rationalized until a previous noise assessment report on the office area from independent acoustic consultants was shared by IH staff. This report found that the main noise source in the corresponding PMF Production area to the south originated from the chain meshing of internal gears from a drive gear box. The PMF machine was directly coupled to five structural beams extending north under the floor into the office with five "I" beams attached to the wall between PMF Production and the office. Natural frequencies of the five "I" beams and structural beams were very close to chain meshing frequency, which may result in vibrational resonance phenomena. Vibration was transmitted from the "I" beams to the wall. In turn by converting vibration to noise, the south wall became the office noise source. In our area survey, all vibration measurements with high crest factors were directly in line with a structural beam running under the office floor, as displayed in floor plans. Future surveys should be expanded further to the west around the other four structure beams running under the office area, looking for similarly high crest factors.

Based on the results from noise area surveys, the conclusion was made that serious occupational hazards from noise were not present in the PMF office and risk for hearing loss was low. Since three positions in line with the structural beam running under the floor had high crest factors, there was a possibility of hazards from WBV to workers in the office area. Suggestions were offered that the cubical be decoupled from the support column and moved a few meters east or west out of line with the support beam under the floor. It was also suggested that employees working over the other four structural beams might be exposed to hazardous WBV levels and should be allowed to move a few meters out of line with those beams. For workers still experiencing adverse symptoms, recommendations were offered that the company provides vibration dampening chairs or isolation pads under desks to reduce or prevent vibrational exposure to workers.

One limitation of this study concerned the measurement of vibration on carpet. Accelerometers must be securely affixed to a surface (with wax or a bolt) to determine vibrational levels. A thin plastic tile was placed over the carpet with tape to provide this surface. It was unclear to what extent the tile was attenuating vibrational levels from the carpet. The difference between average vibration measurements for wall and floor mounts only varied by 0.003 m/s^2 so the influence vibrational attenuation may be low.

4.3.3 Engineering Controls in the PMF Enclosures and PR Area

PMF IH staff requested that the noise reduction effectiveness of engineering controls in two parts of the PMF building be evaluated. Utilizing methodologies similar to those employed by O'Brien (2003) and Dasch *et al* (2005) for evaluation of aerosol engineering controls, area surveys with a SLM were used to evaluate noise reductions by these two engineering controls. The first evaluation was conducted inside three protective noise enclosures in PMF Production

(see Sections 2.2.1 and 3.4 for details). The western and eastern enclosures were similar, having an open doorway with a plastic noise attenuating cover. Noise reduction in these enclosures varied from 4-5 dBA. The central enclosure had a wooden door with an interior noise reduction of 10 dBA. None of these Leq values exceeded the OSHA action limit (≥85 dBA) for implementation of a HCP, if workers were to spend entire 8 hour shifts in the enclosures. Based on these results, we concluded that the three noise enclosures provided adequate noise reduction engineering controls in protecting employees to be deemed "not required" for hearing protector usage.

The second evaluation of engineering controls was conducted one level below PMF Production at a partial barrier surrounding a plastic recycling (PR) machine (see Section 3.4 for details). Evaluation of noise reduction for the partial barrier was accomplished with a combination of noise area surveys and octave band analysis. Expected overall and specific frequency reductions were not observed with noise intensity levels in front of opened and closed modular acoustic screens. These overall and frequency specific measurements were identical within the boundaries of instrumental accuracy (± 1 dBA) with the exception of a single frequency band (160 Hz), where only a 4 dB drop was observed, as shown in Figure 7.31. Octave band analysis revealed that the highest contributors to hazardous noise were confined to the low and middle frequency bands, which were less hazardous than high frequency bands (Ward *et al*., 2003). Noise at such low frequencies is hard to control due to its ability to drift around barriers by reflecting off surfaces.

The acoustic screens in the PR area rose from the ground only covering three quarters of the distance to the ceiling. The remaining top quarter from the barrier to the ceiling was blocked by a network of ducts, wires, and piping so installation of a full barrier was not possible. This

network offered plentiful reflective surfaces, allowing noise to easily reflect over the curtain with no reduction in noise. Based on these results, conclusions were made that the partial enclosure had no effect on reducing noise in the adjacent hallway. Since noise levels in the hallway were approximately 92 dBA, a recommendation was offered to maintain administrative controls redirecting foot traffic or install a full wall and ceiling barrier with noise attenuating properties.

4.4 Occupational Noise and Diesel Exhaust (DE) Hazards at the EECL

At the EECL, noise intensity levels were highly variable based on stationary noise dosimeter researcher analysis. Noise hazard mapping techniques for day 1 were successful in identifying both the expected noise source at the active engine in the northwest corner and the unexpected noise sources in the southeast corner from exterior construction activities. Leq values in the northern room and the upper part of the southern room exceeded the OSHA action limit (≥85 dBA) for implementation of an HCP, if workers remained in the area for 8 hours, so their current policy of required hearing protectors during engine operation was appropriate to protect workers. Noise hazard mapping techniques for day 2 were successful in identifying the active engine in the center of the southern room as the sole noise source. Almost all Leq values in the northern and southern room, if workers remained in the area for 8 hours, exceeded the OSHA action limit for implementation of an HCP so their current policy of required hearing protectors during all engine operation was appropriate to protect workers.

For the EECL on day 1, hazard mapping of $PM_{2.5}$ mass concentration, as shown in Figure 3.14, was successful in identifying the particulate source with highest concentration around the northwestern engine for stationary measurements. For roving measurements the source could only be generally located around the door between the northern and southern rooms. Observed particle size distributions from combined Nanoscan SMPS and OPS instruments revealed a count

median diameter (CMD) of 31.6 nm and geometric standard deviation (GSD) of 2.1 with 99.8 % < 1μm and 92 % < 100 nm.

Since most of the particle sizes were in the ultrafine range, particle number concentration would be a more appropriate sampling metric for detecting this aerosol type in future mapping studies. For example, in an engine and production facility, aerosol mapping was used by Peters *et al* (2006) to demonstrate the necessity of mapping with particle number concentration rather than mass concentration for identifying ultrafine particles (due to their low mass but high number when compared to coarse and fine particles). In that study, mapping with mass concentration was only successful in locating sources of fine particle emissions at poorly enclosed metalworking operations, while mapping with number concentration was only able to locate sources of ultrafine particle emissions at direct-fired natural gas heaters. Aerosol mapping also demonstrated the ability of ultrafine particles to diffuse more readily and persist longer in the air than larger particles.

For measurements from aerosol photometers at stationary measurement positions in the EECL for day 1, $PM_{2.5}$ photometer optical samples from DE measured averaged mass concentrations ranging from 0.067 to 0.099 mg/m^3. These measurements, if workers remained in the area for 8 hours, did not exceed the action levels (half of the OEL) for the OHSA PEL or ACGIH TLV, as detailed previously in Section 1.3. They also did not exceed the Mining Safety and Health Administration (MSHA) diesel particulate standard of 0.16 mg/m^3 TWA for sub-micrometer total carbon ($PM_{1.0}$) (Rogers and Davies, 2005). While these measurements did not exceed any OELs, they did exceed the inhalation reference dose concentration (RFC) for DPM so the incidence of adverse health effects was possible under those conditions. The recommendation was offered that the engine exhaust ventilation be leak tested and repaired.

5 Conclusions and Future Work

Researchers were successful in developing novel sampling techniques employing common, relatively lower-cost direct-reading instruments (DRIs, instruments that report hazard intensity at near real-time resolution) for hazard mapping. Spatial and temporal resolutions was enhanced by deploying stationary (static) personal DRIs that captured temporal variability when distributed throughout the facility and roving personal DRIs that captured spatial and temporal variability over multiple traverses throughout whole work shifts.

Hazard mapping with these novel techniques was conducted at a Plastic Manufacturing Facility (PMF) and the Engine and Energy Conversion Laboratory (EECL). Researcher analysis of stationary noise dosimeters at the PMF for Processes I and II revealed homogeneous noise intensity levels over time. Based on noise hazard mapping from stationary noise dosimeters, roving noise dosimeters, and sound level meters (SLM), researchers were successful in identifying noise sources and hazardous areas of concern. With homogeneous noise intensities over time, researcher analysis of the similarity between hazard maps revealed that sampling techniques with similar spatial resolutions had a tendency to produce more similar hazard maps.

At the EECL, researcher analysis of stationary noise dosimeters for days 1 and 2 indicated highly variable noise intensity levels over time and space. Based on noise hazard maps from different sampling techniques, researchers were successful in identifying similar noise sources and hazardous areas of concern. Under these variable noise intensity levels over time, sampling techniques with similar temporal resolutions, more so than spatial resolutions, had a tendency to interpolate for more similar hazard maps. On day 1 these novel techniques were

expanded to utilize stationary and roving aerosol DRIs to measure diesel exhaust (DE) throughout the facility. Stationary and roving measurements, when averaged over time, interpolated for dissimilar aerosol hazard maps, which identified the same relative DE source. On day 2 since these novel sampling techniques had not been validated, researchers determined that measurements taken from stationary personal noise dosimeters, roving personal noise dosimeters, and a SLM were reasonably similar, when collected at the same time in close spatial proximity, based on predicted instrumental accuracy and literature precedence.

Several occupational hazard assessments were also conducted at these locations. These assessments included determination of "required" hearing protector usage in the main PMF work area based on the high probability of noise induced hearing loss (NIHL) over time. Three noise enclosures in this area were assessed as offering enough noise reduction to "not require" hearing protection usage. While noise hazards were not identified in a PMF office area, potential hazards from whole body vibration (WBV) were uncovered, corresponding to localized areas over vibrating structural beams under the floor. Researcher analysis of noise area surveys and octave bands around a PMF plastic recycling (PR) machine revealed that a partial barrier was completely ineffective at reducing noise intensity levels in an adjacent hallway. At the EECL, currently "required" hearing protector usage policies during engine runtimes were appropriate to protect workers from observed noise intensity levels on days 1 and 2. At the EECL aerosol hazard mapping and particle size distribution revealed no hazards from engine DE on day 1.

Future work will include statistical methods for combining stationary and roving monitor measurements into master hazard maps that will offer enhanced information on overall and transient variation in hazard intensities over space and time. Another future project could concern the assessment of personal exposures to hazards with maps generated from stationary

monitors. Predicted dose hazard maps from stationary monitors could be paired with personal real-time tracking methods (relative indoor tracking or Global Positions System) to predict personal exposures. These estimated exposures would be compared to observed personal exposures from workers fitted with personal DRIs, measuring time-weighted average exposures, to develop and refine the technique.

6 References

ACGIH. (2001a). Documentation of the Threshold Limit Values for Physical Agents Noise. American Conference of Governmental Industrial Hygienists.

ACGIH. (2001b). Documentation of the Threshold Limit Values for Physical Agents Whole-Body Vibration. American Conference of Governmental Industrial Hygienists.

Abu-Allaban M, Coulomb W, Gertler A W, Gillies, J, Pierson W R, Rogers C F, Sagebiel J C, Tarnay L *et al*. (2002) Exhaust Particle Size Distributions Measurements at the Tuscarora Mountain Tunnel. Aerosol Sci Technol; 36: 771-789.

Benton-Vitz K, Volckens J. (2008) Evaluation of the pDR-1200 Real-Time Aerosol Monitor. J Occup Environ Hyg; 5: 353-359.

Byrne, DC, Reeves ER. (2008) Analysis of Nonstandard Noise Dosimeter Microphone Positions. J Occup Environ Hyg; 5: 197-209

Campo P, Morata TC, Hong O *et al*. (2013). Chemical exposure and hearing loss. Disease-a-Month; 59: 119-138.

Daniell WE, Swan SS, McDaniel MM, Stebbin JG *et al*. (2006) Noise exposure and hearing loss prevention programmes after 20 years of regulations in the United States. Occup Environ Med; 63: 343-351.

Dasch J, D'Arcy J, Gundrum A, Sutherland J, Johnson J, Carlson D *et al*. (2005) Characterization of Fine Particles from Machining in Automotive Plants. J Occup Environ Hyg; 2: 609-625.

Fischer ML, Price PN, Thatcher TL, Schwalbe CA, Craig MJ, Wood EE, Sextro RG, Gadgil AJ *et al*. (2001) Rapid measurements and mapping of tracer gas concentrations in a large indoor space. Atmospheric Environment; 35: 2837-2844.

Hesterberg TW, Long CM, Bunn WB, Sax SN, Lapin CA, Valberg PA *et al*. (2009) Non-cancer health effects of diesel exhaust: A critical assessment of recent human and animal toxicological literature. Crit Rev Toxicol; 39: 195-227.

Hong O, Keer MJ, Poling GL, Dahr S *et al*. (2013) Understanding and preventing noise-induced hearing loss. Disease-a-Month; 59: 110-118.

Koehler KA, Peters TM. (2013) Influence of Analysis Methods on Interpretation of Hazard Maps. Ann Occup Hyg; 57: 558-570.

Koehler KA, Volckens, J. (2011) Prospects and Pitfalls of Occupational Hazard Mapping: 'Between These Lines There Be Dragons'. Ann Occup Hyg; 55: 829-840.

Larson Davis. (2004) System 824 Reference Manual. Larson Davis Inc. Available from: URL: http://www.larsondavis.com/Manuals_DataSheets_Brochures.pdf (accessed 25 June 2013).

Leventhall, HG. (2004) Low Frequency Noise and Annoyance. Noise and Health; 6: 59-72.

Li J, Heap AD. (2008) Non-Geostatistical Interpolators. A Review of Spatial Interpolation methods for Environmental Scientists. Geoscience Australia. P. 6-26. ISBN 978 1 921498 30 5.

McMeeking, GR, Kreidenswesi SM, Carrico CM, Collett JL. (2005) Observations of smoke-influenced aerosol during the Yosemite Aerosol Characterization Study: 2. Aerosol scattering and absorbing properties. J. Geophys. Res., 110, D09206, doi:10.1029/2004JD005389.

Metwally FM, Aziz HM, Mahdy-Abdallah H *et al.* (2012). Effect of combined occupational exposure to noise and organic solvents on hearing. Toxicol. Ind. Health; 28: 901-604.

Murphy E, King EA. (2010) Strategic environmental noise mapping: methodological issues concerning the implementation of the EU Environmental Noise Directive and their policy implications. Environ Int; 36: 290-309.

NIOSH. (1998) Criteria for a Recommended Standard: Occupational Noise Exposure. U.S. Department of Health and Human Services, Public Health Service, Centers for Disease Control and Prevention, National Institute of Occupational Safety and Health. Available from: URL: http://www.cdc.gov/niosh/docs/98-126/pdfs/98-126.pdf (accessed 16 June 2013).

NIOSH. (2001) Work Related Hearing Loss. U.S. Department of Health and Human Services, Public Health Service, Centers for Disease Control and Prevention, National Institute of Occupational Safety and Health. Available from: URL:http://www.cdc.gov/niosh/docs/2001-103/ (accessed 16 June 2013).

Oberdorster G, Sharp Z, Atudeorei V, Elder A, Gelein R, Lunts A, Keyling W, Cox C. (2002) Extrapulmonary Translocation of Ultrafine Carbon Particles Following Whole-Body Inhalation Exposure of Rats. J Toxicol Environ Health A; 65: 1531-1543.

O'Brien DM. (2003) Aerosol Mapping of a Facility with Multiple Cases of Hypersensitivity Pneumonitis: Demonstration of Mist Reduction and a Possible Dose/Response Relationship. Appl Occ Environ Hyg; 18: 947-952.

Ologe FE, Akande TM, Olajide TG *et al*. (2006) Occupational noise exposure and sensorineural hearing loss among workers of a steel rolling mill. Eur Arch Otorhinolaryngol; 263: 618-621.

OSHA. (2002) Hearing Conservation. U.S. Department of Labor, Occupational Safety and Health Administration. Available from: URL: http://www.osha.gov/Publications/osha3074.pdf(accessed 16 June 2013).

OSHA. (2012) Particulates Not Otherwise Regulated (Respirable Fraction). U.S. Department of Labor, Occupational Safety and Health Administration. Available from: URL: http://www.osha.gov/dts/chemicalsampling/data/CH_259635.html(accessed 27 June 2013).

OSHA. (2013) OSHA Technical Manual Chapter 5 Noise Appendix I: A. Physics of Sound. U.S. Department of Labor, Occupational Safety and Health Administration. Available from: URL: https://www.osha.gov/dts/osta/otm/noise/health_effects/physics.html (accessed 8 January 2014

Peters TM, Heitbrink WA, Evans DE, Slavin TJ, Maynard AD *et al*. (2006) The mapping of fine and ultrafine particle concentrations in an engine machining and assembly facility. Ann Occup Hyg; 50: 249–57.

Pollice A, Losinio GJ. (2010) Spatiotemporal analysis of the PM10 concentration over the Taranto area. Environ Monit Assess; 162: 177-190.

Prashanth KVM, Venugopalachar S. (2011) The possible influence of noise frequency components on the health of exposed industrial workers - A review. Noise Health; 13: 16-25.

Reich RM, Davis R. (2008) Spatial Modeling. Quantitative Spatial Analysis. Fort Collins, CO, USA: Colorado State University. p. 354-482.

Ris C. (2007). U.S. EPA Health Assessment for Diesel Engine Exhaust: A Review. Inhal. Toxicol; 19: 229-239.

Rogers A, Davies B. (2005) Diesel Particulates—Recent Progress on an Old Issue. Ann Occup Hyg; 49: 453-456.

Royster LH, Berger, EH, Royster JD *et al*. (2003): Noise Surveys and Data Analysis. In Berger EH, Royster LH, Royster JD, Driscoll DP, Layne M *et al*. editors. The Noise Manual 5th Edition. Virginia: American Industrial Hygiene Association. p. 165-244. ISBN: 1931504024.

Seong JC, Park TH, Ko JH, Chang SI, Kim M, Holt JB, Mehdi MR et al. (2011) Modeling of road traffic noise and estimated human exposure in Fulton County, Georgia, USA. Environ Int: 37: 1336-1341.

Singer Safety Co. (2013): "Product Data Sheet for Sound Stopper Modular Acoustic Screen 22-310148." Chicago, IL.

"The R Project for Statistical Computing." [Online] Available at: URL: http://www.r-project.org/(Accessed October 30, 2013).

Valoski MP, Seiler JP, Crivaro MA, Durkt G. (1995) Comparison of Noise Exposure Measurements Conducted with Sound Level Meters and Noise Dosimeters Under Field Conditions. U.S. Department of Labor, Mine Safety and Health Administration. Informational Report No. 1230. Available from: URL: http://www.msha.gov/techsupp/pshtcweb/ptadirs/IR1230.pdf (accessed 8 January 2014)

Ward DW, Royster LH, Royster JD *et al*. (2003): Anatomy and Physiology of the Ear. In Berger EH, Royster LH, Royster JD, Driscoll DP, Layne M *et al*. editors. The Noise Manual 5th Edition. Virginia: American Industrial Hygiene Association. p. 165-244. ISBN: 1931504024.

Widstrom B-O, Kjellberg A, Landstrom (1994). Health effects of long-term occupational exposure to whole-body vibration: A review. Int J Ind Ergonom; 14:273-292.

7 Appendices

7.1 MATLAB Data Extraction from Roving DRI Time Series Measurements

Code for MATLAB custom scripts are listed below for extraction of individual measurements from roving pathway time series data. Roving measurements were downloaded as time series CSV files. The script used the time series with known sampling durations and an additional CSV file of sampling times to extract individual measurements from roving pathways.

```
datename = '-3-21-13';
ext = '.csv';
rovmonitor=[17683
   17682]
[rov1]=xlsread('20130321all_loc_times.xls', 'kirsten');
x1=rov1(:,1);
y1=rov1(:,2);
rovtime1 = datenum('21-Mar-2013') + datenum(rov1(:,3));
rovtime1 = datenum_round_off(rovtime1, 'second');
[rov2]=xlsread('20130321all_loc_times.xls', 'kirk');
x2=rov2(:,1);
y2=rov2(:,2);
rovtime2 = datenum('21-Mar-2013') + datenum(rov2(:,3));
rovtime2 = datenum_round_off(rovtime2, 'second');
%Read in Noise files
 for i=1:length(rovmonitor)
    filename=strcat(num2str(rovmonitor(i)), datename, ext);
    fid = fopen(filename);
    Input=textscan(fid, '%f %s %s %f %f %f %*s %*s %*s %*s %*f %*s %*s',
'delimiter', ',', 'headerlines', 43)%, ,'MultipleDelimsAsOne',1,'TreatAsEmpty', 'MIC');

%[Number,Date,Time,leq,Max,Min,Peak,TWA1,TWA2,TWA3,TWA4,Overload,Mic_D
isconnect]
    fclose(fid);
    if i==1
      %Set up new vectors
    date1 = datenum(Input{1,2}, 'dd-mmm-yy') + datenum(Input{1,3}, 'HH:MM:SS') -
datenum('00:00:00','HH:MM:SS');
    date1 = datenum_round_off(date1, 'second');
    Leq1 = Input{1,4};
```

```
    min1 = Input{1,5};
    max1 = Input{1,6};
    end
    if i==2
       %Set up new vectors
      date2=nan(length(Input{1,1}), 1);
      Leq2=nan(length(Input{1,1}), 1);
      min2=nan(length(Input{1,1}), 1);
      max2=nan(length(Input{1,1}), 1);
    date2 = datenum(Input{1,2}, 'dd mmm yyyy') + datenum(Input{1,3}, 'HH:MM:SS') -
datenum('00:00:00','HH:MM:SS');
    date2 = datenum_round_off(date2, 'second');
    Leq2 = Input{1,4};
    min2 = Input{1,5};
    max2 = Input{1,6};
    end
 end
%Find times for measurements
for i=1:length(rovtime1)
   a=find(rovtime1(i)==date1);
   rov1Leq(i)=mean(Leq1(a:a+14,1));
end
for i=1:length(rovtime2)
   a=find(rovtime2(i)==date2);
   rov2Leq(i)=mean(Leq2(a:a+14,1));
end
%Read in Pdr data
pdrmonitor=[5835];
    filename=strcat(num2str(pdrmonitor), datename, ext);
    fid = fopen(filename, 'rt');
    Input=textscan(fid, '%f %s %s %f', 'delimiter', ',', 'headerlines', 16)%,
,'MultipleDelimsAsOne',1,'TreatAsEmpty', 'MIC');
    %[Number,Date,Time,Conc(mg/m3)]
    fclose(fid);
      %Set up new vectors
    datep1 = datenum(Input{1,2}, 'dd mmm') + datenum(Input{1,3}, 'HH:MM:SS') -
datenum('00:00:00','HH:MM:SS');
    datep1 = datenum_round_off(datep1, 'second');
    PDR1 = Input{1,4};
%Find times for measurements
for i=1:length(rovtime1)
   a=find(rovtime1(i)==datep1);
   rov1PDR(i)=mean(PDR1(a:a+14,1));
end
```

7.2 Code for Hazard Mapping with R

All hazard maps were produced using the free statistical package R ("The R Project for Statistical Computing", 2013). An example of R codes utilized for creating the hazard maps is listed below.

```
## R code example for universal Kriging is listed below.
##Commands for loading the data are listed.
noisest<-data.matrix(read.csv("C:/RSpatial/EECLDAY2ROVING.csv"))
noisest<-list(x=noisest[,2],y=noisest[,3],z=noisest[,1])
##Commands for fitting ordinary least squares p-degree polynomial to data set are listed.
noisest.ls <- surfls(2,noisest$x,noisest$y,noisest$z)
##Plotting estimated variograms with varying bins (10, 20, 30, 40) are listed to visually
##estimate nugget effect, range, and smoothness (matern only, usually 2.5)
##parameters for covariance model.
par(mfrow=c(2,2))
noisest.var <- variogrm(noisest$x, noisest$y, noisest.ls$resid, 10)
noisest.var <- variogrm(noisest$x, noisest$y, noisest.ls$resid, 20)
noisest.var <- variogrm(noisest$x, noisest$y, noisest.ls$resid, 30)
noisest.var <- variogrm(noisest$x, noisest$y, noisest.ls$resid, 40)
##Visually estimated model parameters are inputted into the functions below.
##The function uses iterative fitting to determine the best model parameters.
##Correlation models are optimizing for best fit by lowest AICC.
#Exponential covariance model fitting by polynomial number (np) without nugget
#parameter is listed.
noisest0.exp<-
fit.geospatial(noisest$x,noisest$y,noisest$z,np=0,c(1.67),cov.model="exp",Opt=T)
noisest1.exp<-
fit.geospatial(noisest$x,noisest$y,noisest$z,np=1,c(1.67),cov.model="exp",Opt=T)
noisest2.exp<-
fit.geospatial(noisest$x,noisest$y,noisest$z,np=2,c(1.67),cov.model="exp",Opt=T)
noisest3.exp<-
fit.geospatial(noisest$x,noisest$y,noisest$z,np=3,c(1.67),cov.model="exp",Opt=T)
#Exponential covariance model fitting by polynomial number (np) with nugget
#parameter is listed.
noisest0.expw<-
fit.geospatial(noisest$x,noisest$y,noisest$z,np=0,c(1.67,0.2),cov.model="exp",Opt=T)
noisest1.expw<-
fit.geospatial(noisest$x,noisest$y,noisest$z,np=1,c(1.67,0.2),cov.model="exp",Opt=T)
noisest2.expw<-
fit.geospatial(noisest$x,noisest$y,noisest$z,np=2,c(1.67,0.2),cov.model="exp",Opt=T)
noisest3.expw<-
fit.geospatial(noisest$x,noisest$y,noisest$z,np=3,c(1.67,0.2),cov.model="exp",Opt=T)
```

```
#Gaussian covariance model fitting by polynomial number (np) without nugget parameter
#is listed.
noisest0.gau<-
fit.geospatial(noisest$x,noisest$y,noisest$z,np=0,c(2.5),cov.model="gau",Opt=T)
noisest1.gau<-
fit.geospatial(noisest$x,noisest$y,noisest$z,np=1,c(2.5),cov.model="gau",Opt=T)
noisest2.gau<-
fit.geospatial(noisest$x,noisest$y,noisest$z,np=2,c(2.5),cov.model="gau",Opt=T)
noisest3.gau<-
fit.geospatial(noisest$x,noisest$y,noisest$z,np=3,c(2.5),cov.model="gau",Opt=T)
#Gaussian covariance model by polynomial number (np) with nugget parameter is listed.
noisest0.gauw<-
fit.geospatial(noisest$x,noisest$y,noisest$z,np=0,c(1.67,0.2),cov.model="gau",Opt=T)
noisest1.gauw<-
fit.geospatial(noisest$x,noisest$y,noisest$z,np=1,c(1.67,0.2),cov.model="gau",Opt=T)
noisest2.gauw<-
fit.geospatial(noisest$x,noisest$y,noisest$z,np=2,c(1.67,0.2),cov.model="gau",Opt=T)
noisest3.gauw<-
fit.geospatial(noisest$x,noisest$y,noisest$z,np=3,c(1.67,0.2),cov.model="gau",Opt=T)
#Matern covariance model by polynomial number (np) without nugget parameter is
#listed.
noisest0.mat<- fit.geospatial(noisest$x,noisest$y,noisest$z,np=0,c(1.67,2.5),
cov.model="matern" ,Opt=T)
noisest1.mat<- fit.geospatial(noisest$x,noisest$y,noisest$z,np=1,c(1.67,2.5),
cov.model="matern" ,Opt=T)
noisest2.mat<- fit.geospatial(noisest$x,noisest$y,noisest$z,np=2,c(1.67,2.5),
cov.model="matern" ,Opt=T)
noisest3.mat<- fit.geospatial(noisest$x,noisest$y,noisest$z,np=3,c(1.67,2.5),
cov.model="matern" ,Opt=T)
#Matern covariance model by polynomial number (np) with nugget parameter is listed.
noisest0.matw<- fit.geospatial(noisest$x,noisest$y,noisest$z,np=0,c(1.67,0.2,2.5),
cov.model="matern" ,Opt=T)
noisest1.matw<- fit.geospatial(noisest$x,noisest$y,noisest$z,np=1,c(1.67,0.2, 2.5),
cov.model="matern" ,Opt=T)
noisest2.matw<- fit.geospatial(noisest$x,noisest$y,noisest$z,np=2,c(1.67,0.2,2.5),
cov.model="matern" ,Opt=T)
noisest3.matw<- fit.geospatial(noisest$x,noisest$y,noisest$z,np=3,c(1.67,0.2,2.5),
cov.model="matern" ,Opt=T)
##Best covariance function is zero order polynomial gaussian with nugget effect
##(noisest0.gauw with AICC=197.38).
##Command for Kriging with optimal covariance function is listed.
krig1<-krig.geospatial(noisest0.gauw,0,15.2,0,40.4,50)
##Command for plotting the Kriged object is listed.
filled.contour(krig1,color = function(x)rev(heat.colors(x)),
plot.title=title(main="EECL Day 1: Roving Dosimeter"), plot.axes = { axis(1); axis(2);
```

points(noisest$x,noisest$y,pch=20);rect(0.1,0.1,4.4,33.99,col="grey");rect(5.87,0,14,5.89
,col="grey");rect(7.37,17.98,13.06,20.58,lty=2);rect(7.37,33.6,40.4,33.9,col="black");
rect(14.9,17.89,15.2,33.9,col="black");
rect(0.1,0.1,15.1,40.3)}, key.title = title(main = "Leq dBA"))

7.3 PMF Personal Noise Dosimetry Time Series

A total of 20 personal noise dosimetry samples were collected for five job titles (Leader, Casting, Finishing, Windup, and Quality) in PMF Production during Process I (day 1 and 2) and II (day 1 and 2) by industrial hygiene staff, as shown by Leq time series format in Figures 7.1-7.20.

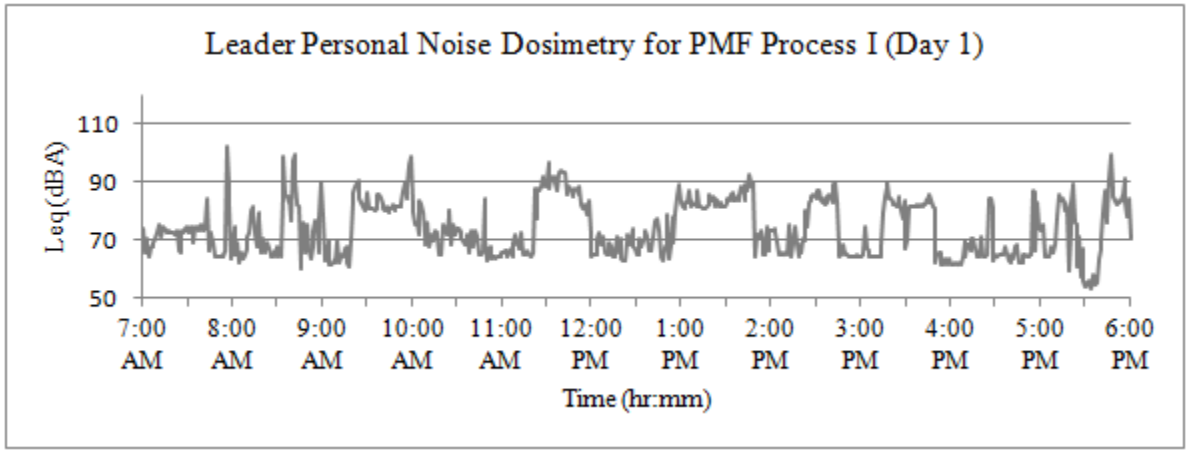

Figure 7.1: Personal noise dosimetry time series for Leader worker is displayed for Process I (day 1).

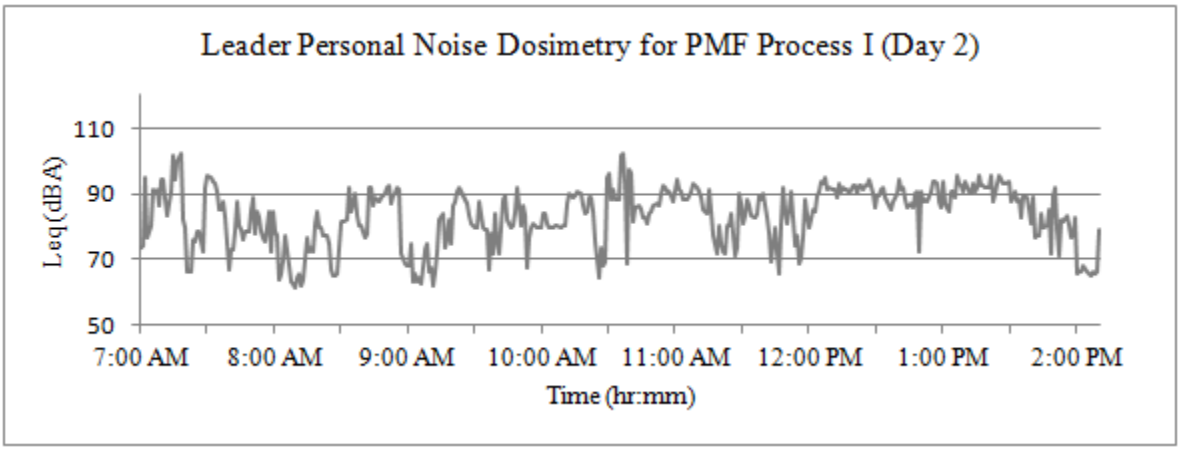

Figure 7.2: Personal noise dosimetry time series for Leader worker is displayed for Process I (day 2).

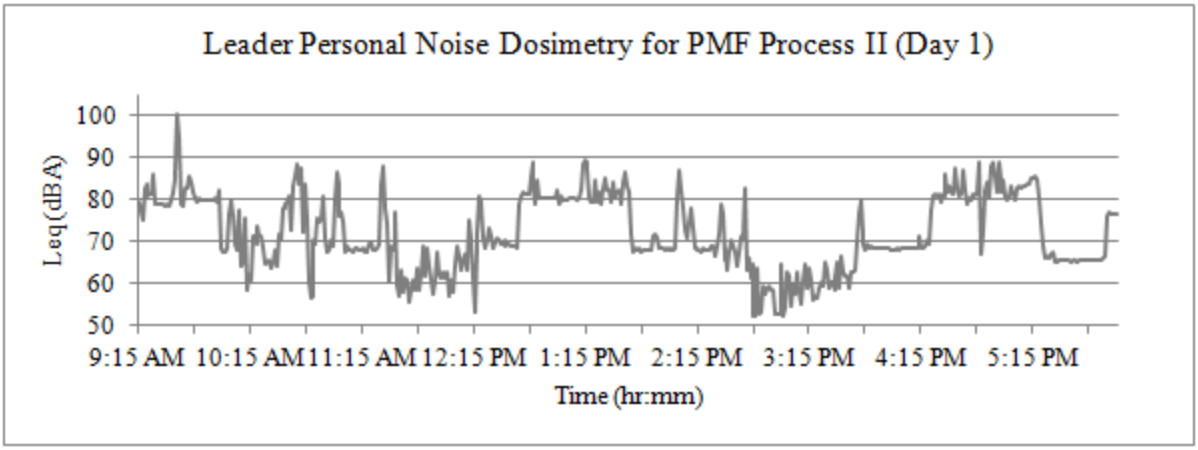

Figure 7.3: Personal noise dosimetry time series for Leader worker is displayed for Process II (day 1).

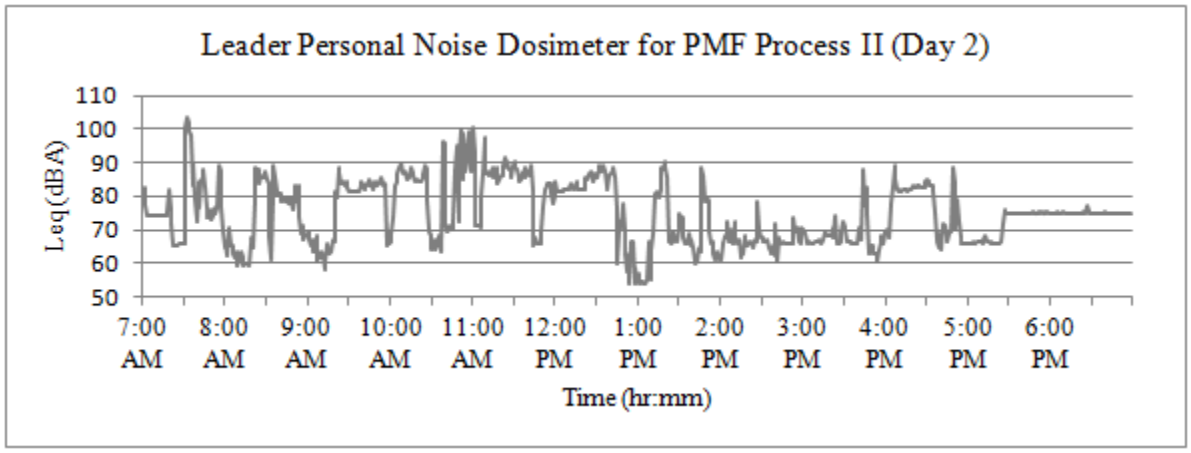

Figure 7.4: Personal noise dosimetry time series for Leader worker is displayed for Process II (day 2).

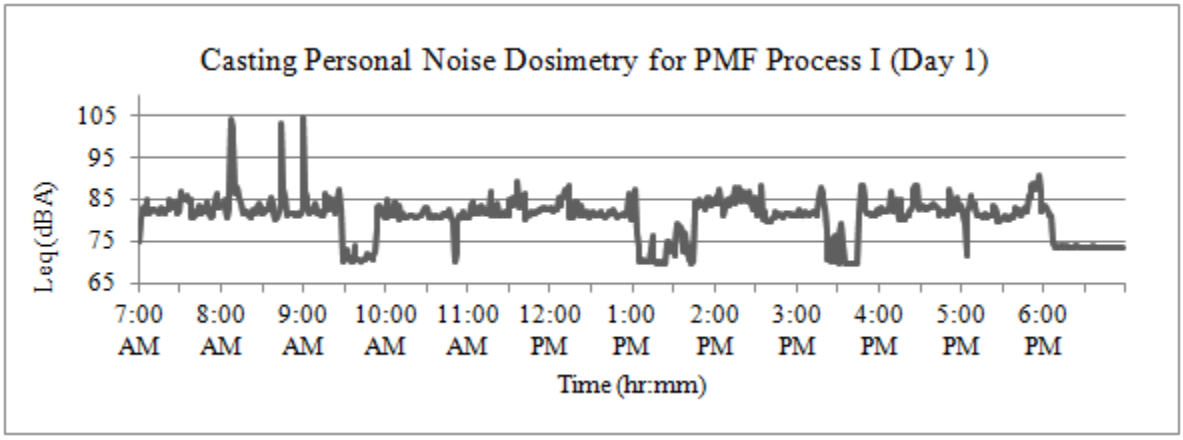

Figure 7.5: Personal noise dosimetry time series for Casting worker is displayed for Process I (day 1).

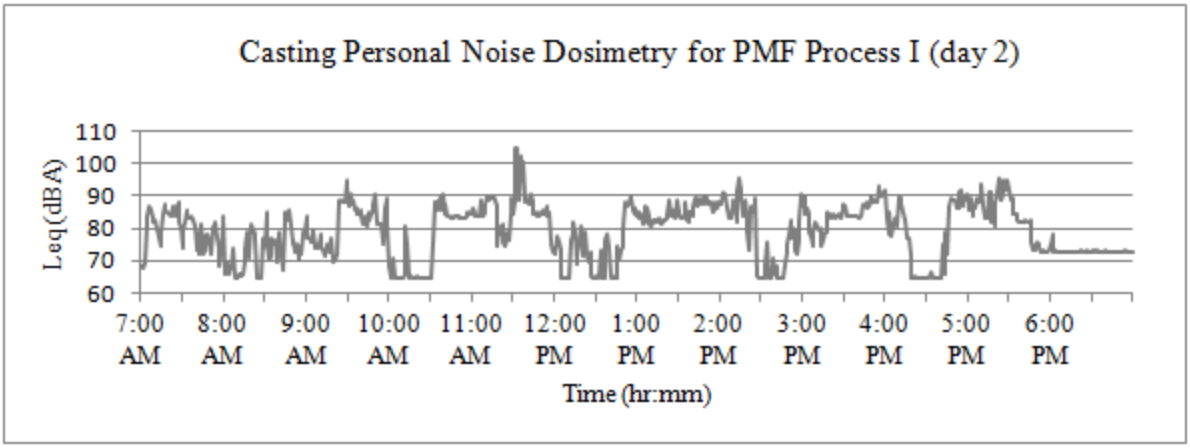

Figure 7.6: Personal noise dosimetry time series for Casting worker is displayed for Process I (day 2).

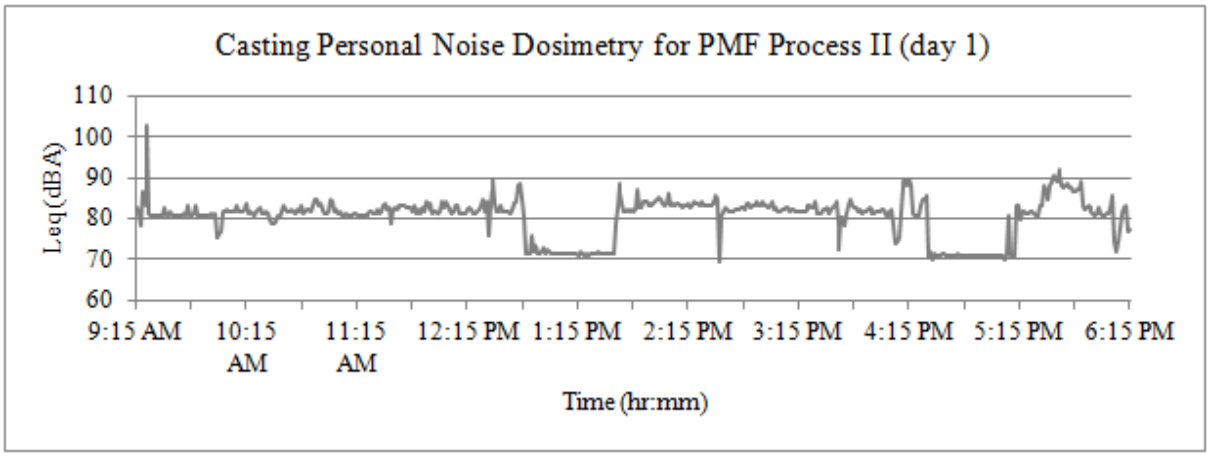

Figure 7.7: Personal noise dosimetry time series for Casting worker is displayed for Process II (day 1).

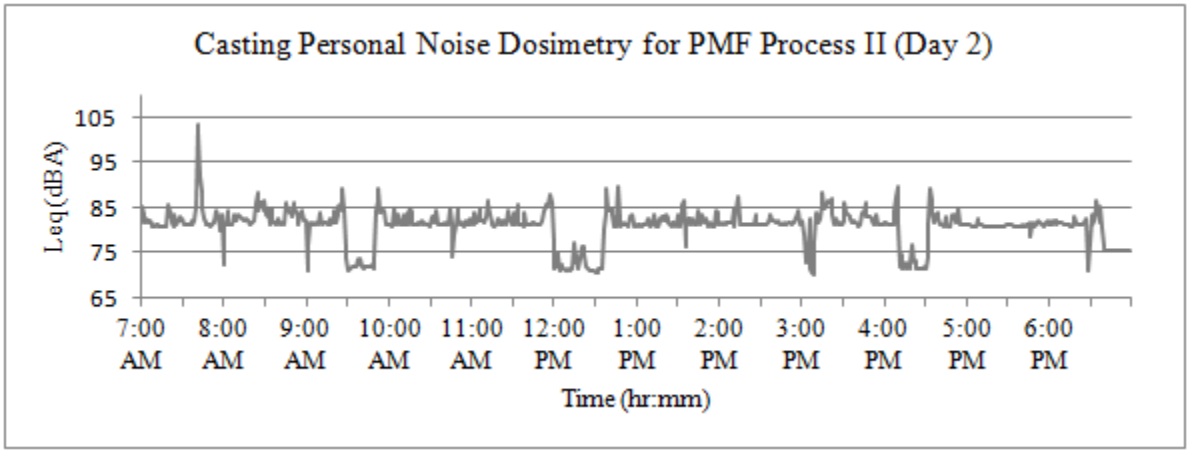

Figure 7.8: Personal noise dosimetry time series for Casting worker is displayed for Process II (day 2).

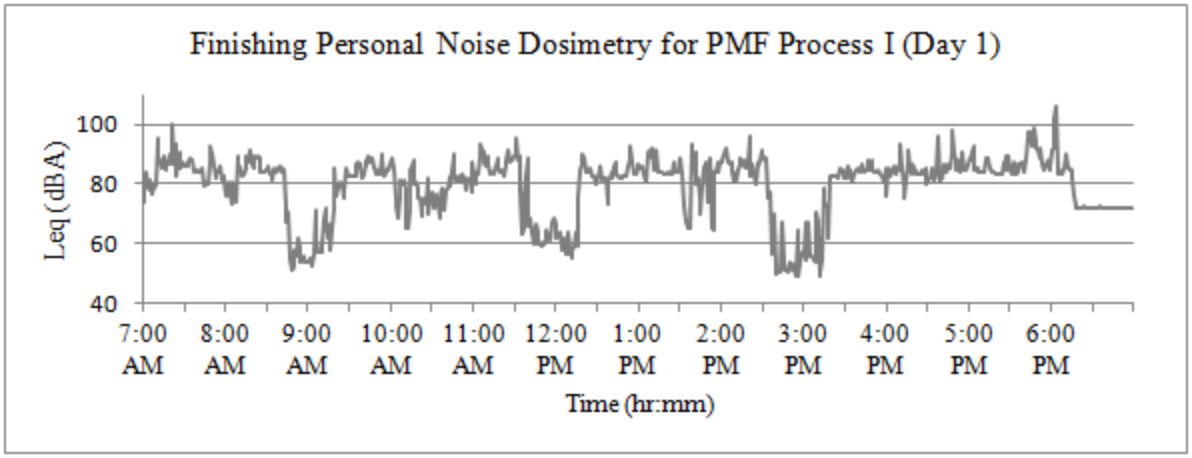

Figure 7.9: Personal noise dosimetry time series for Finishing worker is displayed for Process I (day 1).

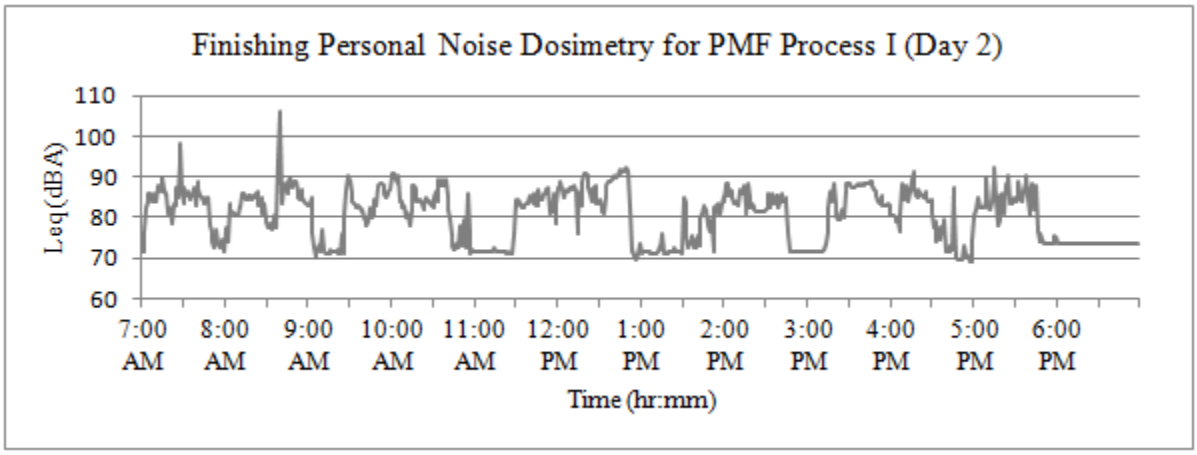

Figure 7.10: Personal noise dosimetry time series for Finishing worker is displayed for Process I (day 2).

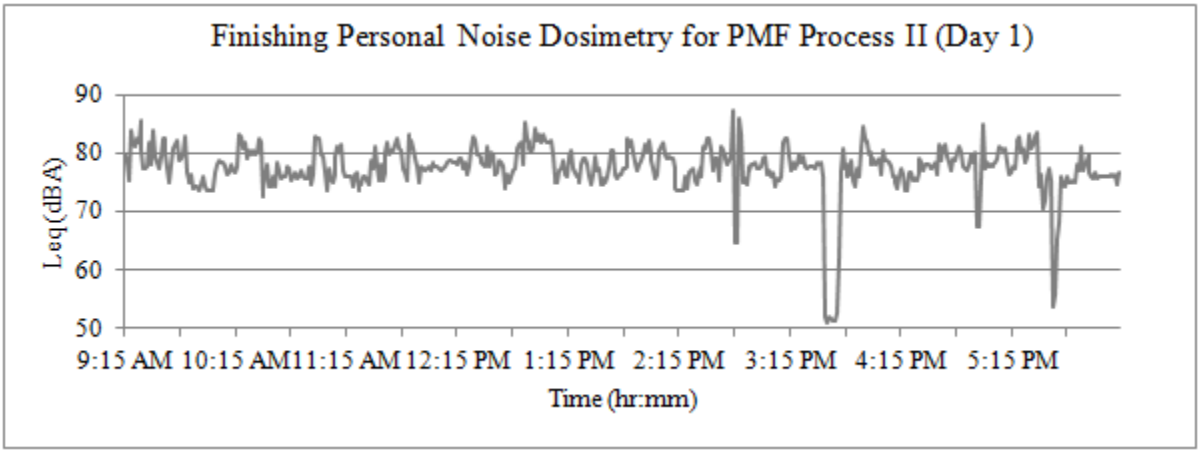

Figure 7.11: Personal noise dosimetry time series for Finishing worker is displayed for Process II (day 1).

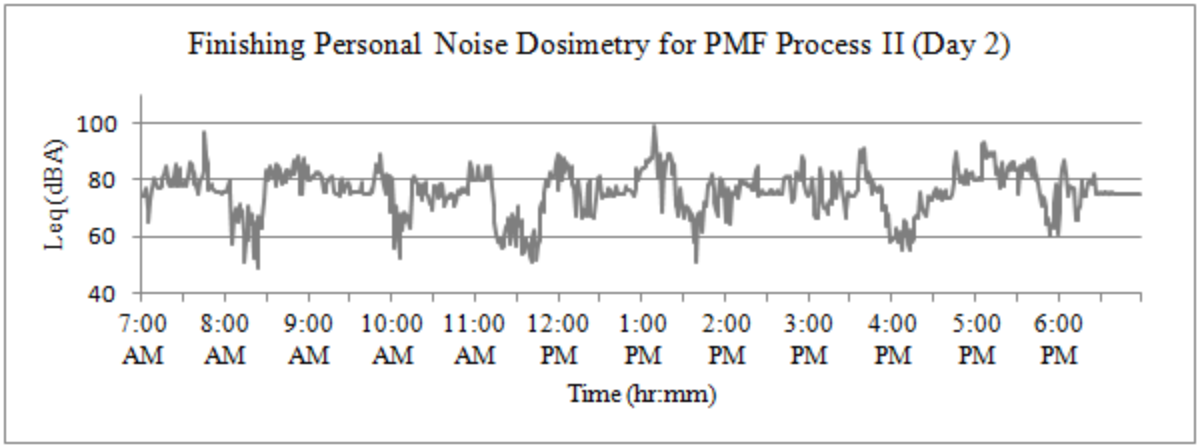

Figure 7.12: Personal noise dosimetry time series for Finishing worker is displayed for Process II (day 2).

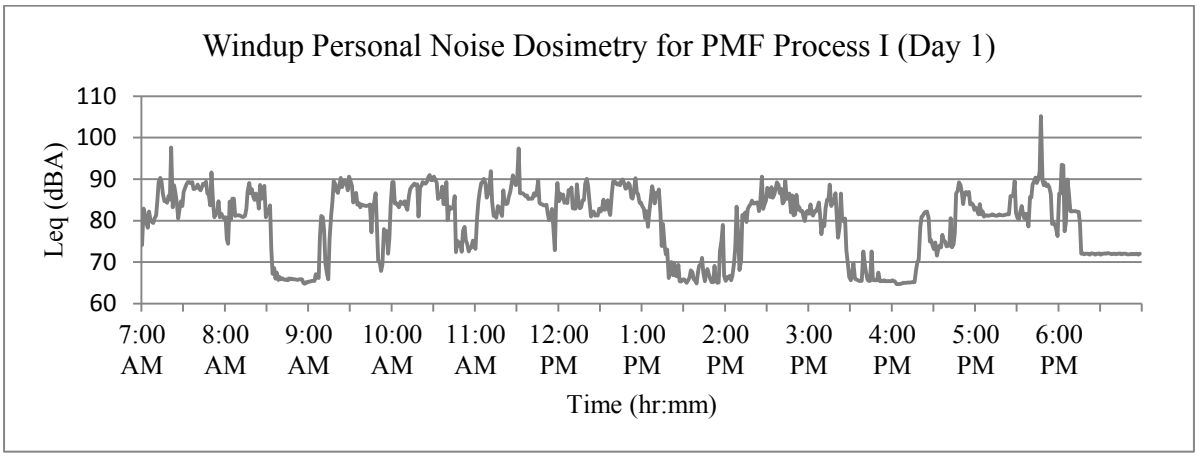

Figure 7.13: Personal noise dosimetry time series for Windup worker is displayed for Process I (day 1).

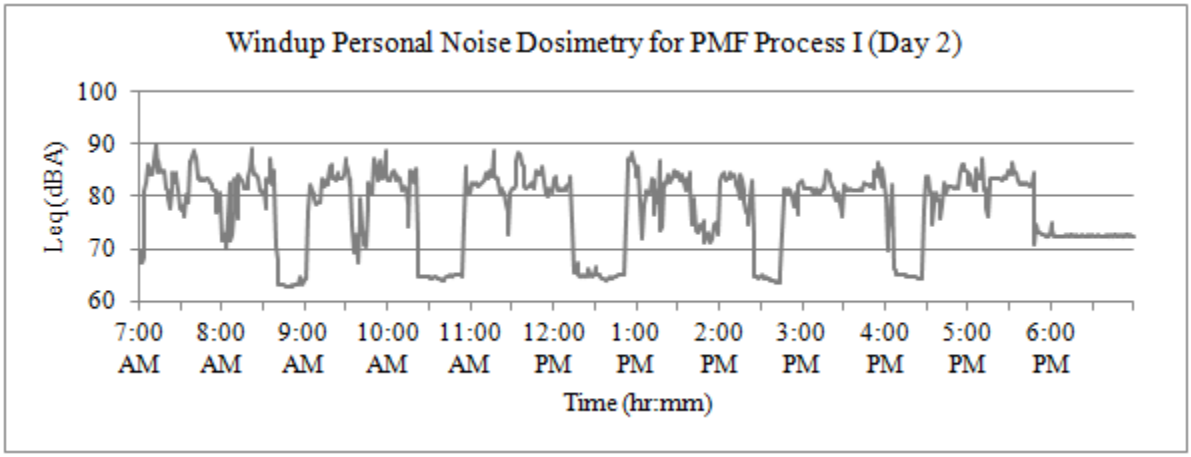

Figure 7.14: Personal noise dosimetry time series for Windup worker is displayed for Process I (day 2).

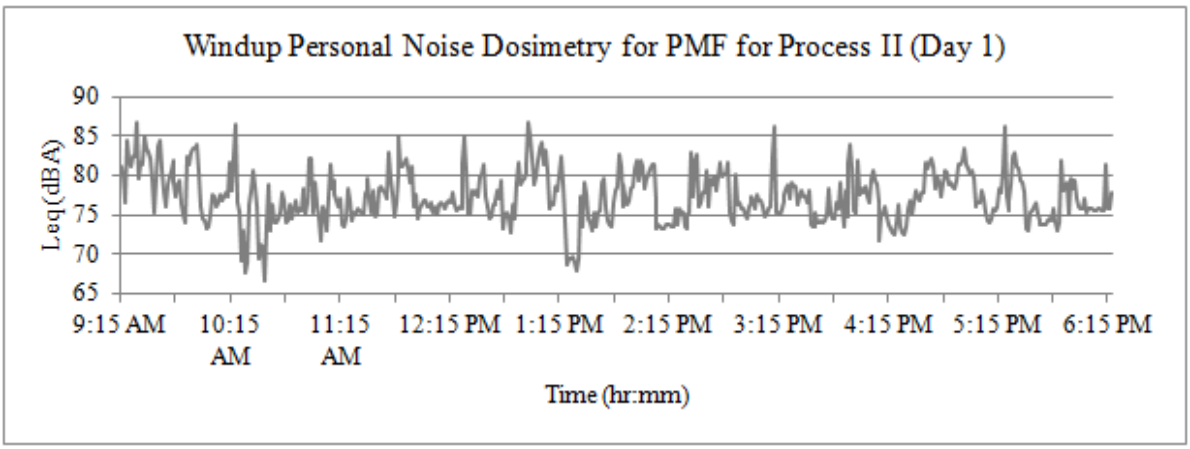

Figure 7.15: Personal noise dosimetry time series for Windup worker is displayed for Process II (day 1).

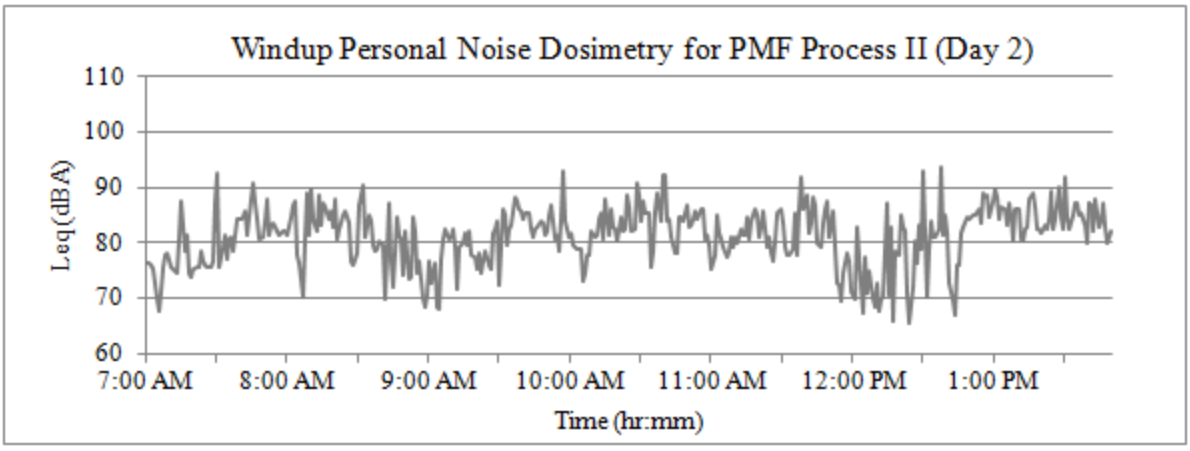

Figure 7.16: Personal noise dosimetry time series for Windup worker is displayed for Process II (day 2).

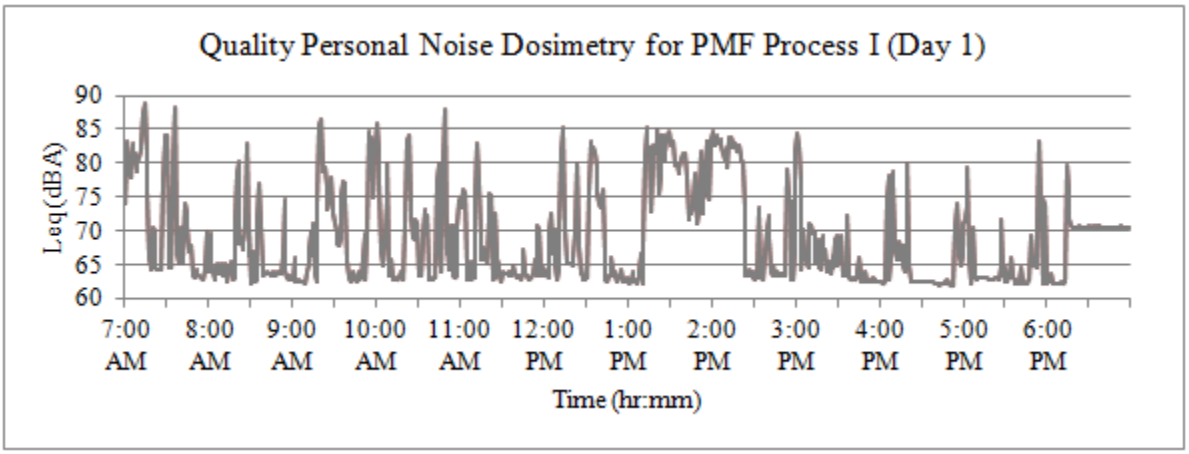

Figure 7.17: Personal noise dosimetry time series for Quality worker is displayed for Process I (day 1).

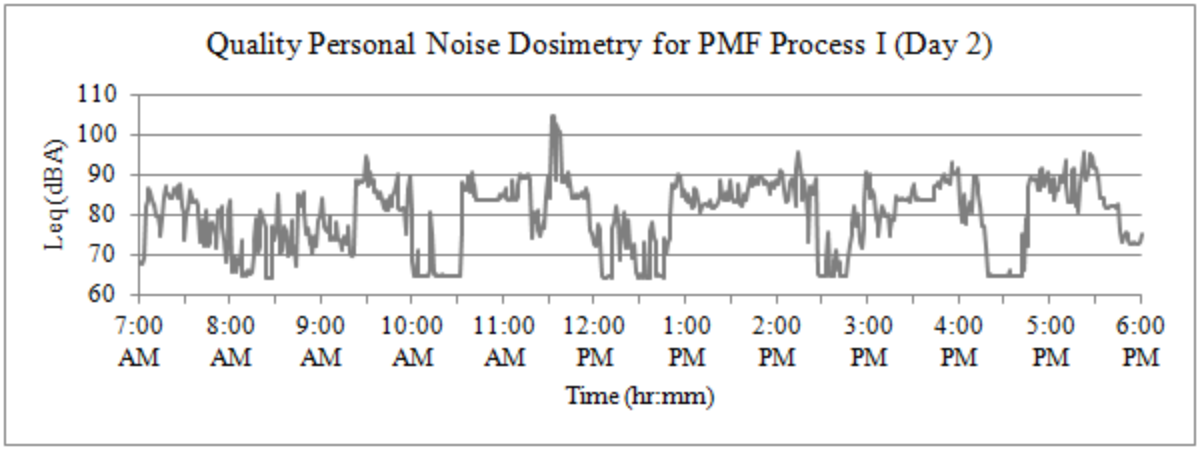

Figure 7.18: Personal noise dosimetry time series for Quality worker is displayed for Process I (day 2).

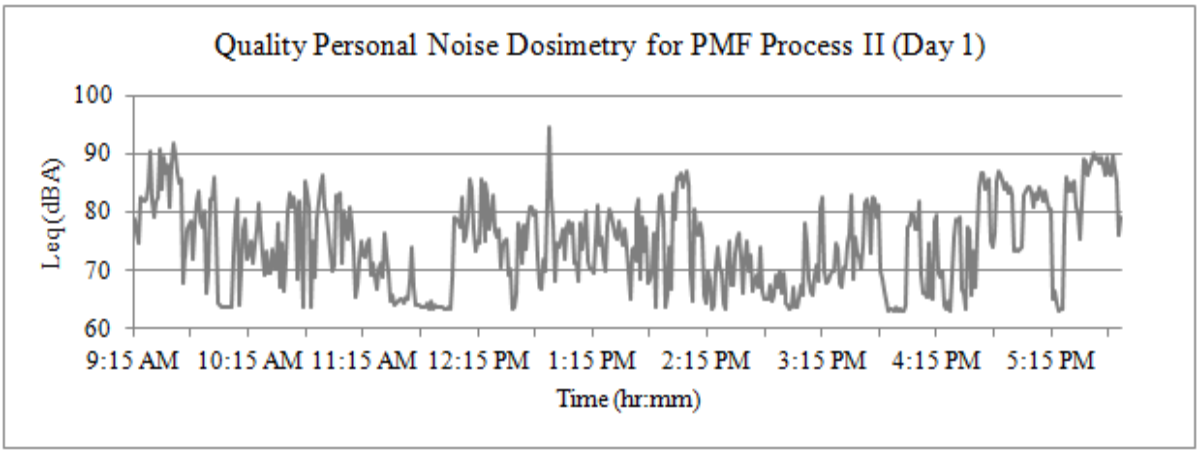

Figure 7.19: Personal noise dosimetry time series for Quality worker is displayed for Process II (day 1).

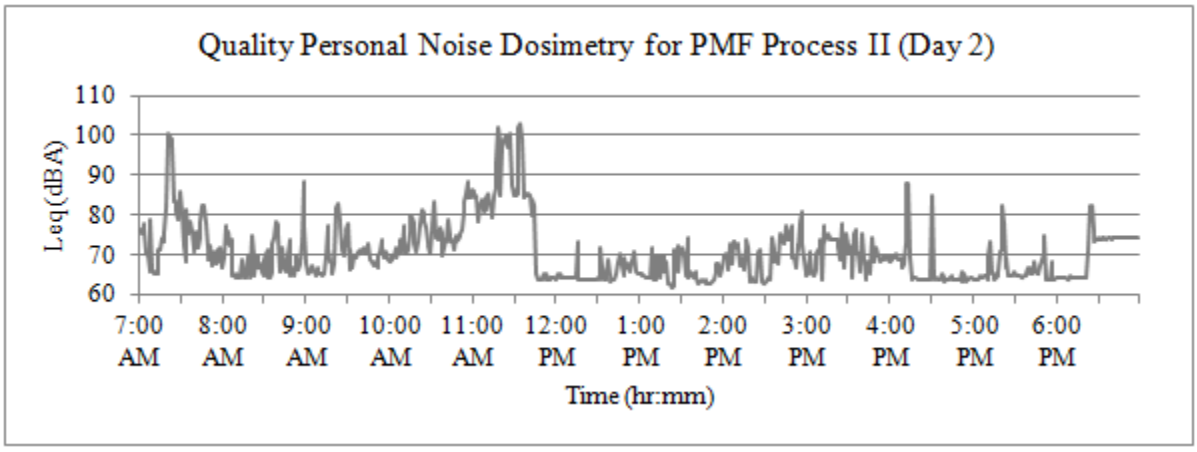

Figure 7.20: Personal noise dosimetry time series for Quality worker is displayed for Process II (day 2).

7.4 Area Noise and Aerosol Surveys

Noise area surveys were conducted in PMF Production for Process I and II (Figures 7.21-7.23 and Tables 7.1-7.3), PMF Production protective noise enclosures and the office for Process I (Figure 7.24 and Table 7.4), the PR area for Process I, and the EECL for day 1 and 2 (Figures 7.25-7.27 and Tables 7.5-7.7). Averaged Leq measurements are listed as means with standard deviation (SD). Times allowed for full dose were calculated by Equation 2. $PM_{2.5}$ area survey was conducted at EECL for day 1. Optical measurements from stationary photometers are listed by sampling time and mass concentration, as shown in Figure 7.28 and Table 7.8.

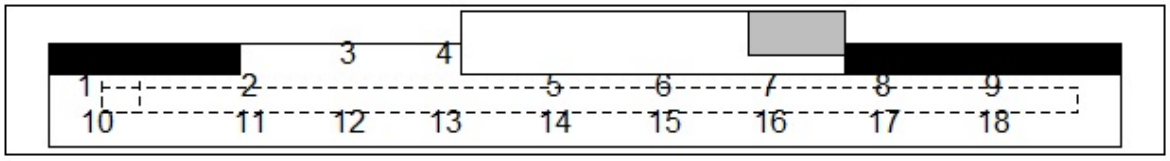

Figure 7.21: Noise area survey sampling positions for PMF Process I from stationary dosimeter data are displayed.

Table 7.1: Noise area survey results and estimated time allowed to full dose at PMF Process I from stationary dosimeter data are listed.

Position	Mean Leq dBA	SD	Time Allowed hr	Position	Mean Leq dBA	SD	Time Allowed hr
1	77.7	0.4	44.0	10	78.6	0.1	38.9
2	86.3	0.1	13.4	11	87.2	0.1	11.8
3	74.4	0.3	69.6	12	79.5	0.6	34.3
4	79.1	0.1	36.3	13	81.7	0.1	25.3
5	86.8	0.1	12.5	14	85.4	0.4	15.1
6	89.5	0.6	8.6	15	89.2	1.3	8.9
7	87.6	0.1	11.2	16	85.9	0	14.1
8	84	0.2	18.4	17	83.9	0.8	18.6
9	81.9	0.4	24.6	18	78.6	0.1	38.9

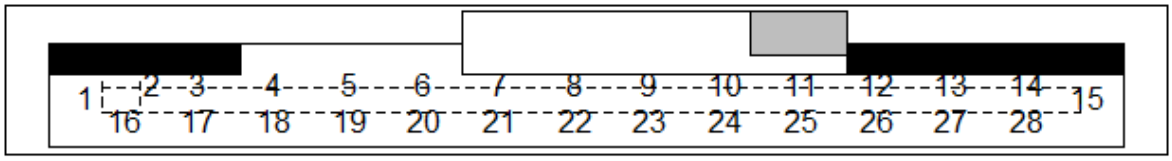

Figure 7.22: Noise area survey sampling positions for PMF Process I (Day 3) from SLM data are displayed.

Table 7.2: Noise area survey results and estimated time allowed to full dose at PMF Process I from SLM data are listed.

Position	Leq dBA	Time Allowed hr	Position	Leq dBA	Time Allowed hr
1	77.9	42.8	15	80.2	31.1
2	87	12.1	16	81.3	26.7
3	83.8	18.9	17	85.8	14.3
4	79.3	35.3	18	83.8	18.9
5	79	36.8	19	77.8	43.4
6	84.2	17.9	20	82.3	23.3
7	87.1	12.0	21	83.6	19.4
8	86.9	12.3	22	86	13.9
9	86.9	12.3	23	86.1	13.7
10	87.6	11.2	24	87	12.1
11	84.1	18.1	25	84.1	18.1
12	81.8	24.9	26	83.1	20.8
13	80.4	30.3	27	79.1	36.3
14	76.3	53.4	28	80.9	28.2

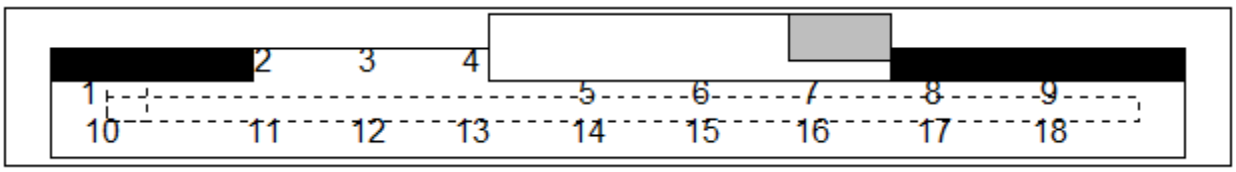

Figure 7.23: Noise area survey sampling positions for PMF Process II from stationary dosimeter data are displayed.

Table 7.3: Noise area survey results and estimated time allowed for full dose at PMF Process II from stationary dosimeter data are listed.

Position	Mean Leq dBA	SD	Time Allowed hr	Position	Mean Leq dBA	SD	Time Allowed hr
1	74.9	0.6	64.9	10	74.6	0.6	67.6
2	80.8	1.2	28.6	11	77.3	1.1	46.5
3	79.8	0.1	32.9	12	80.4	2.7	30.3
4	77.9	0.5	42.8	13	82.2	0.9	23.6
5	87.5	0.6	11.3	14	86.1	1.1	13.7
6	90.1	1	7.9	15	90.5	1.2	7.5
7	87.5	0.7	11.3	16	86.5	1.1	13.0
8	83.6	0.4	19.4	17	84	0.6	18.4
9	83.7	1.3	19.2	18	78.3	0.2	40.5

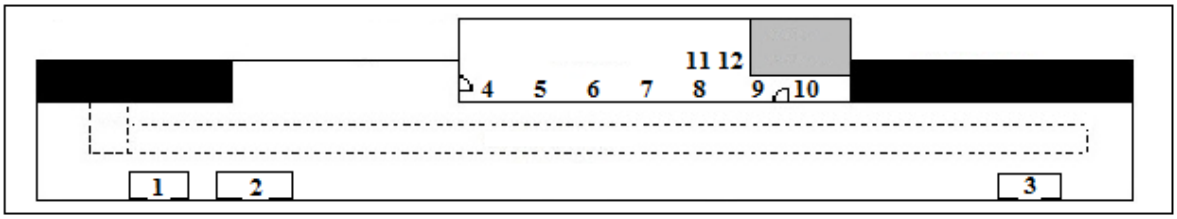

Figure 7.24: This floor plan of the PMF identifies sampling positions in sound dampening enclosures (1-3) and around the office (4-12) from SLM noise area surveys during Process I (enclosures not to scale).

Table 7.4: Leq values for PMF enclosures and office sampling positions for Process I.

Position	Leq dBA	Position	Leq dBA	Position	Leq dBA
1	81	5	68	9	69
2	74	6	70	10	72
3	78	7	71	11	72
4	66	8	70	12	71

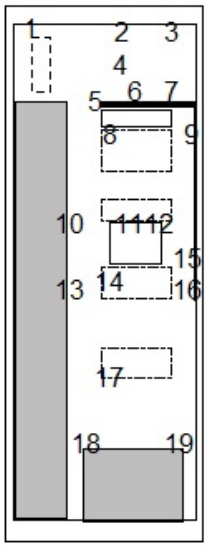

Figure 7.25: Noise area survey sampling positions for EECL Day 1 from stationary dosimeter data are displayed.

Table 7.5: Noise area survey results and estimated time allowed for full does at EECL Day 1 from stationary dosimeter data are listed.

Position	Leq dBA	Time Allowed hr	Position	Leq dBA	Time Allowed hr
1	88.6	10	11	72.8	87
2	83.5	20	12	72.7	88
3	81.1	28	13	72.6	89
4	85.2	16	14	72.3	93
5	83.6	19	15	75.5	60
6	84.9	16	16	72.2	94
7	82.8	22	17	71.7	101
8	79	37	18	72.7	88
9	73.6	78	19	83.4	20
10	74.2	72			

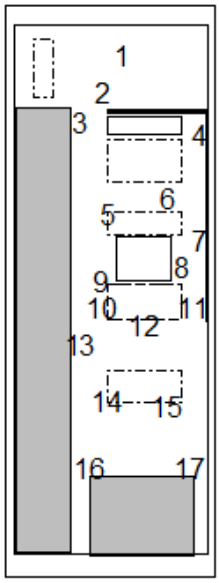

Figure 7.26: Noise area survey sampling positions for EECL Day 2 from stationary dosimeter data are displayed.

Table 7.6: Noise area survey results and estimated time allowed to full dose at EECL Day 2 from stationary dosimeter data are listed.

Position	Leq dBA	Time Allowed hr	Position	Leq dBA	Time Allowed hr
1	86.6	12.8	10	98.1	2.6
2	88.6	9.7	11	94.1	4.5
3	91	7.0	12	101.4	1.6
4	91.3	6.7	13	96.4	3.3
5	94.8	4.1	14	92.8	5.4
6	92.9	5.4	15	93.8	4.7
7	94.1	4.5	16	92.6	5.6
8	95.8	3.6	17	91.3	6.7
9	98.1	2.6			

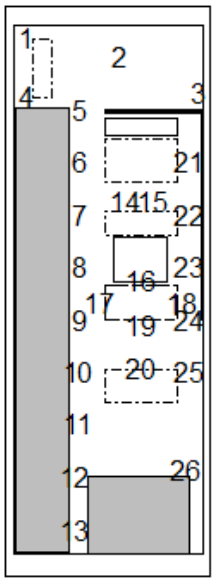

Figure 7.27: Noise area survey sampling positions for EECL Day 2 from SLM data are displayed.

Table 7.7: Noise area survey results and estimated time allowed for full dose at EECL Day 2 from SLM data are listed.

Position	Leq dBA	Time Allowed hr	Position	Leq dBA	Time Allowed hr
1	84.2	17.9	14	94.8	4.1
2	85.8	14.3	15	94.6	4.2
3	82.4	22.9	16	104	1.1
4	83.2	20.5	17	99.9	2.0
5	93.2	5.1	18	97.1	3.0
6	95.6	3.7	19	104.9	1.0
7	97.4	2.9	20	100	2.0
8	99	2.3	21	95.9	3.5
9	99.7	2.1	22	97	3.0
10	98.3	2.5	23	98.9	2.3
11	95.7	3.6	24	97.7	2.8
12	93.5	4.9	25	96.8	3.1
13	92.6	5.6	26	95.6	3.7

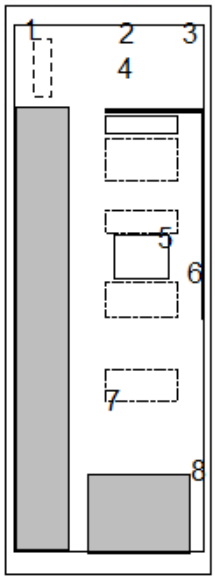

Figure7.28: $PM_{2.5}$ area survey sampling positions for EECL Day 1 are displayed from stationary aerosol photometers.

Table 7.8: $PM_{2.5}$ area survey results for optical measurements at EECL Day 1 from stationary aerosol photometers are listed.

Position	Sampling Time min	$PM_{2.5}$ Mass Concentration mg/m^3	Position	Sampling Time min	$PM_{2.5}$ Mass Concentration mg/m^3
1	175.1	0.0987	5	66.7	0.0918
2	223	0.0696	6	175.1	0.0872
3	175.2	0.0669	7	166.5	0.0787
4	223	0.0787	8	223	0.0711

7.5 Third Octave Band Analysis

A SLM was used to conduct third octave band analysis at the PMF and EECL. Third octave bands in PMF Production during Process I were obtained by averaging individual bands for all SLM positions in the area, as shown in Figure 7.29. In the PMF office during Process I, third octave bands were obtained by averaging individual bands for all SLM positions in the office, as shown in Figure 7.30. During evaluation of engineering controls in the PMF PR area, third octave bands were obtained at 1 m from the PR machine, outside the partial barrier with the

modular acoustic curtains closed, and outside the partial barrier with the curtains open, as shown in Figure 7.31. Third octave bands for EECL day 2 were obtained by averaging individual bands surrounding the engine at 1 m distance on all four sides, as shown in Figure 7.32.

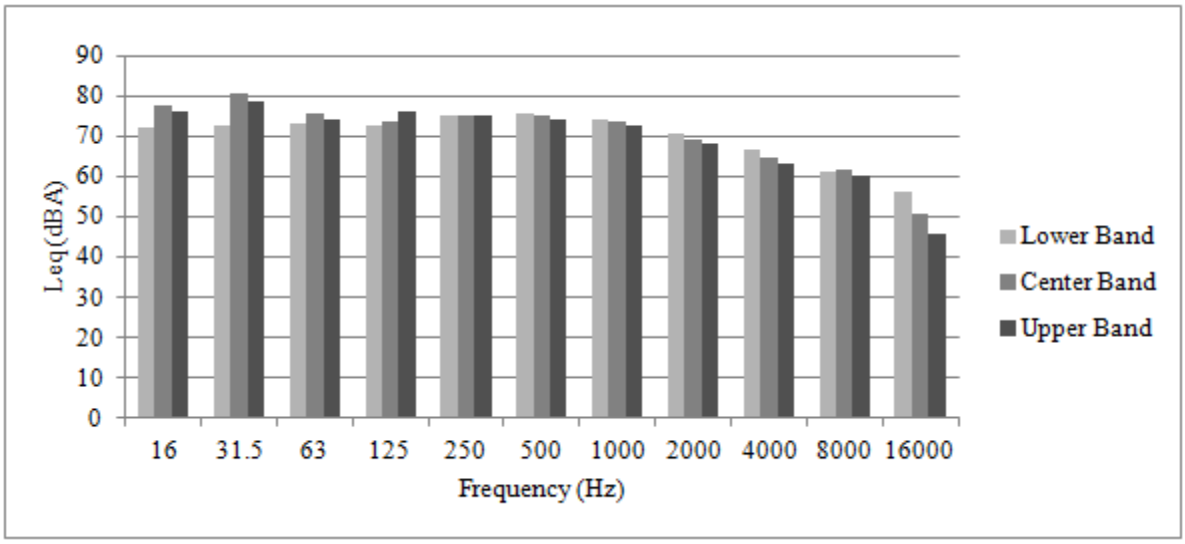

Figure 7.29: Third octave bands for PMF Production are displayed.

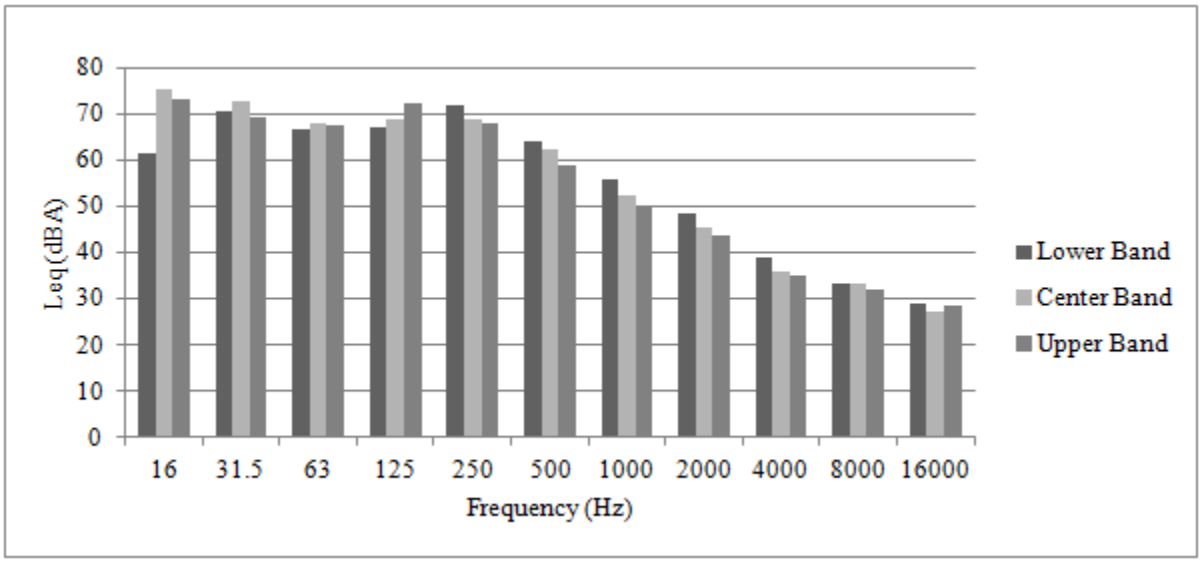

Figure 7.30: Third octave bands for the PMF office are displayed.

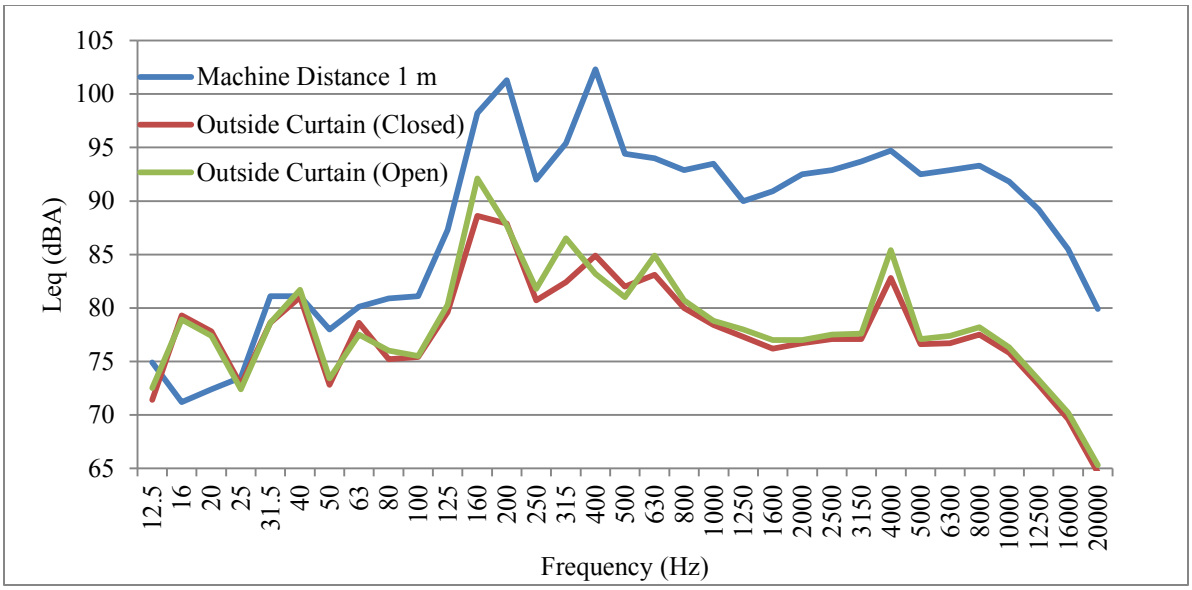

Figure 7.31: Third octave bands for the PMF PR are displayed.

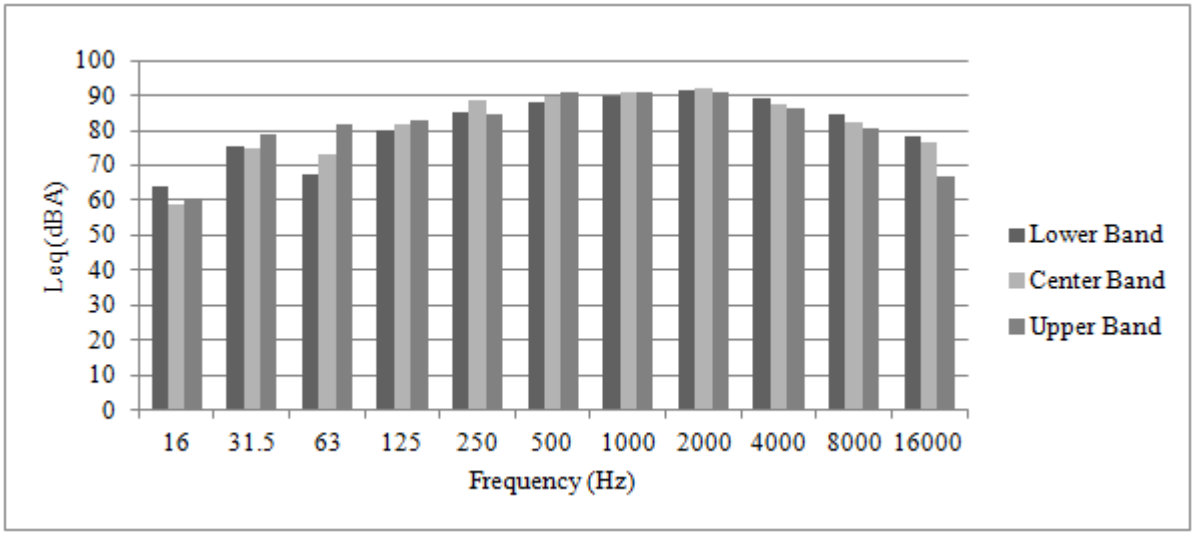

Figure 7.32: Third octave bands for EECL day 2 are displayed.